THE ROLE OF MAST CELLS IN THE MICROENVIRONMENT OF TUMORS

Inaugural Dissertation

zur
Erlangung des Doktorgrades
Dr. nat. med.
der Medizinischen Fakultät
und
der Mathematisch-Naturwissenschaftlichen Fakultät
der Universität zu Köln

vorgelegt von

Dipl. Biol. Anja Rabenhorst
aus Wismar

Köln, 2012

Berichterstatter/-in:	PD Dr. Roswitha Nischt
	PD Dr. Hildegard Büning
Tag der letzten mündlichen Prüfung:	23.01.2013

Table of content

Summary **1**

Zusammenfassung **2**

Abbreviations **3**

1. Introduction **7**

1.1. Mast cells 7

1.2. Models for investigating mast cell functions *in vivo* 8

1.3. Hallmarks of cancer 11

1.3.1. Sustaining proliferative signaling 12

1.3.2. Evading growth suppressors 12

1.3.3. Avoiding immune destruction 12

1.3.4. Enabling replicative immortality 12

1.3.5. Tumor-promoting inflammation 13

1.3.6. Activating invasion and metastasis 13

1.3.7. Inducing angiogenesis 13

1.3.8. Genome instability and mutation 14

1.3.9. Resisting cell death 14

1.3.10. Deregulating cellular energetics by reprogramming the energy metabolism 14

1.4. Mast cell mediators and their potential role in tumorigenesis 15

1.5. Mast cells in tumors 17

1.6. Primary cutaneous lymphoma 18

2. Aims **20**

3. Material and Methods **22**
3.1. Material 22
3.1.1. Chemicals and solutions 22
3.1.2. Buffers 23
3.1.3. Single-stranded oligonucleotides 24
3.1.3.1. Genotyping 24
3.1.3.2. Real-time PCR 24
3.1.4. Laboratory equipment 25
3.1.5. Software 25
3.2. Methods 26
3.2.1. Collection of cutaneous biopsies from patients with primary cutaneous lymphoma 26
3.2.2. Histology 27
3.2.2.1. Human samples 27
3.2.2.2. Murine samples 28
3.2.3. *In vitro* experiments 29
3.2.3.1. Cell isolation 29
3.2.3.2. Cell culture 29
3.2.3.3. Inhibition and stimulation of mediator release from mast cells 31
3.2.3.4. Cytometric bead array in cell culture supernatants 31
3.2.3.5. Quantitative real-time PCR 32
3.2.3.5.1. RNA isolation and reverse transcription into cDNA 32
3.2.3.5.2. RNA and cDNA quantification 32
3.2.3.5.3. Real-time PCR 32
3.2.3.6. Cell proliferation measurement 33
3.2.4. *In vivo* experiments 34
3.2.4.1. Mouse strains 34
3.2.4.2. Genotyping 34
3.2.4.2.1. DNA isolation 34
3.2.4.2.2. Polymerase chain reaction (PCR) 35
3.2.4.2.3. Gel electrophoresis 35
3.2.4.3. Administration of diphtheria toxin 36

3.2.4.4. Subcutaneous injection of tumor cell lines and measuring tumor growth 36
3.2.4.5. Two-step model of chemically induced skin carcinogenesis 37
3.2.5. Statistical analysis 38

4. Results 39
4.1. Mast cells in the microenvironment of human PCL 39
4.1.1. Clinical characteristics of PCL patients participating in the study 39
4.1.2. Mast cell numbers are increased in primary cutaneous lymphoma 42
4.1.3. Mast cell numbers correlate with progression of primary cutaneous lymphoma 45
4.1.4. Mast cell degranulation is increased in primary cutaneous lymphoma 47
4.1.5. Microvessel density is increased in mycosis fungoides 49
4.1.6. Mast cells release mediators that promote tumor growth 52
4.1.7. Unstimulated PCL cells produce proinflammatory cytokines 53
4.1.8. Mast cell supernatant induces changes in cytokine production of primary cutaneous lymphoma cells 55
4.1.9. Mast cell supernatant induces proliferation of primary cutaneous lymphoma cells 56
4.2. Mast cells in the microenvironment of murine tumors 58
4.2.1. Murine mast cell supernatant induces cytokine release and proliferation of the mouse T-cell lymphoma cell line EL4 58
4.2.2. Mast cell-deficient mouse models for the investigation of tumor growth 60
4.2.3. Mast cell-deficient mice show decreased growth of subcutaneously injected tumors 62
4.2.4. Mast cell-deficient mice show decreased chemically induced carcinogenesis 65

5. Discussion **67**

5.1. Increased mast cell number and microvessel density in primary cutaneous lymphoma 67

5.2. Stimulation of tumor growth by mast cells *in vitro* and *in vivo* 69

5.2.1. Potential effects of mast cells on different hallmarks of cancer 70

5.2.1.1. Sustaining proliferative signaling 72

5.2.1.2. Avoiding immune destruction 72

5.2.1.3. Activating invasion and metastasis 73

5.2.1.4. Inducing angiogenesis 74

5.2.2. Decreased growth of subcutaneously injected tumors and decreased chemically induced carcinogenesis in mast cell-deficient mice 75

6. References **77**

Figure Index **89**

Table Index **91**

Acknowledgments **92**

Erklärung **93**

Curriculum vitae **95**

Summary

Mast cells exert important functions in innate and adaptive immunity and are therefore strategically located at inner and outer body surfaces, such as skin, gastrointestinal tract and blood vessels. Once mast cells are activated, they release a broad array of prestored or newly synthesized mediators, including a series of cytokines and chemokines. Recent studies showed that mast cells also infiltrate many types of solid cancers and hematologic malignancies. Here, mast cell products can participate in creating a microenvironment that either promotes or inhibits tumor growth. However, the role of mast cells in tumor biology is still controversial and underlying mechanisms remain largely undefined. In the present study, we show for the first time that mast cell numbers are significantly increased in skin biopsies from patients with primary cutaneous lymphoma. Mast cell infiltration is most prominent in the periphery, at lymphoma rims. Also, degranulation of mast cells is significantly increased. Interestingly, patients with advanced stages of the disease show higher mast cell counts than stable patients. Similarly, numbers of mast cells correlate with disease progression. In addition, mast cell numbers correlate with the density of microvessels. Supernatant of cultured mast cells induces *in vitro* production of cytokines and proliferation in primary cutaneous lymphoma cells. To further elucidate the contribution of mast cells to tumor biology, we use new transgenic mouse models of inducible or constitutive selective deficiency of connective tissue mast cells and show that growth of subcutaneously injected tumors and chemically induced carcinogenesis is significantly decreased in mast cell-deficient mice. Taken together, these experiments demonstrate that mast cells play a tumor-promoting role in human primary cutaneous lymphoma and different murine tumor models. Moreover, our data provide a rationale for exploiting tumor-associated mast cells as prognostic marker and therapeutic target in primary cutaneous lymphoma and other tumors.

Zusammenfassung

Mastzellen üben entscheidende Funktionen in der angeborenen und adaptiven Immunantwort aus. Sie kommen deshalb in besonders großer Zahl an inneren und äußeren Körperoberflächen vor, wie z.B. in der Haut, im Magen-Darm-Trakt und in der Nähe von Blutgefäßen. Wenn Mastzellen aktiviert werden, sezernieren sie viele verschiedene gespeicherte oder neu synthetisierte Mediatoren, z.B. zahlreiche Zytokine und Chemokine. Infiltrate aus Mastzellen finden sich auch in vielen soliden Tumoren und hämatologischen Neoplasien. Die Produkte der Mastzellen können hier eine Umgebung schaffen, die entweder das Tumorwachstum fördert oder hemmt. Die genaue Funktion der Mastzellen in der Tumorbiologie wird jedoch noch kontrovers diskutiert und die zugrunde liegenden Mechanismen sind weitgehend unbekannt. Die vorliegende Arbeit zeigt erstmals, dass Mastzellen auch in Hautbiopsien von Patienten mit primären kutanen Lymphomen signifikant vermehrt sind. Die Infiltrate aus Mastzellen finden sich vor allem im Randbereich der Lymphome. Die Degranulation von Mastzellen ist ebenfalls deutlich gesteigert. Interessanterweise zeigen Patienten mit fortgeschrittenen Krankheitsstadien höhere Mastzellzahlen als stabile Patienten. Vergleichbar korreliert die Mastzellzahl auch mit dem Fortschreiten der Krankheit. Weiterhin korreliert die Zahl der Mastzellen mit der Dichte der Gefäße. *In vitro* induziert der Überstand von kultivierten Mastzellen die Produktion von Zytokinen und Proliferation von primären kutanen Lymphomzellen. Um den Beitrag von Mastzellen zur Tumorbiologie weiter aufzuklären, haben wir neue transgene Mausmodelle verwendet, die eine induzierbare oder konstitutive Defizienz von Bindegewebsmastzellen aufweisen, und zeigen, dass das Wachstum von subkutan injizierten Tumoren und chemisch induzierten Papillomen in diesen Tieren signifikant erniedrigt ist. Zusammenfassend belegen diese Experimente, dass Mastzellen eine Tumor-fördernde Funktion bei primären kutanen Lymphomen und verschiedenen murinen Tumormodellen besitzen. Die Daten liefern zudem die Basis für weitere Untersuchungen zur Nutzung von Tumor-assoziierten Mastzellen als prognostischer Marker und therapeutisches Target in primären kutanen Lymphomen und anderen Tumoren.

Abbreviations

%	percentage
°	degree
µg	mikrogram
µl	mikroliter
µM	mikromolar
A	tumor area
AD	atopic dermatitis
Ang	angiopoietin
BAC	bacterial artificial chromosome
BCL	primary cutaneous diffuse large B-cell lymphoma
BMMC	bone marrow-derived mast cells
bp	base pairs
C	celsius
Ca I	calcium ionophore
CBA	cytometric bead array
CBCL	cutaneous B-cell lymphoma
CCL2	MCP-1
CCL5	RANTES
CD	cluster of differentiation
CD30+ALCL	CD30 positive primary cutaneous anaplastic large cell lymphoma
cDNA	complementary DNA
CFBCL	primary cutaneous follicle center lymphoma
COX	cyclooxygenase
CSF	colony stimulating factor
CTCL	cutaneous T-cell lymphoma
CTMC	connective tissue mast cell
Ctrl	control
CXCL10	IP-10
CXCL8	IL-8
CXCL9	MIG
DC	dendritic cell

DMBA	7,12-Dimethylbenz(a)anthracene
DMEM	dulbecco´s modified eagle medium
DMSO	dimethyl sulfoxide
DNA	deoxyribonucleic acid
dNTP	deoxynucleoside triphosphate
DT	diphtheria toxin
DTR	diphtheria toxin receptor
ED	extensively degranulated
EDTA	ethylenediaminetetraacetic acid
ELISA	enzyme-linked immunosorbent assay
EORTC	European Organization of Research and Treatment of Cancer
FACS	fluorescence-activated cell sorting
FBS	fetal bovine serum
FGF	fibroblast growth factor
FMF	folliculotropic mycosis fungoides
Fwd	forward
g	gram
GAPDH	glyceraldehyde 3-phosphate dehydrogenase
G-CSF	granulocyte-colony stimulating factor
GM-CSF	granulocyte-macrophage colony-stimulating factor
h	hours
H&E	hematoxylin/eosin
HBSS	hank´s balanced salt solution
Hetero	heterozygous
Homo	homozygous
HPLC	high-performance liquid chromatography
HSC	hematopoietic stem cell
i.p.	intraperitoneal
IFN	interferon
Ig	immunoglobulin
IL	interleukin
IMDM	iscove´s modified dulbecco´s medium
ISCL	International Society of Cutaneous Lymphoma

kb	kilo-base pair
LP	lymphomatoid papulosis
LT	leukotriene
M	molar
MC	mast cell
MCP	mast cell progenitor
Mcpt5	mast cell protease-5
MD	moderately degranulated
MDSC	myeloid-derived suppressor cells
MF	mycosis fungoides
mill	million
min	minute
MIP	macrophage inflammatory protein
ml	milliliter
mm	millimeter
mM	millimolar
MMC	mucosal mast cell
MMP	matrix metalloproteinase
mRNA	messenger RNA
MTS	3-(4,5-dimethyl-2-yl)-5-(3-carboxymethoxyphenyl)-2-(4-sulfophenyl)-2H-tetrazolium
MZL	primary cutaneous marginal zone B-cell lymphoma
n	number
ND	not degranulated
NEA	non-essential amino acid solution
NGF	nerve growth factor
NHL	non-Hodgkin lymphoma
nm	nanometer
nM	nanomolar
NO	nitric oxide
ns	not significant
PAF	platelet-activating factor
PCL	primary cutaneous lymphoma
PCR	polymerase chain reaction

PDGF	platelet-derived growth factor
pg	picogram
PG	prostaglandin
pH	negative logarithm of the hydrogen ion concentration
PLEO	primary cutaneous small/medium-sized pleomorphic T-cell lymphoma
Pseudolym	pseudolymphoma
Rev	reverse
RNA	ribonucleic acid
rpm	rounds per minute
RPMI	roswell park memorial institute medium
s.c.	subcutaneous
SCF	stem cell factor
SD	standard deviation
SDS	sodium dodecyl sulfate
sec	seconds
SEM	standard error of the mean
SS	Sézary syndrome
TGF	transforming growth factor
TNF	tumor necrosis factor
TPA	12-O-tetradecanoylphorbol 13-acetate
U	unit
UV	ultraviolet
V	volt
VEGF	vascular endothelial growth factor
Vol	tumor volume
w/v	weight per volume
WHO	World Health Organization
WT	wildtype
x	fold

1. Introduction

1.1. Mast cells

In 1878, Paul Ehrlich discovered cells with large cytoplasmic granules that he named "mast cells".[1] First, mast cells were believed to be a component of the connective tissue, derived from undifferentiated mesenchymal cells.[2,3] Today, we know that mast cells are bone marrow-derived hematopoietic cells. Hematopoietic stem cells give rise to mast cell progenitors, which circulate in the blood and enter the tissues, where differentiation and maturation into mature mast cells takes place (Figure 1).[4] However, it is still controversially discussed whether the mast cell progenitor is derived directly from a pluripotent precursor or from the myeloid lineage.

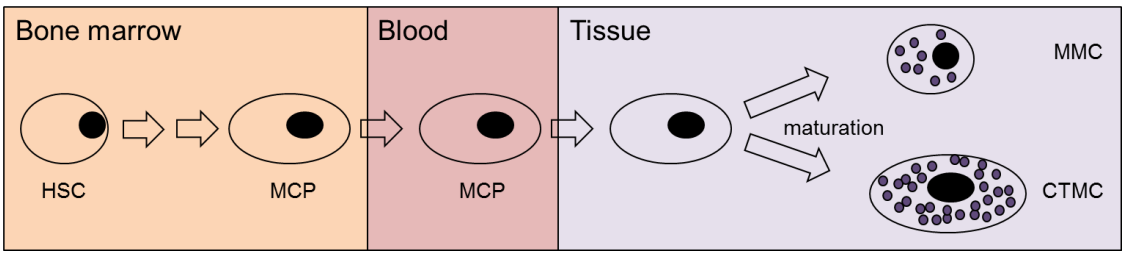

Figure 1. Mast cell development. Mast cells originate from hematopoietic stem cells (HSC) in the bone marrow that give rise to mast cell progenitors (MCP). These mast cell progenitors are released into the blood and circulate until they migrate into the tissues, where they finally differentiate into mature mast cells. MMC, mucosal mast cells; CTMC, connective tissue mast cells.

The phenotype of mature mast cells varies depending on the tissue microenvironment. Human mast cell subpopulations are divided into MC_{TC} cells, designated to their tryptase and chymase content, and MC_T cells that only contain tryptase. In analogy to human mast cells, also different types of murine mast cells exist. In mice, one can distinguish between mucosal mast cells (MMC), located within mucosal epithelia and connective tissue mast cells (CTMC), located in skin, peritoneal cavity and submucosa.[5] Because human MC_T cells predominantly appear in the alveolar septa of the lung and in the small intestinal mucosa, they most closely correspond to mouse MMC, whereas human MC_{TC} cells resemble mouse CTMC.[6]

Due to the preferred location of mast cells in tissues exposed to the environment such as skin, airways and gastrointestinal tract[7-9], they are one of the first immune cells to interact with invading pathogens[10,11] or antigens.[12,13] Thus, mast cells are predestined for performing important functions in innate[10,14,15] and adaptive[14,16-18] immunity. Furthermore, several studies reported on a possible role of mast cells in wound healing, tissue remodeling and transplant tolerance.[19-21] Additionally, mast cells seem to contribute to diet-induced obesity and diabetes.[22] Moreover, a pathogenic role of mast cells was described for rheumatoid arthritis, multiple sclerosis and atherosclerosis[23-26] as well as for different human malignancies, as described in detail in section 1.5.

Mast cells are long-lived cells that can re-enter the cell cycle and proliferate after appropriate stimulation.[27] Furthermore, the increased recruitment and/or retention, and local maturation of mast cell progenitors can contribute to the expansion of mast cell populations.[6,28] The best-characterized activation pathway in mast cells is their activation through immunoglobulin E (IgE), which binds to the high affinity IgE receptor Fcε-receptor I (FcεRI).[29] In mice, activation through IgG1 and FcγRIII is also possible. Besides, a large variety of other immunological and non-immunological signals can induce mast cell activation.[27] Depending on the type and concentration of the activation signal, mast cells can release either all classes of mediators at high levels via degranulation or may release certain mediators more selectively by secretion.[14] This offers the possibility to respond to the requirements of the specific biological process with large variation. In addition, being rechargeable, mast cells can also participate in multiple cycles of mediator release. Furthermore, mast cells can functionally interact with other cell types, including T-cells, B-cells, dendritic cells (DC) and eosinophils, both by releasing mediators and by cell-cell interactions.

1.2. Models for investigating mast cell functions *in vivo*

Over the past 30 years, *Kit*-mutant mice like WBBF1-*Kit*$^{W/W\text{-}v}$ and C57BL/6 *Kit*$^{W\text{-}sh/W\text{-}sh}$ have usually been used for the investigation of mast cell biology *in vivo*.[4,30] *Kit*^{W} contains a point mutation that encodes for a truncated Kit protein, which lacks the transmembrane domain and is therefore not expressed on the cell surface, *Kit*$^{W\text{-}v}$ shows a mutation in the Kit tyrosine kinase domain that decreases the kinase activity of the receptor and *Kit*$^{W\text{-}sh}$ contains an inversion

mutation of the transcriptional regulatory elements upstream of the *Kit* transcription start site on mouse chromosome 5.[14,17,27] Adult WBBF1-*Kit*$^{W/W\text{-}v}$ and C57BL/6 *Kit*$^{W\text{-}sh/W\text{-}sh}$ mice are deficient in mast cells and melanocytes.[4] In the WBBF1-*Kit*$^{W/W\text{-}v}$ strain, the number of mast cells in the skin, stomach, cecum and mesentery is reduced to less than 1% compared to congeneic controls. Additionally, WBBF1-*Kit*$^{W/W\text{-}v}$ mice have several other abnormalities, such as macrocytic anemia, a decrease in the number of bone marrow and blood neutrophils, sterility and a decreased number of intestinal cells of Cajal.[4,28,30]
The mast cell-deficient strain C57BL/6 *Kit*$^{W\text{-}sh/W\text{-}sh}$ is fertile and not anemic.[30,31] C57BL/6 *Kit*$^{W\text{-}sh/W\text{-}sh}$ animals are largely devoid of mast cells in the tongue, trachea, lung, stomach, spleen, small intestine, mesentery, peritoneum and inguinal lymph nodes. In the skin, 1.2% of the normal number of mast cells are still present.[30] However, C57BL/6 *Kit*$^{W\text{-}sh/W\text{-}sh}$ mice also show abnormalities like splenomegaly, thrombocytosis, neutrophilia, and decreased numbers of F4/80-positive cells in the bone marrow.[32]
In contrast to the *Kit*-mutant lines used up to now, recently developed mouse models of inducible (*Mcpt5-Cre/iDTR*) and constitutive (*Mcpt5-Cre/R-DTA*) mast cell deficiency[33,34] show an otherwise normal immune system. For creating these new mouse models, bacterial artificial chromosome (BAC) transgene technology was employed to express *Cre* recombinase under the control of the mast cell-specific promoter mast cell protease-5 (*Mcpt5*).[33] The constructs were injected into C57BL/6 oocytes for random integration into the mouse genome. To develop a mouse model of inducible mast cell deficiency, *Mcpt5-Cre/iDTR*[33,34] mice were generated by breeding the mast cell-specific transgenic line *Mcpt5-Cre* to the *iDTR* line, which is characterized by expression of a simian diphtheria toxin receptor (DTR) in cells that have deleted a *lox*P-flanked stop cassette by *Cre*-mediated recombination (Figure 2).[35] *Mcpt5-Cre+/iDTR+* mice show efficient and specific depletion of connective tissue mast cells upon intraperitoneal injections with diphtheria toxin (DT). A mouse model of constitutive mast cell deficiency, was obtained by crossing the mast cell-specific transgenic line *Mcpt5-Cre* to the *R-DTA* line[36] (Figure 3). These mice express diphtheria toxin (DT) under the control of a *lox*P-flanked stop cassette. The *lox*P-flanked cassette prevents DT expression in the absence of *Cre* activity.

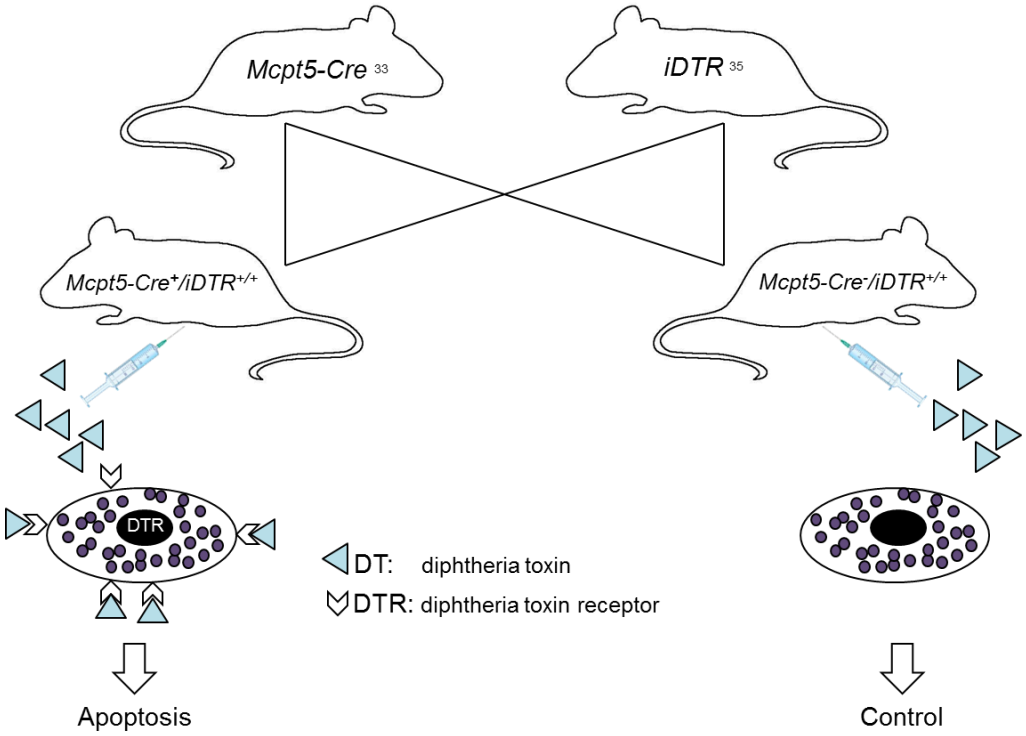

Figure 2. *Mcpt5-Cre/iDTR – A* mouse model of inducible mast cell deficiency. Intraperitoneally injected diphtheria toxin (DT) binds to the receptors on the surface of connective tissue mast cells, which leads to apoptosis of these cells. DTR, diphtheria toxin receptor; DT, diphtheria toxin

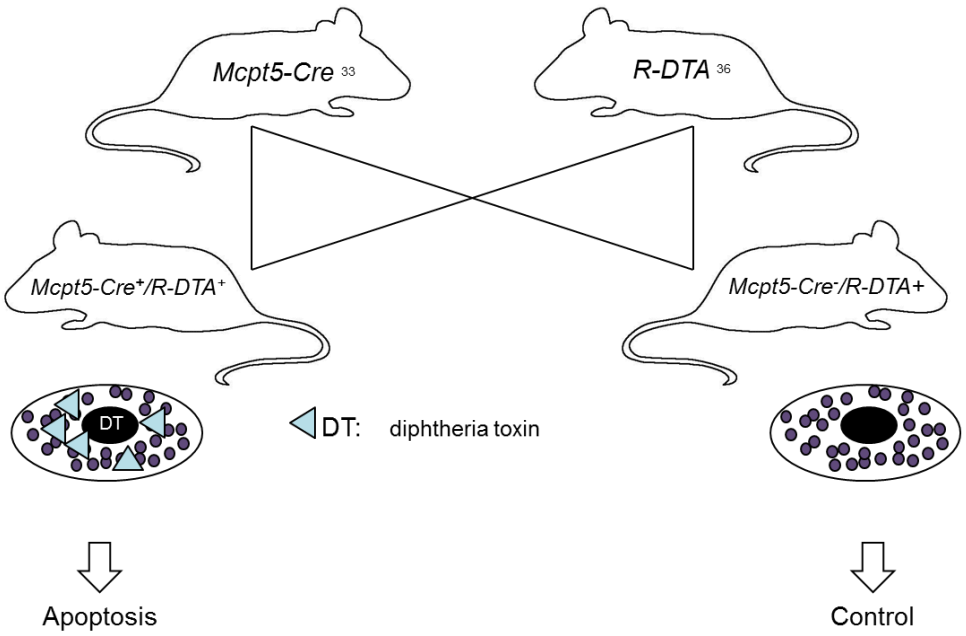

Figure 3. *Mcpt5-Cre/R-DTA – A* mouse model of constitutive mast cell deficiency. Upon *Cre* activity connective tissue mast cells express diphtheria toxin (DT), which leads to apoptosis of these cells. DT, diphtheria toxin

1.3. Hallmarks of cancer

The hallmarks of cancer (Figure 4) include, according to Hanahan and Weinberg[37], ten different mechanisms as shown below:

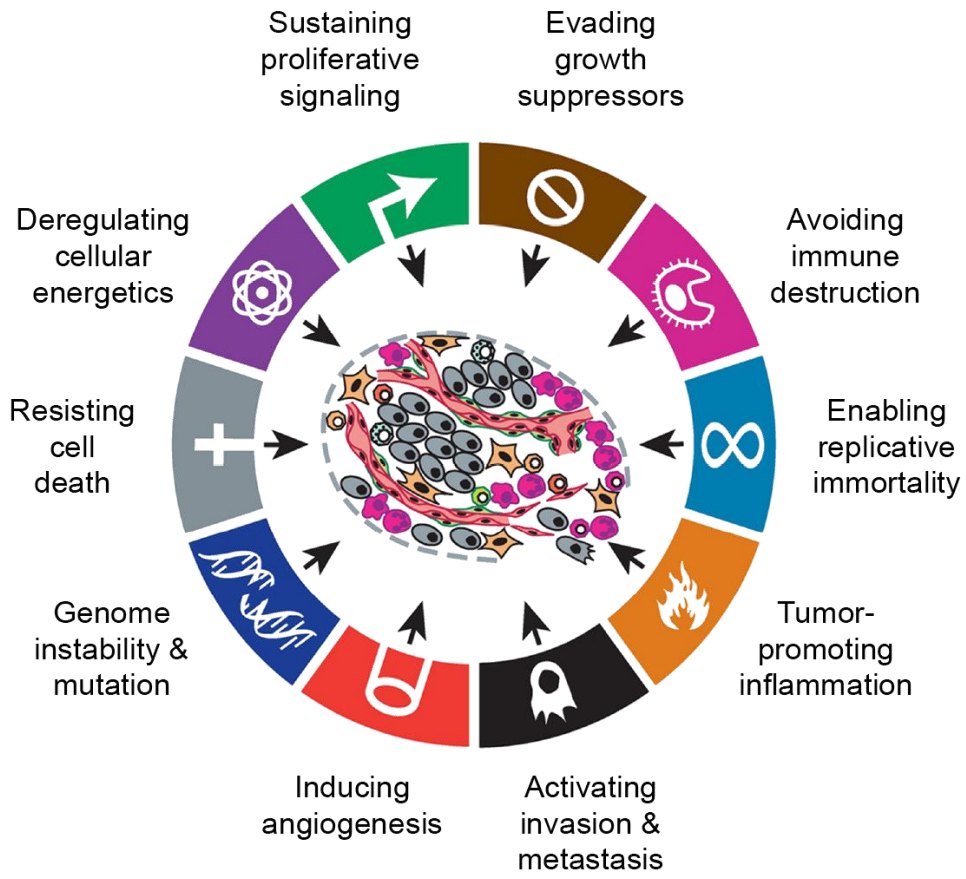

Figure 4. Hallmarks of cancer. Adapted from Hanahan and Weinberg, 2011[37]

1.3.1. Sustaining proliferative signaling

Whereas normal tissue controls the production and release of growth-promoting signals to ensure constant cell numbers and intact tissue architecture, tumor cells deregulate these signals. The enabling signals are conveyed by growth factors that bind cell surface receptors. Sources of these proliferative signals are still largely unknown.

1.3.2. Evading growth suppressors

Besides limitless growing, tumor cells are able to circumvent programs that negatively regulate cell proliferation, which are mostly dependent on tumor suppressors. Additionally, contact inhibition which, in dense cell populations, also yields to a suppressed cell proliferation is abolished in many cancers. Furthermore, deactivating the TGF-β pathway, known for its antiproliferative effects, promotes malignancy.

1.3.3. Avoiding immune destruction

Immune surveillance is usually responsible for recognizing and eliminating the majority of abnormal cells. Tumor cells are often able to avoid detection by the immune system or can limit the extent of being killed. For example, tumor cells can "paralyze" infiltrating cells of the immune system by secreting TGF-β or other immunosuppressive factors. Moreover, they can also actively recruit immunosuppressive cells, such as regulatory T-cells and myeloid-derived suppressor cells.

1.3.4. Enabling replicative immortality

In order to generate tumors, tumor cells aquire unlimited replicative potential. In contrast, normal cells can only pass through a limited number of successive cell growth and cell divison cycles. In the end, normal cells become senescent, meaning they enter a nonproliferative, but viable state. It may occur that some of these cells escape from this state and acquire unlimited replicative potential. Cells that undergo this transition are then called "immortalized". They may proceed to form tumors due to their ability to maintain telomeric DNA at lengths sufficient to avoid undergoing senescence or apoptosis, achieved by upregulating the expression of telomerase.

1.3.5. Tumor-promoting inflammation

Tumors are infiltrated by cells of the innate and adaptive immune system and mirror inflammatory conditions. Historically, such immune responses were thought to reflect an attempt of the immune system to eradicate tumors. Today, it is well recognized that the tumor-associated inflammatory response can also have the opposite effect of enhancing tumorigenesis and progression. Inflammation can contribute to different hallmarks of cancer by supplying a large variety of molecules to the tumor microenvironment that promote tumors, for example growth factors to sustain proliferative signaling, survival factors that limit cell death, proangiogenic factors and extracellular matrix-modifying enzymes that facilitate angiogenesis, invasion and metastasis.

1.3.6. Activating invasion and metastasis

Invasion and metastasis is a multistep process, starting with local invasion, followed by intravasation of tumor cells into nearby blood and lymphatic vessels, transition of tumor cells through the lymphatic and hematogenous systems, extravasation of tumor cells from the lumina of these vessels into the parenchyma of distant tissues, formation of micrometastasis and finally by growth of micrometastatic lesions into macroscopic tumors.

1.3.7. Inducing angiogenesis

Tumors need nutrients and oxygen and can eliminate metabolic waste and carbon dioxide. Therefore, angiogenesis, which means sprouting of new vessels from existing ones, is necessary to generate a tumor-associated vasculature. During tumor progression, an "angiogenic switch" causes continuous sprouting of normal vasculature. Tumor vasculature is marked by early capillary sprouting, convoluted and excessive vessel branching, distorted and enlarged vessels, erratic blood flow, leakiness and abnormal levels of endothelial cell proliferation and apoptosis.[38] The best-studied inducer of angiogenesis is vascular endothelial growth factor (VEGF). VEGF gene expression is upregulated by hypoxia as well as by oncogene signaling. Furthermore, VEGF ligands are sequestered in the extracellular matrix in latent forms that are subject to release and activation by extracellular matrix-degrading proteases, like for example matrix metalloproteinase-9 (MMP-9).

In addition, other proangiogenic signals, like fibroblast growth factor (FGF), have been implicated in sustaining tumor angiogenesis.

1.3.8. Genome instability and mutation

As tumor progression is a multistep process, every step offers the opportunity for mutations and deregulating gene expression. Due to the inherent ability to detect and resolve DNA defects, the rate of spontaneous mutations is usually very low. Tumor cells often show increased rates of mutations. This mutability is also achieved through increased sensitivity to mutagenic agents, through a breakdown in one or several components of the genomic maintenance machinery, or through both mechanisms. Additionally, the accumulation of mutations is accelerated by comprising the surveillance systems that normally monitors genomic integrity and transfers genetically damaged cells into senescence or apoptosis.

1.3.9. Resisting cell death

Programmed cell death by apoptosis is a natural barrier to cancer development. Tumor cells have developed many different strategies to limit or circumvent apoptosis, for example loss of tumor suppressor functions, increased expression of antiapoptotic regulators (Bcl-2, Bcl-x_L) or survival signals (Igf1/2) and downregulation of proapoptotic factors (Bax, Bim, Puma).

1.3.10. Deregulating cellular energetics by reprogramming the energy metabolism

Under aerobic conditions, normal cells process glucose via glycolysis into pyruvate and thereafter into carbon dioxide through mitochondrial oxidative phosphorylation. Tumor cells can reprogram their glucose metabolism by shifting their energy production largely to glycolysis. Besides, reliance on glycolysis is of particular importance under hypoxic conditions within many tumors. Furthermore, increased glycolysis allows the distribution of glycolytic intermediates into various biosynthetic pathways, which facilitate the biosynthesis of macromolecules required for assembling new cells.

1.4. Mast cell mediators and their potential role in tumorigenesis

Upon activation, mast cells exert their biological functions by releasing preformed as well as *de novo* synthesized mediators. Mast cells produce a broad array of such mediators and cell-cell signaling molecules. About thirty different cytokines, chemokines as well as other metabolites have been shown to be produced by mast cells.[39] They can be grouped into three major classes.[12] First, preformed and granule-associated mediators are produced like histamine, serotonin, proteases like tryptase and chymase as well as TNF, VEGF and FGF. Second, newly synthesized lipid mediators are released, namely the leukotrienes LTC_4 and LTB_4 and the prostaglandins PGD_2 and PGE_2. Third, *de novo* synthesized cytokines and chemokines are produced. In tumor biology, these mediators can either have "beneficial" effects on tumor growth, causing progression and spread of the tumor, or "detrimental" effects, limiting the growth of the tumor. To mention just some of these mediators, histamine and growth factors like NGF, SCF, PDGF and TGF-β promote tumor development, whereas heparin, VEGF, FGF and CXCL8 (IL-8) are known to induce angiogenesis, which is an essential feature for tumorigenesis. Some of these growth factors can also serve as mast cell chemoattractants in a feedback loop. On the other hand, mast cell-produced cytokines may also participate in anti-tumor responses and tumor rejection by promoting inflammation (IL-1, IL-2, IL-6, IL-10, TNF-α, IFN-γ) or by inducing tumor cell apoptosis (IL-4, IL-13). Table 1 and 2 summarize mast cell mediators and their functions concerning tumor growth. However, investigations on the role of specific mast cell products in tumor development, especially concerning the balance between pro- and anti-inflammatory mechanisms, are still at the very beginning.

	Mediators	Effects and function
+ beneficial effects on tumor growth +	histamine	increase vascular permeability, angiogenesis, immunosuppression
	heparin	angiogenesis, NGF stabilization, increases vascular permeability, matrix reorganization
	tryptase	tissue remodeling, neovascularization, facilitate metastases
	chymase	facilitate metastases, tissue damage/remodeling
	NGF, SCF	promote tumor growth, mast cell chemoattractant
	PDGF, CSF	promote tumor growth
	VEGF	angiogenesis, mitogenesis of endothelial cells
	FGF	promote tumor growth, neovascularization, matrix reorganization and degradation
	TGF-β	tumor growth, mitogenesis of endothelial cells, angiogenesis
	CCL2, CCL5	chemoattraction for mast cells und other immune cells
	CXCL8	neovascularization, matrix reorganization and degradation
	TNF-α	immunosuppression, neovascularization
	IL-3, 4	matrix reorganization and degradation
	Ang-1	angiogenesis, formation of blood vessels

Table 1. Mediators produced by mast cells exerting beneficial effects on tumor growth.

	Mediators	Effects and function
− detrimental effects on tumor growth −	IL-1, 6, 9, 10	inflammation, leukocyte migration
	IL-3	mast cell proliferation, eosinophil production and activation
	IL-4	tumor cell apoptosis, promote T_H2 differentiation
	IL-5	leukocyte migration, eosinophil production and activation
	TNF-α	inflammation, tumor cell death
	IFN-γ	inflammation, leukocyte proliferation and activation
	GM-CSF	inflammatory cell proliferation, eosinophil production
	TGF-β	inflammatory cell proliferation
	PAF	platelet activation, serotonin release, leukocyte chemotaxis
	PGD_2, PGE_2	vasodilation, neutrophil chemotaxis
	LTB_4, LTC_4	leukocyte chemotaxis, increased vascular permeability
	NO	vasodilation, neurotransmission
	MIP-1α	attraction for monocytes, macrophages and neutrophils
	MCP-3/4	chemoattraction for leukocytes
	tryptase	stimulate protease-activated receptors, induce inflammation

Table 2. Mediators produced by mast cells exerting detrimental effects on tumor growth.

1.5. Mast cells in tumors

In a large variety of cancers, immune cells of the tumor microenvironment have been demonstrated to play crucial roles in tumor biology.[37,40] In particular, tumor-associated macrophages, myeloid-derived suppressor cells (MDSC) and T regulatory cells (T_{regs}) participate in the development of tumors by regulating various hallmarks of cancer, like proliferation, angiogenesis, immunomodulation and tissue remodeling.

The accumulation of mast cells especially in the periphery of tumors was first reported by Westphal in 1891.[41] But also recent studies demonstrated impressively that mast cells serve as critical regulators of the tumor microenvironment.[41-43] Many types of solid cancers and hematologic malignancies show an increased number of mast cells.[44-55] Mast cell counts often also correlate with tumor stage, prognosis and invasiveness, suggesting a protumorigenic role of mast cells in these malignancies.[44-51] More precisely, increased numbers of mast cells have been reported to correlate with poor prognosis in lymphoid neoplasms such as Hodgkin´s lymphoma[47], B-cell non-Hodgkin's lymphoma[50] and multiple myeloma[56]. Similar data have been obtained in solid cancers, such as pancreatic cancer[57], hepatocarcinoma and cholangiocarcinoma[49], prostate cancer[44], neurofibroma[48] and melanoma[46,58].

In summary, the previous studies demonstrated that: (1) Mast cells participate in creating a microenvironment that promotes tumor growth. (2) Mast cell-deficient mice show an impaired carcinogenesis and reduced tumor neo-angiogenesis.[59,60] (3) Pharmacological inhibition of mast cell degranulation can inhibit tumor growth.[60]

In contrast to the protumorigenic role of mast cells described for a large number of tumors, mast cells were also reported to exert antitumorigenic effects in certain malignancies, for example by supporting cancer rejection.[52-54] In colorectal cancer, infiltrates of mast cells have been associated with lower rates of lymph node metastasis and distant metastasis.[52] Also, in breast cancer, stromal mast cells were found to correlate with a favorable prognosis.[53,54] Additionally, mast cells even showed plasticity by exerting both detrimental and beneficial effects in the same cancer entity depending on the tumor stage, as for example elegantly demonstrated for prostate adenocarcinoma.[44]

It has been speculated that mast cells remodel the tumor microenvironment through release of cytokines and chemokines upon degranulation as well as through interactions with other cell types.[61] Aggregation of eosinophils together with mast cells has also been described to correlate with poor prognosis, for example in Hodgkin´s lymphoma.[62] Apart from the interaction of mast cells with other immune cells of the tumor microenvironment, it is also conceivable that mast cells modulate other stromal structures such as blood vessels or extracellular matrix. As an example, mast cells may indirectly participate in tumor development by producing VEGF that in turn stimulates tumor growth through enhanced tumor neo-angiogenesis. Supporting this hypothesis, in lung cancer[63] and squamous cell carcinomas of the esophagus[64] and cervix[65], mast cell infiltrates correlated with both microvessel density and tumor progression. The complex functions of mast cells in tumor biology may in part be related to the differential release of mediators, but specific effects on tumor growth are still poorly understood.

1.6. Primary cutaneous lymphoma

Cutaneous lymphomas are clonal lymphoid neoplasms, which belong to the group of extranodal non-Hodgkin´s lymphomas (NHL).[66-69] They usually reflect a clonal proliferation of lymphocytes in the skin. The annual incidence is estimated at 1/100.000.[67] By definition one has to distinguish between secondary cutaneous lymphomas, as manifestations of nodal or other extranodal lymphomas also involving the skin, and primary cutaneous lymphomas (PCL).

As an example for a skin tumor in which the role of mast cells had not been described yet, we investigated primary cutaneous lymphomas (PCL). In PCL, functional interactions between neoplastic cells and their microenvironment are largely unknown. PCL are a clinical and histological distinct group of T- or B-cell malignancies that originate in the skin and usually remain localized to the skin for a longer period of time. In Europe, cutaneous T-cell lymphomas (CTCL) constitute about 75-80% of all PCLs, cutaneous B-cell lymphomas (CBCL) 20-25%, but different distributions have been observed in other parts of the world.[66] Diagnosis and classification of primary cutaneous lymphomas into CTCL and CBCL and their subtypes is based on a combination of clinical, histological and

immunophenotypical data. The most common subtypes of CTCL include mycosis fungoides (MF), Sézary syndrome (SS) and lymphomatoid papulosis (LP), whereas CBCL are subdivided into primary cutaneous marginal zone B-cell lymphoma (MZL), primary cutaneous follicle center lymphoma (CFBCL) and primary cutaneous diffuse large B-cell lymphoma (BCL).

Clinical manifestation and prognosis of PCL are highly variable and depend on the subtype and stage of the disease.[70,71] For example, early stages of MF, characterized by eczematous skin lesions resulting from inflammation associated with proliferation of malignant cells in the epidermis, typically run an indolent course.[70] More advanced stages of MF show intradermal tumors, which arise from poorly differentiated subclones of malignant cells that spread into deeper layers of the skin and later into peripheral blood, lymph nodes and internal organs. In these advanced stages, conventional therapies can achieve only short-term clinical responses and median survival is less than three years. The prognosis is even worse in patients with SS, the leukemic variant of CTCL. In contrast, most patients with CBCL show stable nodular lesions associated with an indolent course.[72]

Involvement of immune cells is suggested by elevated levels of inflammatory cytokines in plasma and skin sections of CTCL patients, such as IL-1β, IL-7, IL-15, IL-17, IL-18 and IL-23.[73-75] Recent investigations reported on significant expression of IL-17 in cells and tissues from patients with MF and SS.[73,74] IL-17 is known to participate in proinflammatory responses by initiating the production of various cytokines (IL-6, G-CSF, GM-CSF, IL-1β, TGF-β1, TNF), chemokines (CXCL8 and CCL2), and prostaglandins (PGE_2) from other cell types such as epithelial cells, keratinocytes, endothelial cells, fibroblasts, macrophages and potentially mast cells. In CTCL, it has been shown that IL-2 and IL-15 are able to up-regulate the expression of IL-17 in neoplastic T-cells.[74] CTCL lesions are known to exhibit increased angiogenesis and several angiogenic and inflammatory proteins that are induced by IL-17 (for example TNF, CCL20, MMP-9, COX-2, VEGF and CXCL8) are also expressed in CTCL lesions.[76-78] Interestingly, a recent study using a mouse model of CTCL reported on increased numbers of macrophages and neutrophils and showed that tumor growth is reduced upon depletion of macrophages.[79]

2. Aims

Mast cells infiltrate many types of cancers. Recent studies demonstrated that mast cells actively participate in modulating tumor growth, either by directly affecting growth and invasiveness of tumor cells or by indirectly regulating the tumor microenvironment, e.g. by interacting with other immune cells, inducing neo-angiogenesis or degrading extracellular matrix, which then promotes tumor growth. However, the precise role of mast cells in tumors remains largely unknown. Therefore, the present study aims to clarify specific functions of mast cells in tumor biology addressing the following four goals:

1. To explore numbers of mast cells and their correlation with tumor growth, we decided to initially investigate mast cell counts in primary cutaneous lymphoma (PCL) as an example of a tumor entity, in which mast cells have not been addressed to date. More specifically, we will analyze the number and distribution of mast cells in different subtypes of PCL compared to normal skin and inflammatory cutaneous diseases, such as psoriasis and atopic dermatitis. In addition, hypothesizing that mast cells are activated in the tumor microenvironment of PCL, we will explore mast cell degranulation in PCL. Furthermore, we will correlate mast cell numbers and degranulation with the course and prognosis of different PCL subtypes.

2. To further elucidate the contribution of mast cells to tumor growth, we will use new transgenic mouse models with inducible or constitutive selective deficiency of connective tissue mast cells and analyze tumorigenesis in these models compared to control mice. Here, we will investigate different subcutaneously injected tumors, namely the murine lymphoma cell line EL4, the pancreatic adenocarcinoma cell line Pan02 and the Lewis lung carcinoma cell line LLC, as well as chemically induced carcinogenesis.

3. To clarify the effect of specific mast cell products on tumor growth, we will first analyze whether supernatant of human or murine mast cells stimulates cytokine production and proliferation of primary PCL cells and human or murine lymphoma cell lines. Next, we will investigate levels of different cytokines in supernatants of human and murine mast cells using a cytometric bead array approach.

4. To address the role of mast cells in tumor neo-angiogenesis, we will analyze vessel density in PCL and in the murine EL4 tumor model. We will also investigate growth of EL4 tumors in mast cell-specific VEGF knockout mice.

3. Material and Methods

3.1. Material

3.1.1. Chemicals and solutions

Standard chemicals and solutions were purchased from:

Biochrom AG, Berlin, Germany

Brenntag, Mülheim, Germany

Gibco/Invitrogen, Karlsruhe, Germany

Merck, Darmstadt, Germany

Roth, Karlsruhe, Germany

Serva, Heidelberg, Germany

Sigma-Aldrich, Taufkirchen, Germany

StarLab, Hamburg, Germany

Product	**Company**
Acetone	Roth
Agarose StarPure	StarLab
Calcium ionophore A23187	Sigma-Aldrich
Cromolyn sodium salt	Sigma-Aldrich
Dimethyl sulphoxide (DMSO)	Sigma-Aldrich
Disodium hydrogen phosphate (Na_2HPO_4)	Merck
Dulbecco´s Modified Eagle Medium (DMEM, 1x)	Gibco/Invitrogen
EDTA (1% (w/v) in PBS, cell culture)	Biochrom AG
Ethanol (≥ 99.5%)	Roth
Ethylenediaminetetraacetic acid (EDTA)	Roth
Fetal bovine serum (FBS)	Biochrom AG
Hanks´ Balanced Salt Solution (HBSS)	Sigma-Aldrich
Hydrochloric acid (HCl)	Roth
Iscove´s Modified Dulbecco´s Medium (IMDM, 1x)	Gibco/Invitrogen
Isopropanol	Brenntag
L-glutamine (200 mM)	Biochrom AG
Non-essential amino acid solution (NEA, 100x)	Sigma-Aldrich
Penicillin/Streptomycin (10.000 U/ml / 10.000 µg/ml)	Biochrom AG
Potassium chloride (KCl)	Roth
Potassium dihydrogen phosphate (KH_2PO_4)	Roth
Roswell Park Memorial Institute (RPMI) medium 1640 (1x)	Gibco/Invitrogen

Roti®-Histofix (4%)	Roth
Sodium acetate ($C_2H_3NaO_2$)	Merck
Sodium chloride (NaCl)	Roth
Sodium dodecyl sulfate (SDS)	Serva
Sodium pyruvate (100 mM)	Gibco/Invitrogen
Tris $(HOCH_2)_3CNH_2$)	Roth
Trypsin (2.5%, 10x)	Gibco/Invitrogen
β-Mercaptoethanol (50 mM)	Gibco/Invitrogen

Table 3. Frequently used chemicals and solutions.

3.1.2. Buffers

Used buffers were prepared with deionized water at room temperature.

Buffer components	Concentration
PBS	
NaCl	136 mM
KCl	2.6 mM
KH_2PO_4	1.5 mM
Na_2HPO_4	10 mM
TE	
Tris-HCl (pH 8.0)	10 mM
EDTA	1 mM
TAE	
Tris-HCl (pH 8.0)	40 mM
$C_2H_3NaO_2$	20 mM
EDTA	1 mM
Tail lysis	
Tris-HCl (pH 8.0)	200 mM
EDTA	50 mM
NaCl	100 mM
SDS	1% (w/v)

Table 4. Chemical composition of frequently used buffers.

3.1.3. Single-stranded oligonucleotides

All single-stranded oligonucleotides were purchased lyophilized, in HPLC quality, from metabion international AG, Martinsried, Germany. 100 µM stock solutions were prepared according to the manufacturer´s instructions in ddH_2O. For use in PCR, stocks were diluted 1:10.

3.1.3.1. Genotyping

Name	Sequence	Bands	
Mcpt5-Cre			
Mcpt5-CreUP	5'ACAGTGGTATTCCCGGGGAGTGT3'	WT	224 bp
CreSeq1b-DO	5'GTCAGTGCGTTCAAAGGCCA3'	Cre+	224 bp
Mcpt5-Ex1-DO3	5'GCTTTGGTGCTGGAACCCAGGA3'		554 bp
iDTR			
Mutant	5'CATCAAGGAAACCCTGGACTACTG3'	WT	603 bp
Common	5'AAAGTCGCTCTGAGTTGTTAT3'	Homo	242 bp
WT Rev	5'GGAGCGGGAGAAATGGATATG3'	Hetero	242 bp
			603 bp
R-DTA			
Fwd	5'AAAGTCGCTCTGAGTTGTTAT3'	WT	no
Rev	5'AAGAACGGAGCCGGTTGGCG3'	R-DTA+	592 bp
VEGF			
VEGF Rev	5'TCCGTACGACGCATTTCTAG3'	WT	100 bp
VEGF Fwd	5'CCTGGCCCTCAAGTACACCTT3'	Homo	150 bp
		Hetero	100 bp
			150 bp

Table 5. Primer used for animal genotyping.

3.1.3.2. Real-time PCR

Name	Sequence	Reference
IL-6		
IL-6 Fwd	5'GGTACATCCTCGACGGCATCTC3'	[80]
IL-6 Rev	5'GTTGGGTCAGGGGTGGTTATTG3'	
TGF-β1		
TGF b1 Fwd	5'CAGAAATACAGCAACAATTCCTGG3'	[81]
TGF b1 Rev	5'TTGCAGTGTGTTATCCGTGCTGTC3'	
GAPDH		
GAPDH sense	5'CGGAGTCAACGGATTTGGTCGTAT3'	[82]
GAPDH antisense	5'AGCCTTCTCCATGGTGGTGAAGAC3'	

Table 6. Primer used for quantitative real-time PCR.

3.1.4. Laboratory equipment

Equipment	Description	Company
Balance	Explorer	Ohaus Europe, Nänikon, Schweiz
Heraeus Biofuge	Fresco	DJB Labcare Ltd, Buckinghamshire, UK
BioPhotometer	-	Eppendorf, Hamburg, Germany
CCTV Monitor	RMB 92	Rainbow CCTV, Costa Mesa, CA, USA
CO_2 Incubator	Heracell 150i	Thermo Scientific, Waltham, MA, USA
Electrophoresis Power supply	EPS 200	Pharmacia Biotech, Amersham, UK
FACS Calibur	E1274	BD Biosciences, Heidelberg, Germany
ELISA Reader	NJ-2000	InterMed, Tokyo, Japan
LaminAir Flow	HB 2448	Thermo Scientific, Waltham, MA, USA
Heraeus Megafuge	1.0	DJB Labcare Ltd, Buckinghamshire, UK
Microscope	DM 4000 B	Leica Camera AG, Solms, Germany
Microwave	-	Bosch, Gerlingen, Germany
pH-Meter	CG 710	Schott, Mainz, Germany
Thermal cycler	StepOne Plus	Applied Biosystems, Carlsbad, CA, USA
Thermocycler	T 3000	Biometra, Göttingen, Germany
Thermomixer	Compact	Eppendorf, Hamburg, Germany
UV light	ECX-26.M	Peqlab, Erlangen, Germany
Vortexer	VF2	IKA Labortechnik, Staufen, Germany
Mitutoyo Quick	Mini caliper	Mitutoyo Europe, Neuss, Germany

Table 7. Frequently used laboratory equipment.

3.1.5. Software

Software	Version	Company
Adobe Photoshop	7.0	Adobe Systems Inc., Dublin, Ireland
CellQuest Pro	5.2.1	BD Biosciences, Heidelberg, Germany
Diskus	4.50.1638	Diskus, Königswinter, Germany
EndNote X4	Bld 4845	Thomson Reuters, New York, NY, USA
FCAP^{TM} Array	1.0	BD Biosciences, Heidelberg, Germany
GraphPad Prism	5.01	GraphPad Inc., San Diego, CA, USA
Microsoft Excel	2010	Microsoft, Redmond, WA, USA
Pannoramic Viewer	1.15	3DHistech Kft., Budapest, Hungary
StepOne Software	2.1	Applied Biosystems, Carlsbad, CA, USA

Table 8. Software used for data collection and analysis.

3.2. Methods

3.2.1. Collection of cutaneous biopsies from patients with primary cutaneous lymphoma

Cutaneous biopsies were obtained from 43 patients with PCL for diagnostic purposes and kindly provided by Dr. Max Schlaak, PD Dr. Peter Kurschat and Prof. Dr. Dr. Cornelia Mauch within the framework of the Z2 project of the SFB829 at the University of Cologne. All patients had attended the Hauttumorzentrum of the Department of Dermatology, University Hospital of Cologne between 1995 and 2010 (heads of the Hauttumorzentrum: Prof. Dr. Dr. Cornelia Mauch, PD Dr. Peter Kurschat; physicians: Dr. Max Schlaak, Prof. Dr. Christine Neumann). The diagnosis of PCL and assignment to disease categories and subtypes according to the WHO-EORTC classification were performed by Dr. Max Schlaak and PD Dr. Peter Kurschat and were based on established criteria.[66,68] In addition, assignment to subtypes of PCL was confirmed by a histopathological reference center for PCL (Kempf and Pfaltz, Laboratory for Histological Diagnostics, Zurich, Switzerland). Out of the 43 patients, 35 patients (81.4%) were diagnosed with CTCL and 8 patients (18.6%) with CBCL. Detailed clinical characteristics of all patients are listed in Table 10 in the results section. For control, 12 biopsies from subjects with normal skin were kindly provided by Dr. Lukas Heukamp and Prof. Dr. Reinhard Büttner (Institute of Pathology, University Hospital of Cologne) and 24 biopsies from patients with inflammatory cutaneous diseases, namely 8 patients with psoriasis, 8 patients with atopic dermatitis and 8 patients with pseudolymphoma, obtained for diagnostic purposes were used. All procedures were approved by the Institutional Ethics Committee of the University of Cologne, Cologne, Germany, under written, informed patient consent and adherence to the declaration of Helsinki (AZ 08-144). Patients with CTCL were grouped in cooperation with Dr. Max Schlaak according to the ISCL/EORTC classification.[71,83] Additionally, to also reflect the clinical course of PCL, patients with CTCL were divided in cooperation with Dr. Max Schlaak into those with stable or progressive disease, defining stable disease as maximally two topical treatments (e.g., UV irradiation, topical corticosteroids) and progressive disease as three or more topical and systemic treatments (e.g,. UV irradiation, topical corticosteroids, surgery, systemic therapy such as bexarotene or interferon

alpha). Progression-free survival was defined in cooperation with Dr. Sebastian Theurich and PD Dr. Dr. Michael von Bergwelt-Baildon (Department I of Internal Medicine, University Hospital of Cologne) as time span from initial diagnosis until first change of systemic therapy due to disease progression and recorded over 30 years. For Kaplan-Meier curves, the event criterion was defined as >100 mast cells/mm^2.

3.2.2. Histology

Staining procedures were performed in cooperation with Dr. Lukas Heukamp and Prof. Dr. Reinhard Büttner (Institute of Pathology, University Hospital of Cologne) within the framework of the Z1 project of the SFB832 at the University of Cologne.

3.2.2.1. Human samples

Histological analysis of mast cells in human PCL was initiated by Dr. Max Schlaak and PD Dr. Karin Hartmann. These initial studies suggested an increase of mast cells in PCL. Therefore, sections of paraffin-embedded cutaneous biopsies from 43 patients with PCL and control subjects with normal skin and inflammatory cutaneous diseases were systematically evaluated by immunohistochemistry with antibodies against mast cell tryptase (pretreatment with 0.1% protease, staining with 1:3.000 dilution of antibody Dako 7052, Dako, Hamburg, Germany) and CD117 (*Kit*; pretreatment with citrate buffer pH 6.0, staining with 1:100 dilution of antibody Dako A4502, Dako, Hamburg, Germany). Evaluation of skin sections was performed by counting the number of tryptase- and CD117-positive mast cells under a Leica microscope with Diskus software at 200x magnification in 5 high power fields. Counts were used to calculate the mean number of mast cells per mm^2. A comparison between stainings with antibodies against tryptase and CD117 showed highly consistent results. Results were, therefore, only expressed as tryptase-positive mast cells. For control, sections were also counted by Silke Leja (MTA, Department of Dermatology), as a second independent reviewer.

To grade degranulation of mast cells, skin sections were assessed at 200x magnification and mast cells were semiquantitatively classified into 3 groups of not degranulated, moderately degranulated or extensively degranulated mast

cells.[34] Sections were also stained by hematoxylin/eosin (H&E) following standard protocols in a routine histology laboratory.

For analysis of microvessel density, sections of paraffin-embedded cutaneous biopsies from patients with MF and control patients with inflammatory cutaneous diseases were evaluated by immunohistochemistry with antibodies against CD31 (pretreatment with citrate buffer pH 6.0, staining with 1:500 dilution of antibody Dako M0823, Dako, Hamburg, Germany) and CD34 (pretreatment with citrate buffer pH 6.0, staining with 1:2000 dilution of antibody Cell Marque 134M-1, Cell Marque, Sierra College Blvd., Rocklin, CA, USA). Evaluation of skin sections was performed by recording the distribution of CD31- and CD34-positive microvessels with a minimal lumen size of 50 μm^2 and by counting their number under a Leica microscope with Diskus software at 100x magnification in 5 high power fields. Counts were used to calculate the mean number of microvessels per mm^2. A comparison between stainings with antibodies against CD31 and CD34 showed highly consistent results. Results were, therefore, only expressed as CD31-positive microvessels.

3.2.2.2. Murine samples

In order to detect mast cells in the different mouse models (as described below), punch biopsies of back skin were fixed in 4% formalin (Roti®-Histofix) over night and embedded in paraffin. Sections were stained by Giemsa stain and toluidine blue following standard protocols in a routine histology laboratory.

For evaluation of microvessel density in the different mouse models (as described below), punch biopsies of back skin were embedded in paraffin and CD31 staining (pretreatment with citrate buffer pH 6.0, staining with 1:50 dilution of antibody Histonova DIA-310, Dianova, Hamburg, Germany) was performed.

3.2.3. *In vitro* experiments

3.2.3.1. Cell isolation

To obtain primary Sézary cells, CD4+ T-cells from a patient with Sézary syndrome were isolated from freshly collected blood, kindly provided by Dr. Max Schlaak, using the Macs Whole Blood Column Kit for CD4+ T-cells (Miltenyi Biotech, Bergisch Gladbach, Germany) and generated by culturing as described in section 3.2.3.2. Additionally, CD4+ T-cells from the blood of healthy donors, kindly provided by PD Dr. Karin Hartmann, were isolated as controls.

Primary murine bone marrow-derived mast cells (BMMC) were isolated under sterile conditions from the femoral lavage of WT C57BL/6 mice.[30]

3.2.3.2. Cell culture

All cell cultures were maintained at 37°C in 5% CO_2 in a humidified atmosphere.

The human CTCL cell line Mac2B, originally derived from a patient with CD30+ALCL[84], was kindly provided by Dr. Marshall Kadin (Department of Dermatology and Skin Surgery, Boston University School of Medicine, Roger Williams Medical Center, Providence, USA) and maintained in RPMI 1640 medium containing 20% FBS, 2 mM L-glutamine, 100 U/ml penicillin and 100 µg/ml streptomycin.

Human CTCL cell lines MyLa, derived from a patient with MF[85], and SeAx, derived from a patient with SS[86], as well as the human B-cell lymphoma cell line BJAB, derived from African Burkitt-like lymphoma[87], were kindly provided by Dr. Maria Karpova (Department of Dermatology, University Hospital Zurich, Zurich, Switzerland). All three cell lines were cultured in RPMI 1640 medium containing 10% FBS, 2 mM L-glutamine, 1 mM sodium pyruvate, 100 U/ml penicillin and 100 µg/ml streptomycin.

The cell line Jurkat (originally called JM), a pseudodiploid human cell line that originated from a patient with acute T-cell leukemia[88], was cultured in RPMI 1640 medium containing 10% FBS, 4 mM L-glutamine, 100 U/ml penicillin and 100 µg/ml streptomycin.

Primary Sézary cells were cultured as described[89] and kept in RPMI 1640 medium containing 20% FBS, 2 mM L-glutamine, 100 U/ml penicillin and 100 µg/ml streptomycin. Isolated CD4+ T-cells were maintained in RPMI 1640

medium containing 10% FBS, 2 mM L-glutamine, 1 mM sodium pyruvate, 100 U/ml penicillin and 100 µg/ml streptomycin.

The human mast cell line HMC1, originally derived from a patient with mast cell leukemia, was kindly provided by Dr. Joseph H. Butterfield (Mayo Clinic, Rochester, USA) and cultured in IMDM medium containing 10% FBS, 2 mM L-glutamine, 50 µM β-mercaptoethanol, 100 U/ml penicillin and 100 µg/ml streptomycin.[90] For our experiments, we used the subclone HMC1.2, which carries 2 *Kit* mutations, V560G and D816V.

For mouse xenograft experiments, we used the mouse T-cell lymphoma cell line EL4, which was kindly provided by A. Gisselsson (Genovis, Malmö, Sweden) maintained in DMEM medium containing 10% FBS, 2 mM L-glutamine, 1 mM sodium pyruvate, 50 µM β-mercaptoethanol, 100 U/ml penicillin and 100 µg/ml streptomycin.

Primary murine bone marrow-derived mast cells (BMMC) were isolated from the femoral lavage of WT C57BL/6 mice[30] and generated by culturing in IMDM medium supplemented with 10 ng/ml recombinant murine IL-3 (PeproTech, Hamburg, Germany), 10% FBS, 100 U/ml penicillin and 100 µg/ml streptomycin.[90]

Primary cells and cell lines described above grew in suspension, whereas the mouse cell lines Pan02 and LLC, which were also used in mouse xenograft experiments, represented adherent cells and were, therefore, cultured on plates and detached by treatment with a PBS/Trypsin/EDTA mixture.

The mouse pancreas adenocarcinoma cell line Pan02, also known as Panc02[91], was a kind gift from Dr. David Linehan´s Lab (Washington University School of Medicine, Department of Surgery, St. Louis, MO, USA). Cells were cultured in RPMI 1640 medium containing 20% FBS, 2 mM L-glutamine, 100 U/ml penicillin and 100 µg/ml streptomycin.

Lewis lung carcinoma (LLC) cells, kindly provided by Dr. Axel Roers (Institute for Immunology, Medical Faculty Carl Gustav Carus, Technische Universität Dresden, Dresden, Germany), derived from spontaneously developing carcinoma of the lung of a C57BL/6 mouse, were maintained in DMEM medium containing 10% FBS, 2 mM L-glutamine, 1 mM sodium pyruvate, non-essential amino acid solution (NEA, 1x), 100 U/ml penicillin and 100 µg/ml streptomycin.

3.2.3.3. Inhibition and stimulation of mediator release from mast cells

To either inhibit or stimulate release of mediators from mast cells, $1x10^6$ HMC1 cells/ml were incubated with 1 ml cromolyn sodium salt (0.025 M) dissolved in HBSS or with 1 ml calcium ionophore A23187 (250 nM) dissolved in DMSO, respectively, for 30 minutes at 37°C. As control, cells were incubated with standard medium. Then, cells were washed and kept in standard medium for 6 hours. After centrifugation, cell culture supernatant was frozen at -20°C and stored for future use in proliferation experiments and cytometric bead array (CBA) measurements, as described below.

3.2.3.4. Cytometric bead array in cell culture supernatants

For measurement of cytokine and chemokine levels in HMC1 supernatant, cells were either blocked or stimulated as described above and secretion of IL-2, IL-4, IL-6, IL-10, IL-17A, TNF and IFN-γ using Human Th1/Th2/Th17 Cytokine Kit (BD Biosciences, Heidelberg, Germany), CXCL8, CCL5, CXCL9, CCL2 and CXCL10 using Human Chemokine Kit (BD Biosciences, Heidelberg, Germany) VEGF and basic FGF using Human Flex Sets (BD Biosciences, Heidelberg, Germany) together with Human Soluble Protein Master Buffer Kit (BD Biosciences, Heidelberg, Germany) as well as TGF-β1 using Human TGF-β1 Single Plex Flex Set (BD Biosciences, Heidelberg, Germany) was measured by cytometric bead array (CBA) according to the manufacturer's guidelines.

For measurement of baseline cytokine levels in mouse BMMCs and EL4 cells, human CTCL cells, cell lines and control cells, $2x10^6$ cells/ml of 4 week-old cells were cultured for 1 week under standard conditions described above and secretion of IL-2, IL-4, IL-6, IL-10, IL-17A, TNF and IFN-γ was measured in supernatants by cytometric bead array (CBA) according to the manufacturer's guidelines (Human/Mouse Th1/Th2/Th17 Cytokine Kit, BD Biosciences, Heidelberg, Germany).

For measurements of changes in cytokine and chemokine production in mouse EL4 cells and human CTCL cell lines Mac2B and SeAx, $6x10^5$ cells/ml freshly thawed cells were incubated with or without mast cell supernatant. Human cell lines were stimulated for 48 hours with HMC1 supernatant and the mouse cell line with supernatant of BMMCs. Thereafter, cells were washed, counted and $5x10^5$ cells/ml were cultured again for 48 hours in standard medium. Cell culture

supernatants were collected and frozen at -20°C for CBA measurements. In 4 separate experiments, each sample was measured 6 times.
After acquisition of sample data using FACS (FACS Calibur, BD Biosciences, Heidelberg, Germany), cytokine and chemokine concentrations were calculated using FCAP™ analysis software (BD Biosciences, Heidelberg, Germany).

3.2.3.5. Quantitative real-time PCR

3.2.3.5.1. RNA isolation and reverse transcription into cDNA

Mac2B and SeAx cells ($6x10^5$ cells/ml) were incubated with or without HMC1 supernatant for 24 hours. After washing, $6x10^5$ cells/ml were cultured again for 6 hours in standard medium.
Total RNA was extracted from harvested cells with RNeasy Mini Kit (Qiagen, Hilden, Germany) completed with QIAshredder (Qiagen, Hilden, Germany) and on-column DNase digestion (RNase-Free DNase Set, Qiagen, Hilden, Germany), according to the manufacturer´s instructions. RNA was then reversely transcribed into cDNA using the QuantiTect Reverse Transcription Kit (Qiagen, Hilden, Germany), according to the manufacturer´s instructions.

3.2.3.5.2. RNA and cDNA quantification

RNA and cDNA concentrations were determined by measuring the absorption at 260 nm on the BioPhotometer. At this wavelength absorption of 1 corresponds to 40 μg/ml RNA and 50 μg/ml cDNA, respectively.

3.2.3.5.3. Real-time PCR

To quantify the amounts of IL-6 and TGF-β1 mRNA expression, real-time PCR was performed using Power SYBR Green PCR Master Mix (Applied Biosystems, Carlsbad, CA, USA), according to the manufacturer´s instructions. The used primer sequences are listed in section 3.1.3.2. Real-time PCR was then performed on a StepOne Plus cycler (Applied Biosystems, Carlsbad, CA, USA) using the following cycling profile: 95°C for 10 min, 40 cycles of 95°C for 15 sec and 60°C for 1 min, followed by a melting curve analysis to prove the specificity of the PCR product by 95°C for 15 sec, 60°C for 1 min and 95°C for 15 sec. Relative quantification of gene expression was determined by

normalization against GAPDH expression using the $2^{-\Delta\Delta CT}$ method.[92] In 4 separate experiments, each sample was measured 3 times.

3.2.3.6. Cell proliferation measurement

Primary T-cells, primary Sézary cells, the CTCL cell lines Mac2B, MyLa and SeAx, Jurkat cells, the BJAB cell line and EL4 cells were cultured with and without mast cell supernatant for 80 hours. Human cell lines were cultured with HMC1 supernatant and mouse EL4 cells with BMMC supernatant. As positive control, cells were also cultured with a cytokine cocktail containing IL-1α, IL-1β, IL-2, IL-4 and IL-7 (Peprotech, Hamburg, Germany), described to stimulate cell growth. Additionally, SeAx and Mac2B cell lines were cultured with mast cell supernatant derived from HMC1 cells blocked by cromolyn as described above. After 48 hours, fresh mast cell supernatant, media or cytokine cocktail was added. Cell proliferation was measured at 4 hour intervals using the Cell Titer 96® AQ_{ueous} One Solution Assay (Promega, Mannheim, Germany). Briefly, 100 µl cells and 20 µl MTS (3-(4,5-dimethyl-2-yl)-5-(3-carboxymethoxyphenyl)-2-(4-sulfophenyl)-2H-tetrazolium) were added per well in a 96-well plate and incubated for 1 h at 37°C and 5% CO_2. Absorbance of formazan, which is converted from living cells by MTS, was measured at 490 nm in an ELISA reader.

3.2.4. *In vivo* experiments

Mice were kept and bred under standard conditions in a pathogen-free barrier facility. All procedures were performed in accordance with institutional guidelines on animal welfare and were approved by the "Landesamt fuer Natur, Umwelt und Verbraucherschutz" of North Rhine-Westphalia (AZ K23, 24/06).

3.2.4.1. Mouse strains

For investigating mast cell biology *in vivo*, different mouse models were used. We used *Mcpt5-Cre/iDTR*[33,34], a mouse model of inducible mast cell deficiency, generated by breeding the mast cell-specific transgenic line *Mcpt5-Cre* to the *iDTR* line[35]. *Mcpt5-Cre+/iDTR+* mice show efficient and specific depletion of cutaneous and peritoneal mast cells upon intraperitoneal injections with diphtheria toxin. Furthermore, we used a mouse model of constitutive mast cell deficiency, breeding the mast cell-specific transgenic line *Mcpt5-Cre* to the *R-DTA* line[36]. To generate mice lacking mast cell-derived VEGF, a VEGF *floxed* mouse strain[93], with *loxP* sites flanking the third exon of the VEGF gene (kindly provided by Napoleone Ferrara, Genentech Inc., South San Francisco, CA, USA) was also bred to *Mcpt5-Cre*. For comparison, we also used the mast cell-deficient C57BL/6 *Kit*$^{W\text{-}sh/W\text{-}sh}$ line[30], which shows several other defects in addition, due to a genetic conversion in the *Kit* gene promotor, as well as WT C57BL/6 animals. Mouse models are also described in detail in the introduction. All mice were generated on the C57BL/6 background.

3.2.4.2. Genotyping

3.2.4.2.1. DNA isolation

Tail biopsies (approx. 5 mm) obtained from 3 week-old mice were incubated in 500 µl tail lysis buffer (see section 3.1.2.) and 5 µl proteinase K (Fermentas, St. Leon-Rot, Germany) in a thermomixer at 800 rpm and 55°C over night. After centrifuging, DNA was isolated from the supernatant by adding 700 µl ice-cold isopropanol. Precipitated DNA was pelleted by centrifuging and discarding the supernatant. DNA was washed with 500 µl 70% ethanol in an additional centrifugation step. Afterwards, the DNA pellet was dried at room temperature for 15 min and at 55°C in a thermomixer at 300 rpm for another 15 min.

Then DNA was dissolved in 50 µl TE buffer (see section 3.1.2.) at 800 rpm and 55°C in a thermomixer over night. DNA was stored at 4°C.

3.2.4.2.2. Polymerase chain reaction (PCR)

For PCR, 3 µl of template DNA were added to 22 µl reaction master mix containing 1x Dream Taq buffer (10x, Fermentas, St. Leon-Rot, Germany), 200 nM of each primer (10 µM), 200 µM dNTP mix (10 mM, Fermentas, St. Leon-Rot, Germany) and 0.05 U/µl Dream Taq Polymerase (5 U/ µl, Fermentas, St. Leon-Rot, Germany). Primers used for genotyping are listed in section 3.1.3.1. and cycling profiles are summarized in Table 9.

Step	**Temperature (°C)**				**Time**				**Cycle number**			
	1	**2**	**3**	**4**	**1**	**2**	**3**	**4**	**1**	**2**	**3**	**4**
1	95	94	94	95	5 min	3 min	3 min	10 min				
2	95	94	94	95	45 sec	30 sec	30 sec	15 sec	29	35	38	29
3	57	61	56	55	1 min	1 min	30 sec	1 min				
4	72	72	72	72	45 sec	1 min	1 min	2 min				
5	72	72	72	72	7 min	2 min	10 min	5 min				
6	10	10	4	10	-	-	-	-				

Table 9. Summary of PCR cycling profiles for genotyping.1:*Mcpt5-Cre*; 2:*iDTR*; 3:*R-DTA*; 4:*VEGF*

Denaturation (step 1) was followed by the appropriate number of cyles of steps 2-4. In step 3, up to 1 min at primer-suitable annealing temperature, and in step 4, 1 min per kb DNA to be amplified at synthesis temperature (72°C), was used. Amplification was completed in a final step at 72°C (step 5).

3.2.4.2.3. Gel electrophoresis

PCR products were mixed with 5 µl loading dye (6x, Fermentas, St. Leon-Rot, Germany) and directly loaded onto a 2% (w/v) agarose gel (1x TAE, 8 µl SYBR Safe DNA gel stain, Molecular Probes/Invitrogen, Karlsruhe, Germany). Gel electrophoresis was performed at 100 V for 30 min and bands were visualized under UV light.

3.2.4.3. Administration of diphtheria toxin

Lyophilized diphtheria toxin (DT) (Sigma-Aldrich, Taufkirchen, Germany) was reconstituted in ddH_2O to a stock solution of 1 mg/ml and aliquots were stored at -20°C. For each DT injection, aliquots were thawed on ice and diluted to a working concentration of 5 ng/µl in sterile PBS. Starting at the age of 6 weeks, *Mcpt5-Cre+/iDTR+* and *Mcpt5-Cre-/iDTR+* controls received 4 injections of 25 ng DT/g bodyweight intraperitoneally at weekly intervals to deplete mast cells. For the first injection, 5 µg/g bodyweight of pyrilamine maleate salt (Sigma-Aldrich, Taufkirchen, Germany), a H_1 histamine receptor antagonist (antihistamine), was added to prevent possible anaphylaxis reactions.

3.2.4.4. Subcutaneous injection of tumor cell lines and measuring tumor growth

For mouse xenograft experiments, 3 different cell lines, namely EL4, Pan02 and LLC were used. For subcutaneous injections, cells were harvested and washed in HBSS (Sigma-Aldrich, Taufkirchen, Germany). LLC cells were additionally treated with accutase solution (Sigma-Aldrich, Taufkirchen, Germany) to prevent cells from clustering and washed again in HBSS. 10 week-old *Mcpt5-Cre+/iDTR+*, *Mcpt5-Cre-/iDTR+* (both after DT treatment), *Mcpt5-Cre+/R-DTA+*, *Mcpt5-Cre-/R-DTA+*, *Mcpt5-Cre/VEGF*$^{fl/fl}$, C57BL/6 *Kit*$^{W\text{-}sh/W\text{-}sh}$ and WT C57BL/6 animals received 100 µl of $1x10^7$ of either EL4, Pan02 or LLC cells/ml HBSS ($1x10^6$ cells/mouse) subcutaneously into the shaved flanks. Subsequently, tumor size was assessed 5 times weekly by direct measurement of the tumor region in three perpendicular directions using a Mitutoyo Quick Mini caliper (Mitutoyo Europe GmbH, Neuss, Germany). Measurements were recorded as tumor area (mm^2) and tumor volume (mm^3) from groups of 2-3 mice each with two tumors per mouse. Tumor area (A) was calculated by the formula: [A= tumor height x tumor width], and tumor volume (Vol) by the formula: [Vol= tumor height x tumor width x tumor depth]. During tumor experiments, *Mcpt5-Cre+/iDTR+* mice and *Mcpt5-Cre-/iDTR+* controls continuously received DT injections (80 µl) subcutaneously around the tumors once weekly to sufficiently deplete mast cells. Experiments were terminated after tumors started to burst and cutaneous punch biopsies were taken from tumor regions and processed as described in section 3.2.2.2.

3.2.4.5. Two-step model of chemically induced skin carcinogenesis

Backs of 10 week-old *Mcpt5-Cre+/iDTR+*, *Mcpt5-Cre-/iDTR+* (both after DT treatment), C57BL/6 *Kit*$^{W\text{-}sh/W\text{-}sh}$ and WT C57BL/6 animals were shaved and treated 3 days later with a single application of the tumor initiator DMBA (7,12-Dimethylbenz[a]anthracene, Sigma-Aldrich, Taufkirchen, Germany). DMBA represents a powerful carcinogen inducing multiple necessary mutations that promote tumor development. Animals were treated with 50 µg DMBA dissolved in 200 µl acetone. During the following weeks, the tumor-promoting reagent TPA (12-O-tetradecanoylphorbol 13-acetate, phorbol 12-myristate 13-acetate, PMA, Sigma-Aldrich, Taufkirchen, Germany) was applied twice weekly (6 µg dissolved in 200 µl acetone per mouse) for a period of up to 20 weeks. Figure 5 and Figure 6 show the treatment regimens for C57BL/6 *Kit*$^{W\text{-}sh/W\text{-}sh}$ and WT C57BL/6 animals and for *Mcpt5-Cre+/iDTR+* and *Mcpt5-Cre-/iDTR+* animals, respectively. As controls, backs of mice were shaved and received topical applications of acetone (200 µl/mouse) instead of DMBA or TPA. The number of papillomas was recorded once weekly. Back skin biopsies were taken from 1 animal of each group every 3 weeks, processed as described in section 3.2.2.2., mast cells were counted under the microscope at 200x magnification in 5 high power fields and the mean value per mm^2 was calculated.

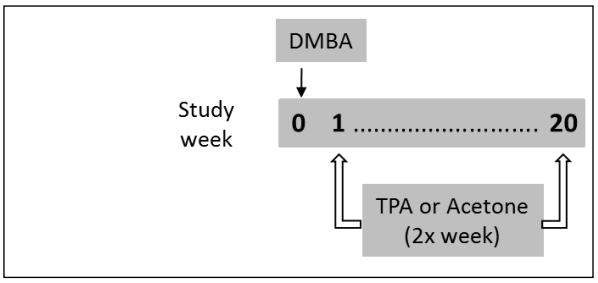

Figure 5. Treatment regimen for C57BL/6 *Kit*$^{W\text{-}sh/W\text{-}sh}$ and WT C57BL/6 animals. Animals were treated once with DMBA and received TPA or acetone applications twice weekly for a period of 20 weeks.

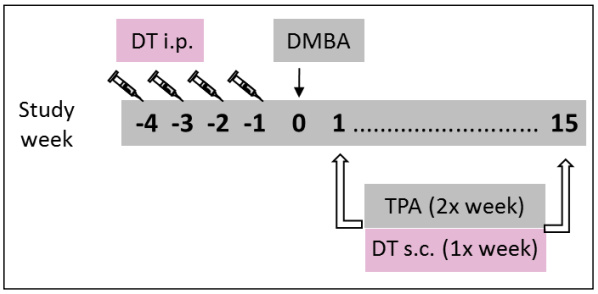

Figure 6. Treatment regimen for *Mcpt5-Cre+/iDTR+* and *Mcpt5-Cre-/iDTR+* animals. For mast cell depletion animals received DT i.p. injections once a week for 4 weeks and were then treated with DMBA. After that, they received TPA or acetone applications twice weekly for a period of 15 weeks. In addition, animals received subcutaneous DT injections once a week.

3.2.5. Statistical analysis

Statistical analyses were performed with GraphPad Prism (Version 5.01) software (GraphPad Software Inc., San Diego, CA, USA) using two-tailed Student's *t* test. Clinical data were analyzed as Kaplan-Meier curves employing Log-rank test. Correlation analyses were performed using Spearman correlation. A *P* value of less than 0.05 was considered statistically significant.

4. Results

While working on this dissertation, parts of this research were originally published in *Blood*. Rabenhorst A, Schlaak M, Heukamp LC, Förster A, Theurich S, von Bergwelt-Baildon M, Büttner R, Kurschat P, Mauch C, Roers A, Hartmann K. Mast cells play a protumorigenic role in primary cutaneous lymphoma. *Blood*. 2012;120(10):2042-2054. © the American Society of Hematology. In particular, data reported below on PCL and EL4 (sections 4.1.1.-4.1.6., partly 4.1.8., 4.1.9., 4.2.1., partly 4.2.3.) were published there.[94]

4.1. Mast cells in the microenvironment of human PCL

4.1.1. Clinical characteristics of PCL patients participating in the study

In order to explore the role of mast cells in the tumor microenvironment of primary cutaneous lymphoma (PCL), we initially investigated the number and distribution of mast cells in different categories of human PCL.

Skin sections from 43 PCL patients (Table 10) were used for counting mast cells microscopically. The group consisted of 29 male (67.4%) and 14 female (32.6%) patients. The age ranged from 23 to 81 years, with a mean age of 56.7 years. As mentioned in the material and methods section, patients were grouped on the basis of the clinical course of the disease. 32 patients (74.4%) exhibited stable disease and 11 patients (25.6%) belonged to the progressive group. Furthermore, out of the 43 patients, 35 patients (81.4%) were diagnosed with CTCL and 8 patients (18.6%) with CBCL. Within the CTCL group, 23 patients had mycosis fungoides (MF), 3 patients folliculotropic mycosis fungoides (FMF), 4 patients CD30-positive primary cutaneous anaplastic large cell lymphoma (CD30+ALCL), 1 patient lymphomatoid papulosis (LP), 1 patient primary cutaneous small/medium-sized pleomorphic T-cell lymphoma (PLEO) and 3 patients Sézary syndrome (SS). Within the CBCL group, 3 patients were diagnosed with primary cutaneous marginal zone B-cell lymphoma (MZL), 3 patients with primary cutaneous follicle center lymphoma (CFBCL) and 2 patients with primary cutaneous diffuse large B-cell lymphoma (BCL).

In addition, CTCL patients suffering from MF, FMF and SS were clustered according to ISCL/EORTC classification[71,83] into 13 patients with stage IA (44.8%), 8 patients with stage IB (27.6%), 1 patient with stage IIA (3.4%), 4 patients with stage IIB (13.8%), 2 patients with stage IIIB (6.9%) and 1 patient

with stage IVA (3.4%). Moreover, patients with MF, FMF and SS were also assigned to clinical stages, namely eczema (13 patients, 44.8%), plaque (10 patients, 34.5%), tumor (3 patients, 10.3%) and SS (3 patients, 10.3%).

For control, 12 subjects with normal skin and 24 patients with inflammatory cutaneous diseases such as psoriasis (n=8), atopic dermatitis (n=8) and pseudolymphoma (n=8) were used.

Parameters	Number of patients
All	43 (100%)
Gender	
Male	29 (67.4%)
Female	14 (32.6%)
Age at time of skin biopsy	
Mean	56.7 years
Range	23 – 81 years
≤ 50 years	12 (27.9%)
> 50 years	31 (72.1%)
Clinical course	
Stable	32 (74.4%)
Progressive	11 (25.6%)
Category	
CTCL	35 (81.4%)
CBCL	8 (18.6%)
CTCL subtypes	
MF	23 (53.5%)
FMF	3 (7.0%)
CD30+ALCL	4 (9.3%)
LP	1 (2.3%)
PLEO	1 (2.3%)
SS	3 (7.0%)
ISCL/EORTC stages of MF, FMF, SS	
IA (T1)	13 (44.8%)
IB (T2)	8 (27.6%)
IIA (T1,2)	1 (3.4%)
IIB (T3)	4 (13.8%)
IIIB (T4)	2 (6.9%)
IVA (T1-4)	1 (3.4%)
Clinical stages of MF, FMF, SS	
Eczema	13 (44.8%)
Plaque	10 (34.5%)
Tumor	3 (10.3%)
SS	3 (10.3%)
CBCL subtypes	
MZL	3 (7.0%)
CFBCL	3 (7.0%)
BCL	2 (4.7%)

Table 10. Clinical characteristics of PCL patients participating in the study.

4.1.2. Mast cell numbers are increased in primary cutaneous lymphoma

Cutaneous biopsies of patients with PCL and controls were stained with antibodies against mast cell tryptase and CD117 (*Kit*). Evaluation of skin sections was performed by counting the number of tryptase- and CD117-positive mast cells under a Leica microscope with Discus software at 200x magnification in 5 high power fields. Counts were used to calculate the mean number of mast cells per mm^2. A comparison between the two different antibodies against mast cell tryptase and CD117 showed highly consistent results. Therefore, results were only expressed as tryptase-positive mast cells per mm^2. As shown in Figure 7A and Figure 8, mast cells were significantly increased in patients with PCL compared to normal skin and inflammatory cutaneous diseases, with a similar increase in CTCL and CBCL. The mean number of mast cells in PCL mounted to an increase of more than 3-fold compared to normal skin and about 2-fold compared to inflammatory cutaneous diseases (144.4 ± 11.5 mast cells/mm^2 in PCL (All), 38.8 ± 3.5 mast cells/mm^2 in normal skin (Ctrl), 78.0 ± 3.6 mast cells/mm^2 in inflammatory cutaneous diseases (All), mean ± SEM). Interestingly, in nearly all CTCL and CBCL sections, infiltration of mast cells was particularly prominent at the periphery of the infiltrate (Figure 7B). Often, mast cells were found to even align along the rim of the infiltrate (Figure 8C). In contrast, the number of mast cells in the center of CTCL and CBCL was comparable with normal skin (Figure 7B). When we compared different subtypes of CTCL and CBCL, even though for some rare subtypes only few samples were available, the CTCL subtypes folliculotropic MF (FMF) and Sézary syndrome (SS) appeared to exhibit the most pronounced mast cell infiltration (Figure 7C). Clinically, both of these subtypes are characterized by a highly progressive course.

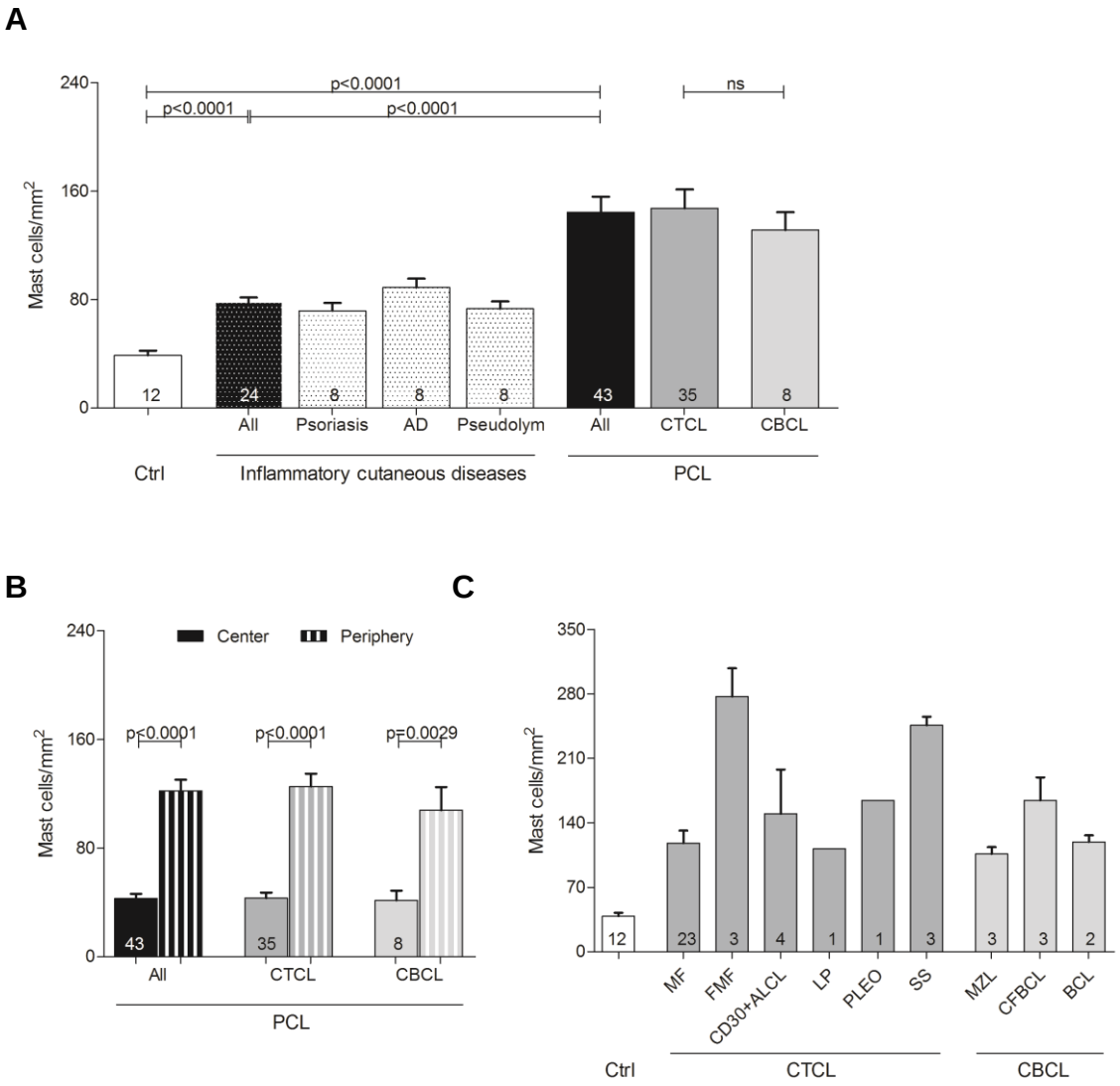

Figure 7. Mast cell numbers are increased in PCL. (A) Skin biopsies from patients with PCL (All; n=43) subdivided into patients with CTCL (n=35) and CBCL (n=8), from subjects with normal skin (Ctrl; n=12) and from patients with inflammatory cutaneous diseases (All; n=24) such as psoriasis (n=8), atopic dermatitis (AD; n=8) and pseudolymphoma (Pseudolym; n=8) were stained by immunohistochemistry with anti-tryptase antibody. The number of tryptase-positive mast cells was analyzed by microscopic counting of 5 high power fields at 200x magnification and calculating the mean number of mast cells per mm^2. Data represent the mean ± SEM. Statistical significance was assessed by two-tailed Student´s *t*-test. **(B)** The number of tryptase-positive mast cells was counted separately in the center (filled columns) and in the periphery (striped columns) of PCLs. Data represent the mean ± SEM. Statistical significance was assessed by two-tailed Student´s *t*-test. **(C)** The number of tryptase-positive mast cells was analyzed in different PCL subtypes subdivided into CTCL patients with MF (n=23), FMF (n=3), CD30+ALCL (n=4), LP (n=1), PLEO (n=1), SS (n=3) and CBCL patients with MZL (n=3), CFBCL (n=3) and BCL (n=2) and from subjects with normal skin (Ctrl; n=12). Data represent the mean ± SEM.

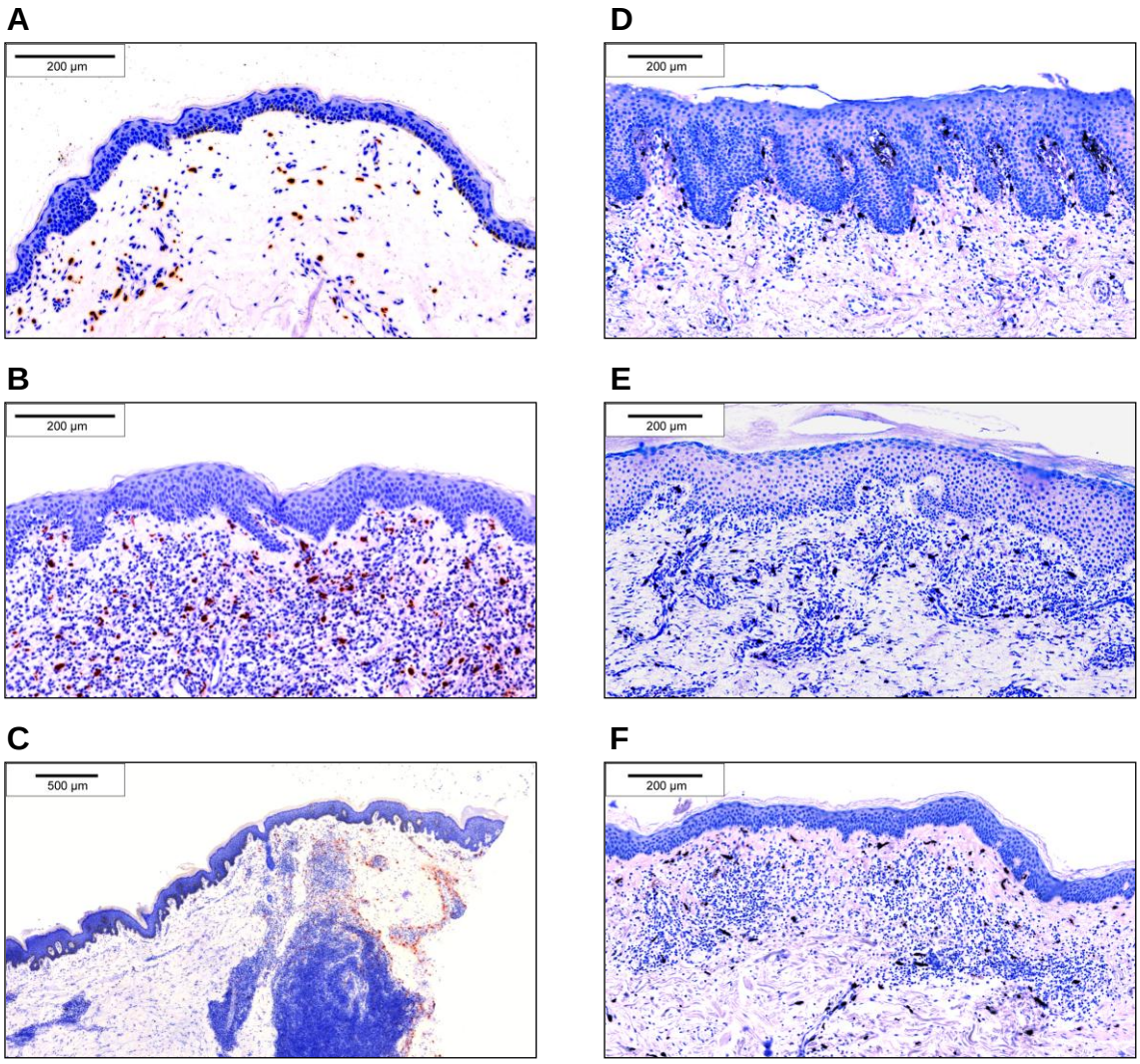

Figure 8. Histological analyses showed that mast cell numbers are increased in PCL. (A) Normal skin, magnification 200x. **(B)** CTCL, plaque stage, magnification 200x. **(C)** CTCL, tumor stage, magnification 50x. **(D)** Psoriasis, magnification 150x. **(E)** Atopic dermatitis, magnification 150x. **(F)** Pseudolymphoma, magnification 150x, staining of mast cells with anti-tryptase antibody (brown).

4.1.3. Mast cell numbers correlate with progression of primary cutaneous lymphoma

To investigate whether progression of CTCL correlates with the number of mast cells, patients with MF, FMF and SS were grouped according to the ISCL/EORTC classification and, additionally, by means of the clinical course into patients with stable or progressive disease (Figure 9A, Table 10). Patients exhibiting more advanced stages of the disease (IIB-IVA; 278.5 ± 21.7 mast cells/mm^2 in stage IIB; 254.8 ± 4.7 mast cells/mm^2 in stage IIIB; 227.8 mast cells/mm^2 in stage IVA; mean ± SEM) showed significantly increased numbers of mast cells compared to patients with stages IA (100.9 ± 7.7 mast cells/mm^2; mean ± SEM) to IB (100.2 ± 13.6 mast cells/mm^2; mean ± SEM). Similarly, patients with progressive disease showed increased mast cell numbers compared to stable patients (271.2 ± 13.7 mast cells/mm^2 in progressive, 100.7 ± 6.8 mast cells/mm^2 in stable patients, mean ± SEM). We also determined progression-free survival and found, as anticipated, that patients with advanced disease stages as well as progressive disease showed a significantly decreased progression-free survival compared to stable patients (Figure 9B). In accordance, patients with the progressive CTCL subtypes FMF and SS showed significantly increased numbers of mast cells compared to MF patients (Figure 9A) and a decreased progression-free survival (Figure 9B). Similarly, dividing CTCL patients into clinically relevant groups exhibiting eczema (mild), plaque (moderate) or tumor (moderate/severe) stages or Sézary syndrome (SS, severe), a significant increase in mast cell numbers was observed correlating with the malignancy of CTCL (Figure 9A). CTCL malignancy was also associated with decreased progression-free survival (Figure 9B). Furthermore, when CTCL patients with MF, FMF and SS were subdivided according to the ISCL/EORTC classification, into groups with stable or progressive disease and into groups with <100 mast cells/mm^2 or >100 mast cells/mm^2, the patients with more advanced stages of the disease (IIB-IVA), with progressive disease and with >100 mast cells/mm^2 showed a significantly shorter progression-free survival (Figure 9C). Together, these results show that mast cell numbers correlate with progression of CTCL.

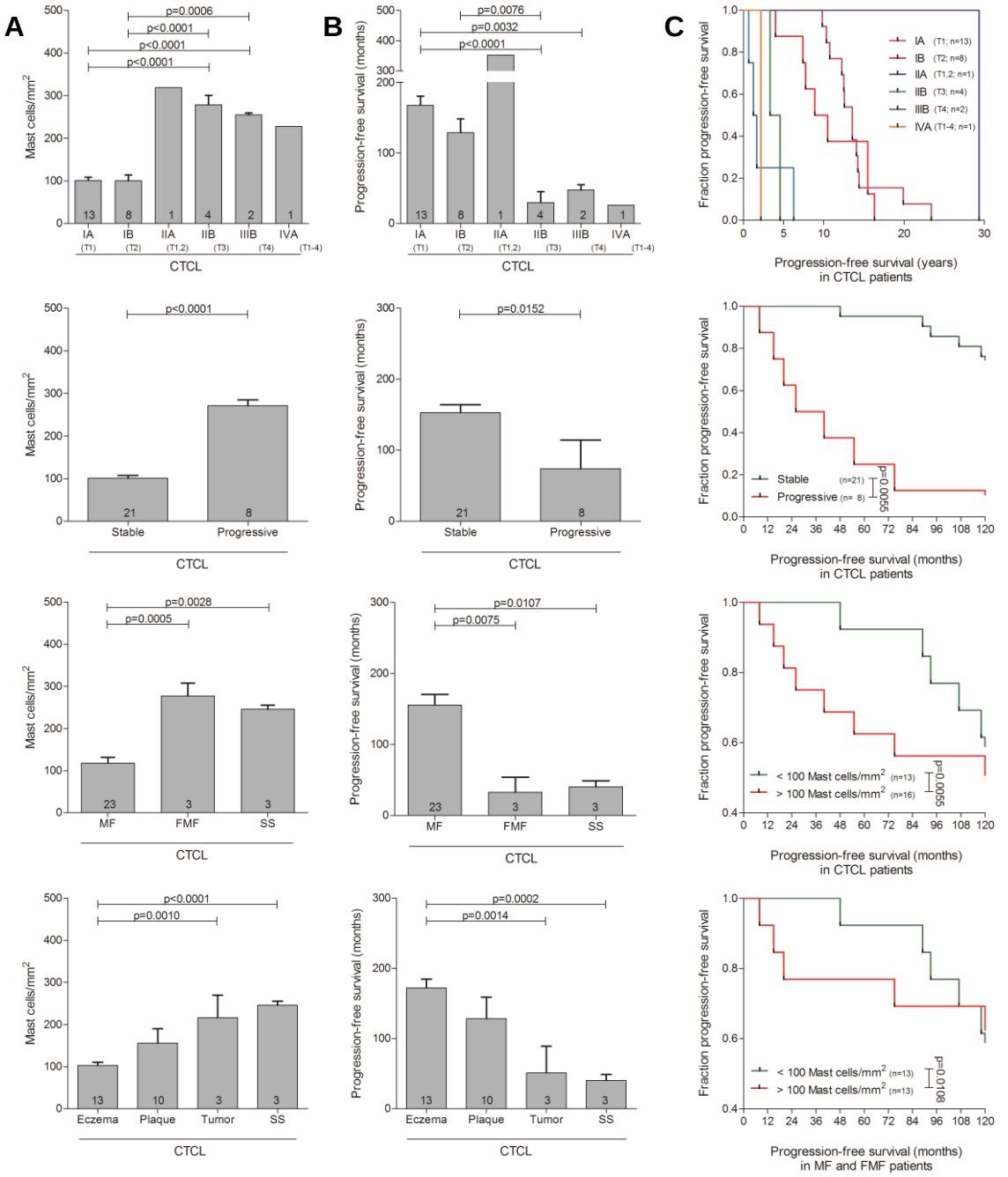

Figure 9. Mast cell numbers correlate with progression of PCL. (A) The number of tryptase-positive mast cells was analyzed by microscopic counting of 5 high power fields at 200x magnification in skin biopsies from CTCL patients with MF, FMF and SS grouped according to ISCL/EORTC classification (IA, n=13; IB, n=8; IIA, n=1; IIB, n=4; IIIB, n=2; IVA, n=1), into patients with stable (n=21) and progressive (n=8) disease, into patients with MF (n=23), FMF (n=3) and SS (n=3) and into patients with different clinical stages (Eczema, n=13; Plaque, n=10; Tumor, n=3; SS, n=3). Data represent the mean ± SEM. Statistical significance was assessed by two-tailed Student´s *t*-test. **(B)** Progression-free survival, defined as duration (years, months) from initial diagnosis until first change of treatment due to disease progression, was determined for each group of patients. Data represent the mean ± SEM. Statistical significance was assessed by two-tailed Student´s *t*-test. **(C)** Kaplan-Meier curves were generated for CTCL patients with MF, FMF and SS grouped according to the ISCL/EORTC classification, into stable and progressive disease, and into <100 mast cells/mm^2 and >100 mast cells/mm^2. Additionally, patients with MF and FMF were grouped into those with <100 mast cells/mm^2 and >100 mast cells/mm^2 (lower right panel). Statistical significance was assessed by Log-rank test.

4.1.4. Mast cell degranulation is increased in primary cutaneous lymphoma

Evaluating mast cell numbers in the different skin sections, we noted at higher magnifications that most mast cells in PCL sections were degranulated, whereas mast cells in normal skin were usually not degranulated. We therefore classified mast cells into 3 groups of not degranulated (Figure 10A), moderately degranulated (Figure 10B) or extensively degranulated (Figure 10C) mast cells[34] and determined the percentage of each group in all patients and controls.

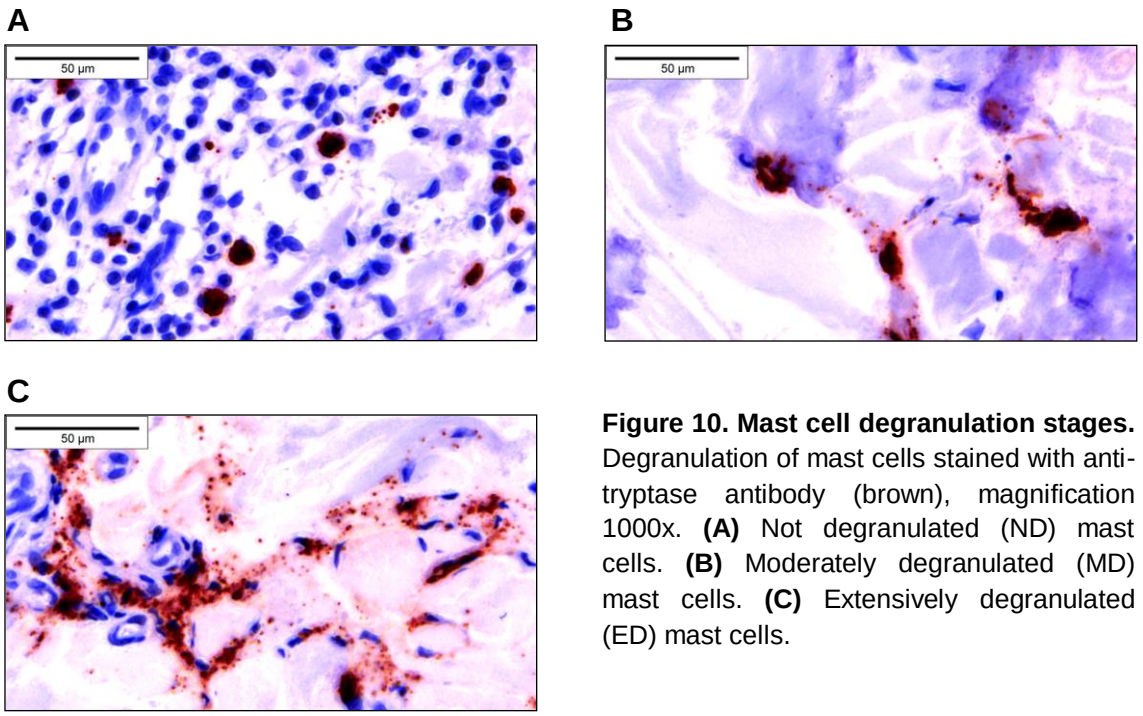

Figure 10. Mast cell degranulation stages. Degranulation of mast cells stained with anti-tryptase antibody (brown), magnification 1000x. **(A)** Not degranulated (ND) mast cells. **(B)** Moderately degranulated (MD) mast cells. **(C)** Extensively degranulated (ED) mast cells.

Patients with PCL showed a significant increase of extensively degranulated mast cells compared to normal skin and inflammatory cutaneous diseases (Figure 11A; 26.4 ± 1.9% extensively degranulated (ED) mast cells in PCL (All), 5.6 ± 0.9% extensively degranulated mast cells in normal skin (Ctrl), 17.0 ± 1.2% extensively degranulated mast cells in inflammatory cutaneous diseases (All), mean ± SEM). CTCL and CBCL patients showed a similar increase in extensively degranulated mast cells (Figure 11A). When we compared stable (CTCL, n=25; CBCL, n=7) and progressive (CTCL, n=10; CBCL, n=1) patients, progressive patients showed significantly more extensively degranulated (ED) mast cells and significantly fewer not degranulated (ND) mast cells (Figure 11B). Thus, in addition to the number of mast cells, the degranulation of mast

cells is increased in CTCL and CBCL, and this is particularly prominent in progressive forms. Interestingly, we also noted that areas with degranulated mast cells were often associated with increased numbers of eosinophils (Figure 11C).

A

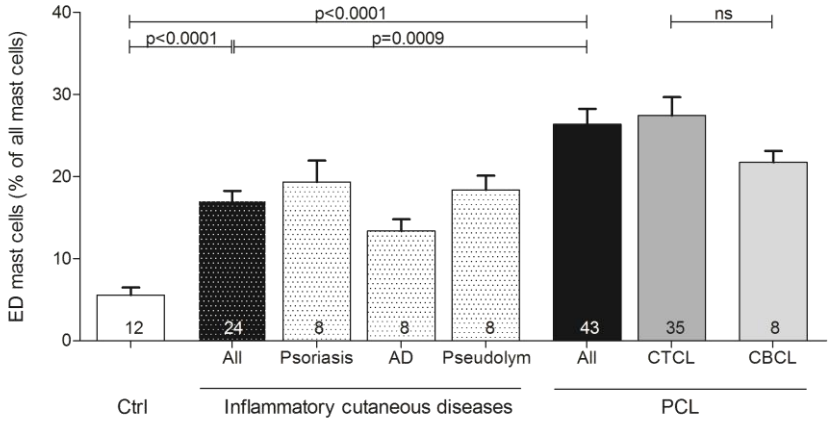

B

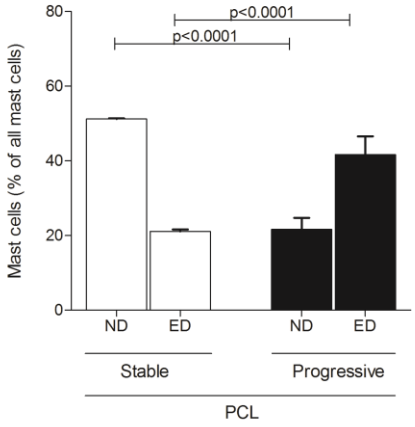

C

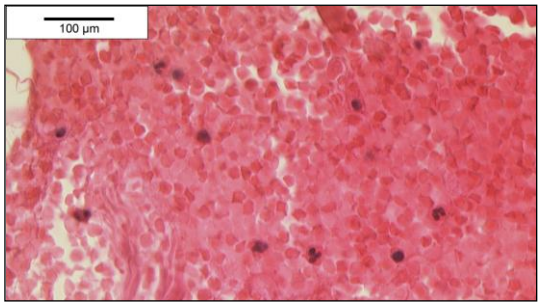

Figure 11. Mast cell degranulation is increased in PCL. Degranulation of mast cells stained with anti-tryptase antibody was evaluated semiquantitatively at 200x magnification in skin biopsies from PCL patients, patients with inflammatory cutaneous diseases and control subjects. **(A)** Extensively degranulated (ED) mast cells were counted in 3 high power fields at 200x magnification in skin biopsies from patients with PCL (All; n=43) subdivided into patients with CTCL (n=35) and CBCL (n=8), from subjects with normal skin (Ctrl; n=12) and from patients with inflammatory cutaneous diseases (All; n=24) such as psoriasis (n=8), atopic dermatitis (AD; n=8) and pseudolymphoma (Pseudolym; n=8). Results are presented as percentage of ED mast cells of all mast cells and expressed as mean ± SEM. Statistical significance was assessed by two-tailed Student´s *t*-test. **(B)** Not degranulated (ND) mast cells and ED mast cells were counted in skin biopsies from patients with stable PCL (n=32) and progressive PCL (n=11). Data represent the mean ± SEM. Statistical significance was assessed by two-tailed Student´s *t*-test. **(C)** Skin biopsies of PCL patients were evaluated by H&E staining and screened for numbers of eosinophils (dark red staining). Progressive PCL, magnification 400x.

4.1.5. Microvessel density is increased in mycosis fungoides

To explore possible effects of mast cell infiltration, we determined microvessel density in MF patients (n=23) subdivided into eczema (n=13), plaque (n=8) and tumor stages (n=2) and in patients with inflammatory cutaneous diseases (n=24) (Figure 12, Figure 13). Skin sections were stained with anti-CD31 antibody and the number of CD31-positive microvessels was counted microscopically. For comparison, sections were also stained with anti-CD34 antibody. Determining the number of CD34-positive cells revealed similar results.

Microvessel density was significantly increased in MF patients compared to inflammatory cutaneous diseases (Figure 12A; 26.4 ± 2.1% microvessel density/mm^2 in MF patients (All), 14.4 ± 0.9% microvessel density/mm^2 in inflammatory cutaneous diseases (All), mean ± SEM). Comparing the different MF stages, we found a significantly increased microvessel density in tumor compared to eczema stage (37.2 ± 7.8% microvessel density/mm^2 in tumor, 23.0 ± 1.6% microvessel density/mm^2 in eczema stage, mean ± SEM). Additionally, when we performed correlation analysis, we observed a highly significant correlation between microvessel density and mast cell numbers in MF patients (Figure 12B; Spearman r=0.89, $p<0.0001$).

A

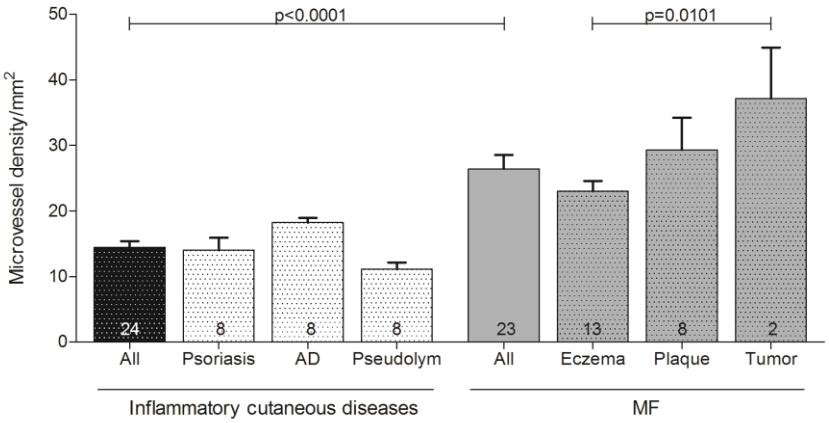

B

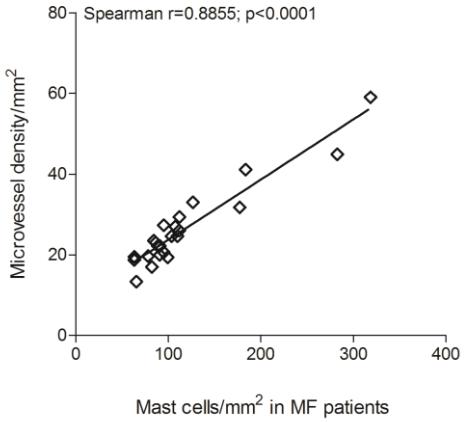

Figure 12. Microvessel density is increased in MF. (A) Skin biopsies from MF patients and patients with inflammatory cutaneous diseases were stained with anti-CD31 antibody. Microvessel density per mm^2 was analyzed by microscopic counting of 5 high power fields at 100x magnification. Data represent the mean ± SEM. Statistical significance was assessed by two-tailed Student´s *t*-test. **(B)** Microvessel density per mm^2 (*y-axis*) positively correlates with mast cell number per mm^2 (*x-axis*) in MF patients (n=23; Spearman r=0.8855; p<0.0001).

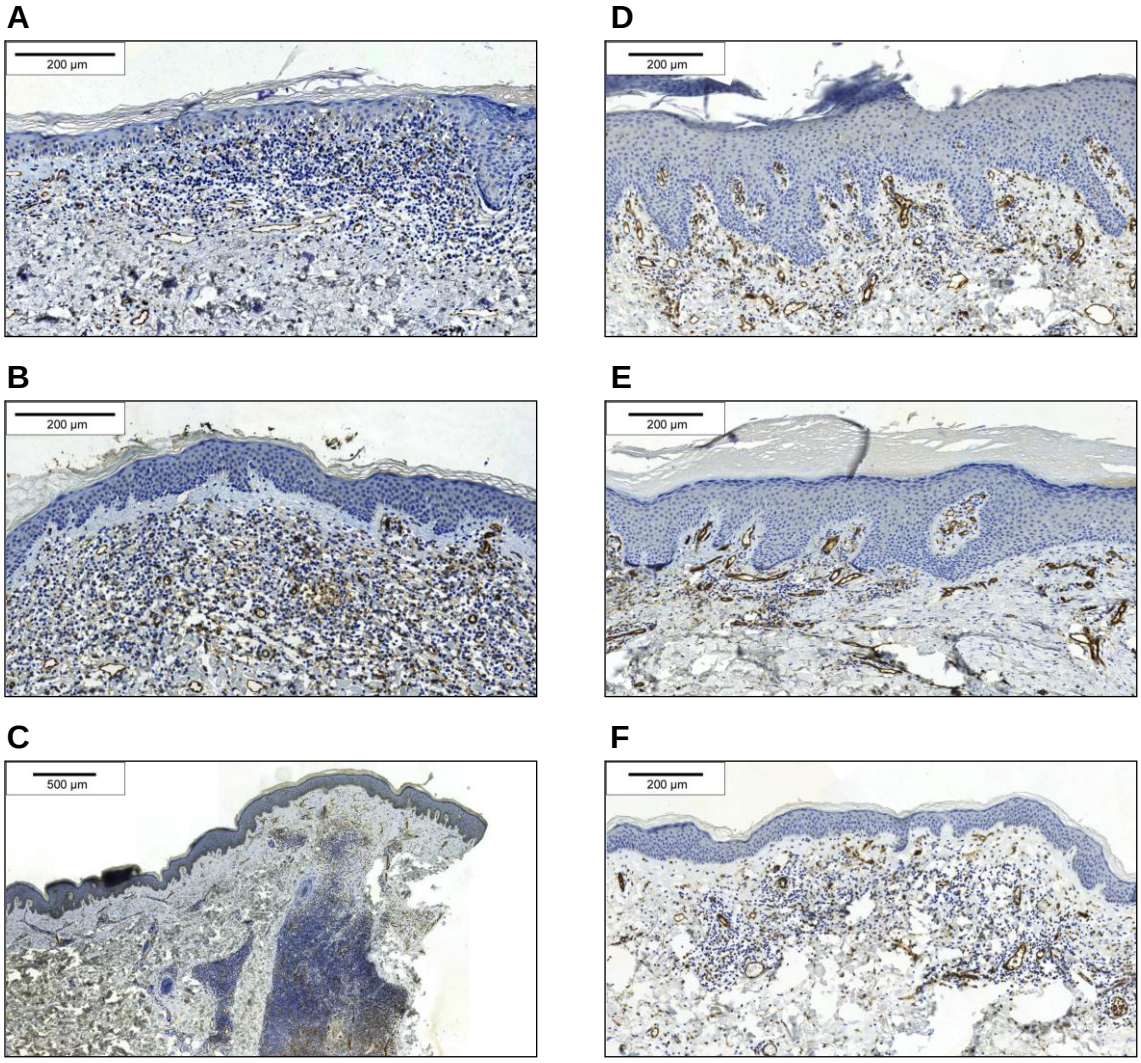

Figure 13. Histological analyses showed that microvessel density is increased in MF. (A) MF, eczema stage, magnification 200x. **(B)** MF, plaque stage, magnification 200x. **(C)** MF, tumor stage, magnification 50x. **(D)** Psoriasis, magnification 150x. **(E)** Atopic dermatitis, magnification 150x. **(F)** Pseudolymphoma, magnification 150x, staining of microvessels with anti-CD31 antibody (brown).

4.1.6. Mast cells release mediators that promote tumor growth

To explore the mechanisms by which mast cells may promote tumor growth, we used cytometric bead array (CBA) analysis to measure multiple inflammatory cytokines and chemokines (IL-2, IL-4, IL-6, IL-10, IL-17A, TNF, IFN-γ, CXCL8, CCL5, CXCL9, CCL2, CXCL10, VEGF, basic FGF and TGF-β1) in the supernatant of the human mast cell line HMC1. At baseline, HMC1 cells mainly produced IL-6, TGF-β1, VEGF, CCL2 and CXCL8 (Figure 14). All these cytokines were induced by treatment with calcium ionophore and inhibited by cromolyn.

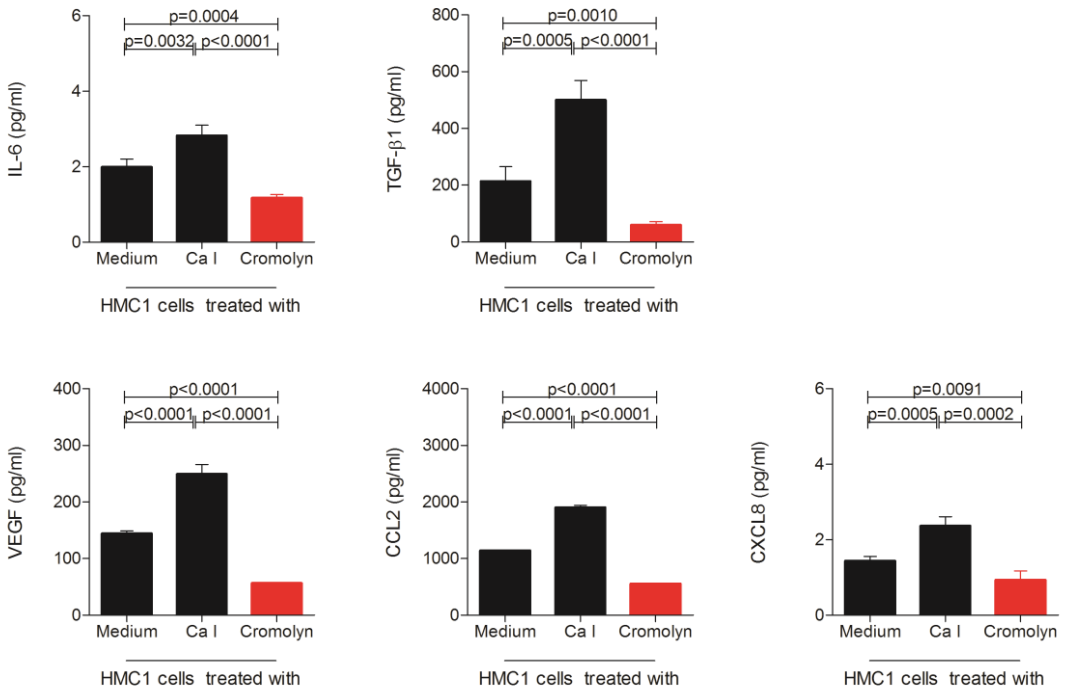

Figure 14. Mast cells release mediators that promote tumor growth. 1x10^6 HMC1 cells were treated with medium, calcium ionophore A23187 (Ca I) or cromolyn for 30 minutes at 37°C, washed and incubated in medium for 6 h. Mast cell products IL-6, TGF-β1, VEGF, CCL2 and CXCL8 were measured in the supernatants using a flow cytometric bead array (CBA). Mean data of 4 separate experiments (n=4) are presented as mean ± SD. Statistical significance was assessed by two-tailed Student´s *t*-test. When error bars are not shown, they were too small to be diagrammed.

4.1.7. Unstimulated PCL cells produce proinflammatory cytokines

As mast cell infiltration and degranulation within the microenvironment of PCL suggested a tumor-promoting role of mast cells, we next sought to investigate whether mast cells are able to induce release of cytokines from PCL cells *in vitro*. Initially, we measured multiple inflammatory cytokines (IL-2, IL-4, IL-6, IL-10, IL-17A, TNF and IFN-γ) in the supernatant of unstimulated primary Sézary cells, derived from a patient with Sézary syndrome, and in the supernatant of different CTCL cell lines, namely the human CTCL cell line MyLa, derived from a patient with MF[85], Mac2B, originally derived from a patient with CD30+ALCL[84], and SeAx, derived from a patient with SS[86] by CBA analysis (Figure 15). At baseline, Sézary cells and the CTCL cell lines SeAx, Mac2B and partly also MyLa produced high levels of TNF. Furthermore, Mac2B and SeAx produced also IL-6, exceeding levels produced by primary T-cells derived from healthy subjects or by the control cell line Jurkat (Figure 15). Moreover, MyLa and SeAx cells and partly also primary Sézary cells were found to release IL-17A, confirming and extending previous reports on production of IL-17A by CTCL cells.[73,74] The human B-cell lymphoma cell line BJAB produced mainly IL-10.

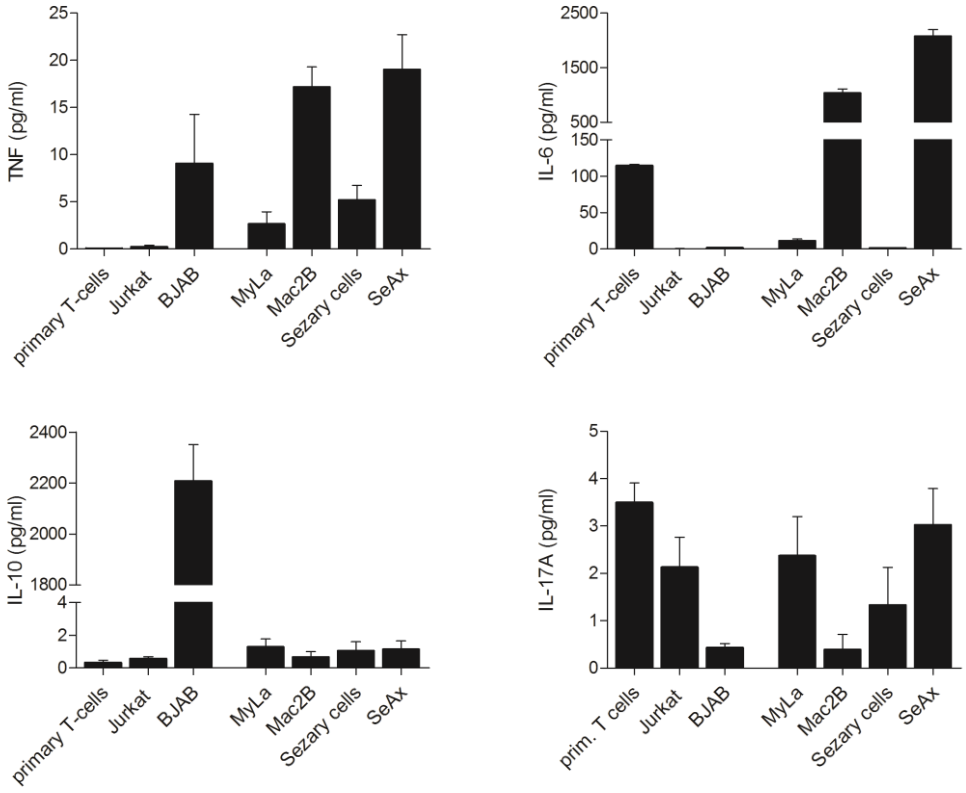

Figure 15. Unstimulated PCL cells produce proinflammatory cytokines. Four week-old primary T-cells, Jurkat cells, CTCL cell lines Mac2B, MyLa and SeAx, primary Sezary cells and human B-cell lymphoma cell line BJAB were cultured for 1 week in medium and the cytokines TNF, IL-6, IL-10 and IL-17A were measured in the supernatant of $2x10^6$ cells/ml each using a flow cytometric bead array (CBA). Mean data of 4 separate experiments (n=4) are presented as mean ± SD. When error bars and bars are not shown, they were too small to be diagrammed.

4.1.8. Mast cell supernatant induces changes in cytokine production of primary cutaneous lymphoma cells

When we incubated the PCL cell lines Mac2B and SeAx with supernatant of HMC1 cells, we observed a significantly increased production of IL-6 mRNA and protein (Figure 16A) as well as a significantly decreased production of TGF-β1 mRNA and protein (Figure 16B) in Mac2B cells and SeAx cells. Secretion of IL-2, IL-4, IL-10, IL-17A, TNF and IFN-γ, as well as CXCL8, CCL5, CXCL9, CCL2 and CXCL10 was not altered. Together, these results demonstrate that mast cells can induce changes in cytokine production of CTCL cells *in vitro*.

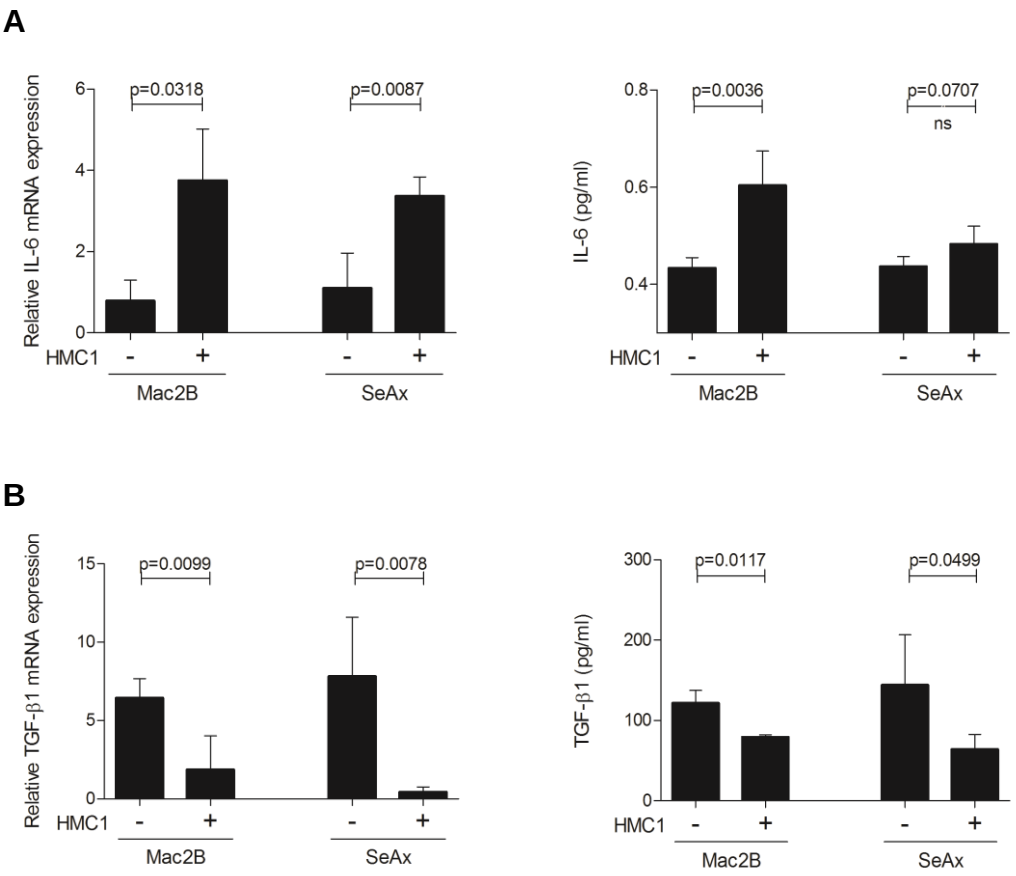

Figure 16. Mast cell supernatant induces changes in cytokine production of PCL cells. Mac2B and SeAx cells were cultured with or without supernatant of HMC1 cells for 24 h, washed and incubated in medium for 6 h. IL-6 **(A)** and TGF-β1 **(B)** mRNA levels relative to GAPDH expression were determined using quantitative real-time PCR. Statistical significance was assessed by two-tailed Student´s *t*-test. Mac2B and SeAx cells were cultured with or without supernatant of HMC1 cells for 48 h, washed and incubated in medium for 48 h. Levels of IL-6 **(A)** and TGF-β1 **(B)** were measured in the supernatant of $5x10^5$ cells/ml using CBA. Statistical significance was assessed by two-tailed Student´s *t*-test (ns, not significant). Mean data of 4 separate experiments (n=4) are presented as mean ± SD.

4.1.9. Mast cell supernatant induces proliferation of primary cutaneous lymphoma cells

To test whether addition of mast cell supernatant also affects proliferation of PCL cells, primary Sézary cells, the CTCL cell lines MyLa, Mac2B and SeAx, as well as primary T-cells, Jurkat cells and the B-cell lymphoma cell line BJAB were incubated with supernatant of HMC1 cells and proliferation was measured for 80 h in 4 hour intervals using the Cell Titer 96® AQ_{ueous} One Solution Assay (Figure 17). Briefly, 100 µl cells and 20 µl MTS (3-(4,5-dimethyl-2-yl)-5-(3-carboxymethoxyphenyl)-2-(4-sulfophenyl)-2H-tetrazolium) were added per well in a 96-well plate and incubated for 1 h at 37°C and 5% CO_2. Absorbance of formazan, which is converted from living cells by MTS, was measured at 490 nm in an ELISA reader. We observed that mast cell supernatant significantly increased proliferation of Sézary cells and all CTCL cell lines. This increase was often comparable to stimulation with a cocktail of several cytokines used as positive control. When we inhibited mediator release by pretreatment of HMC1 cells with cromolyn, mast cell supernatant failed to affect proliferation of the CTCL cell lines Mac2B and SeAx (Figure 17, lower right panels). In contrast to the increased proliferation of PCL cells, primary T-cells and Jurkat cells only showed a limited response to mast cell supernatant (Figure 17, upper panels). Within the first 32 hours, we observed a typical growth curve with an exponential growth starting at 24 hours of incubation, which decreased after around 48 hours. When we added new media or mast cell supernatant after 48 hours, this had only little effect on CTCL cells alone, but, surprisingly, led to a highly increased cell number when mast cell supernatant or cytokine cocktail were added. This effect was most prominent in SeAx cells and primary Sézary cells. In summary, these results demonstrate that mast cells can induce proliferation of CTCL cells *in vitro*. CTCL cells might be more sensitive to mast cell stimulation than primary T-cells.

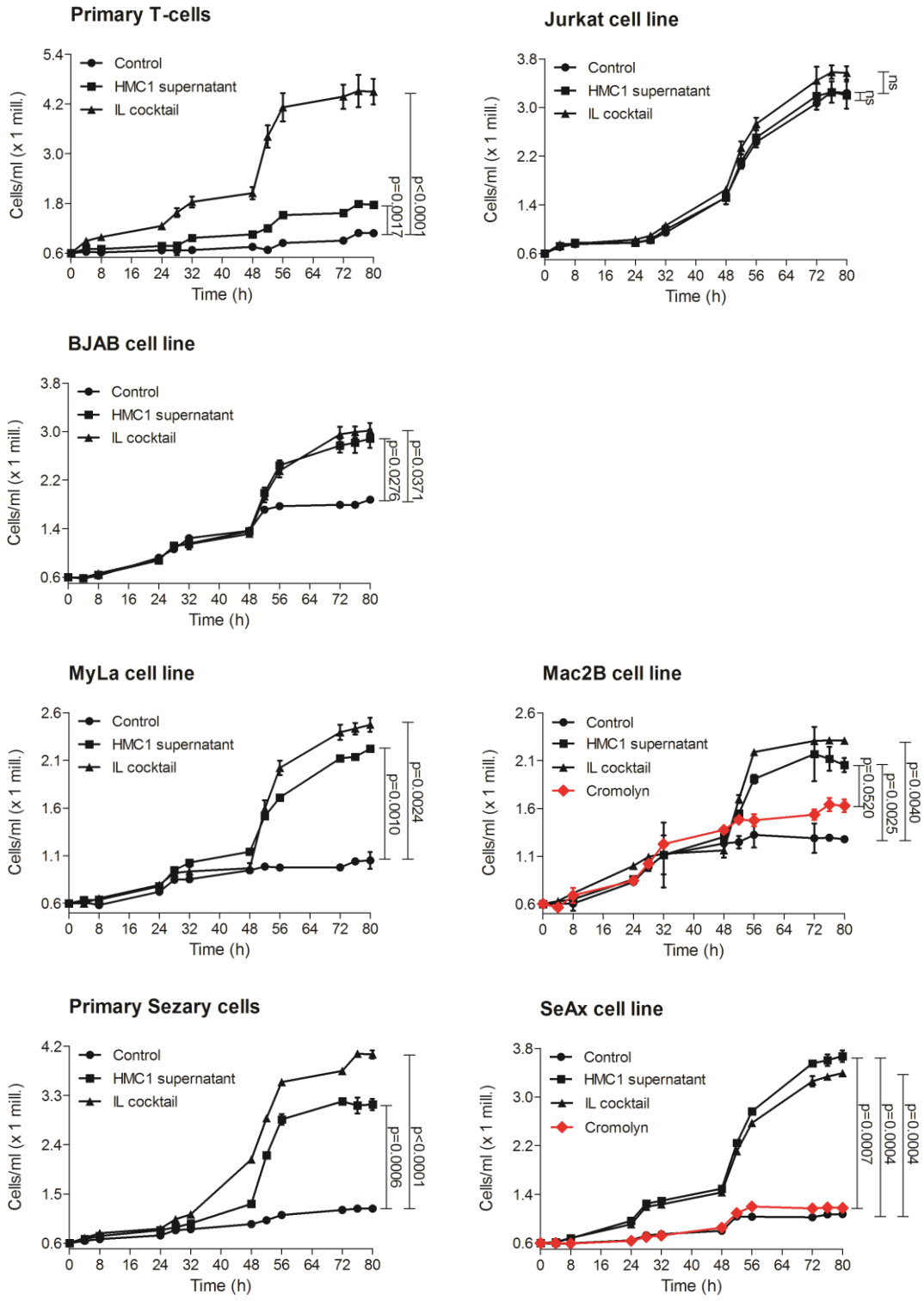

Figure 17. Mast cell supernatant induces proliferation of PCL cells. Primary T-cells, Jurkat cells, primary Sézary cells, the CTCL cell lines SeAx, Mac2B and MyLa as well as the human B-cell lymphoma cell line BJAB were cultured with (HMC1 supernatant) or without (Control) supernatant of HMC1 cells or with a cocktail of several cytokines (IL cocktail; IL-1α, IL-1β, IL-2, IL-4 and IL-7). SeAx cells and Mac2B cells were additionally cultured with mast cell supernatant of HMC1 cells, which were pretreated with cromolyn (Cromolyn). Proliferation was measured for 80 h using the Cell Titer 96® AQ_{ueous} One Solution Assay. Data represent the mean ± SD of 4 separate experiments (n=4). When error bars are not shown, they were too small to be diagrammed. Statistical significance was assessed by two-tailed Student´s *t*-test (ns, not significant).

4.2. Mast cells in the microenvironment of murine tumors

4.2.1. Murine mast cell supernatant induces cytokine release and proliferation of the mouse T-cell lymphoma cell line EL4

To transfer the *in vitro* data obtained with human PCL cells and cell lines to an *in vivo* system, we established a murine lymphoma model injecting subcutaneously the mouse T-cell lymphoma cell line EL4 into the flanks of mast cell-deficient mice and controls. To also investigate cytokine production and proliferation of EL4 cells upon stimulation with mast cells, release of cytokines (IL-2, IL-4, IL-6, IL-10, IL-17A, TNF and IFN-γ) was measured by CBA (Figure 18). EL4 cells were found to express a proinflammatory cytokine pattern at baseline (Figure 18A), similar to human PCL cells. Stimulation of EL4 cells with supernatant of murine bone marrow-derived mast cells (BMMC) induced significant upregulation of TNF, IL-6 and IL-17A (Figure 18B). In addition, supernatant of BMMCs significantly increased proliferation of EL4 cells (Figure 18C).

A

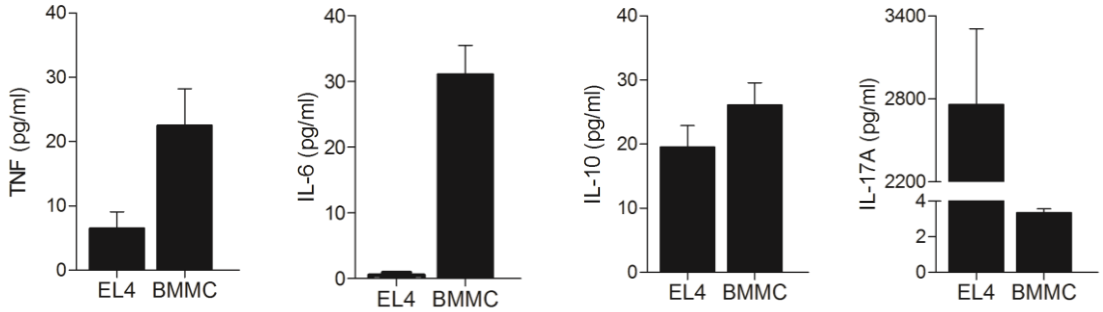

B

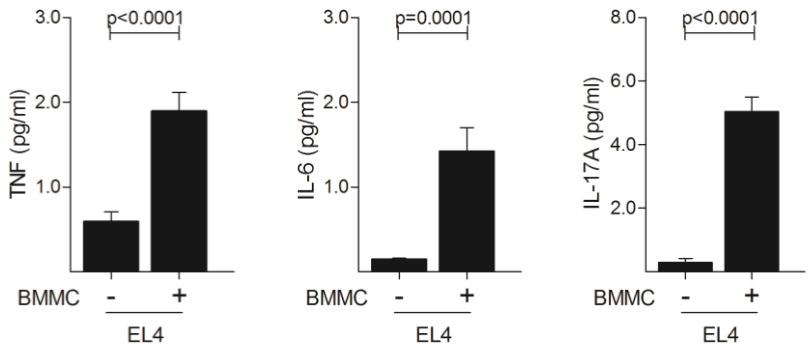

C

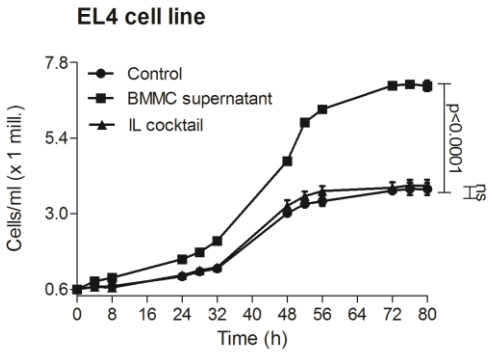

Figure 18. Murine mast cell supernatant induces cytokine release and proliferation of mouse T-cell lymphoma cell line EL4. (A) EL4 cells and murine bone marrow-derived mast cells (BMMC) were cultured for 1 week and the cytokines TNF, IL-6, IL-10 and IL-17A were measured in the supernatant of $2x10^6$ cells/ml using a flow cytometric bead array (CBA). Mean data of 4 separate experiments (n=4) are presented as mean ± SD. **(B)** EL4 cells were cultured with or without supernatant of BMMC for 48 h, washed and incubated in medium for 48 h. Levels of TNF, IL-6 and IL-17A were measured in the supernatant of $5x10^5$ cells/ml using CBA. Statistical significance was assessed by two-tailed Student´s *t*-test. Mean data of 4 separate experiments (n=4) are presented as mean ± SD. **(C)** EL4 cells were cultured with (BMMC supernatant) or without (Control) supernatant of BMMC or with a cocktail of several cytokines (IL cocktail; IL-1α, IL-1β, IL-2, IL-4 and IL-7) and proliferation was measured for 80 h using Cell Titer 96® AQ_{ueous} One Solution Assay. Data represent the mean ± SD of 4 separate experiments (n=4). When error bars are not shown, they were too small to be diagrammed. Statistical significance was assessed by two-tailed Student´s *t*-test (ns, not significant).

4.2.2. Mast cell-deficient mouse models for the investigation of tumor growth

To analyze the functional role of mast cells *in vivo*, we evaluated tumor growth in our recently developed mouse model that allows inducible selective depletion of connective tissue mast cells (Figure 19).[33,34] Breeding the mast cell-specific transgenic line *Mcpt5-Cre* (Figure 19A, right) to the *iDTR* line (Figure 19A, left)[35], we generated *Mcpt5-Cre+/iDTR+* mice that show efficient and specific depletion of cutaneous and peritoneal mast cells upon i.p. injections with diphtheria toxin (Figure 19B, C).

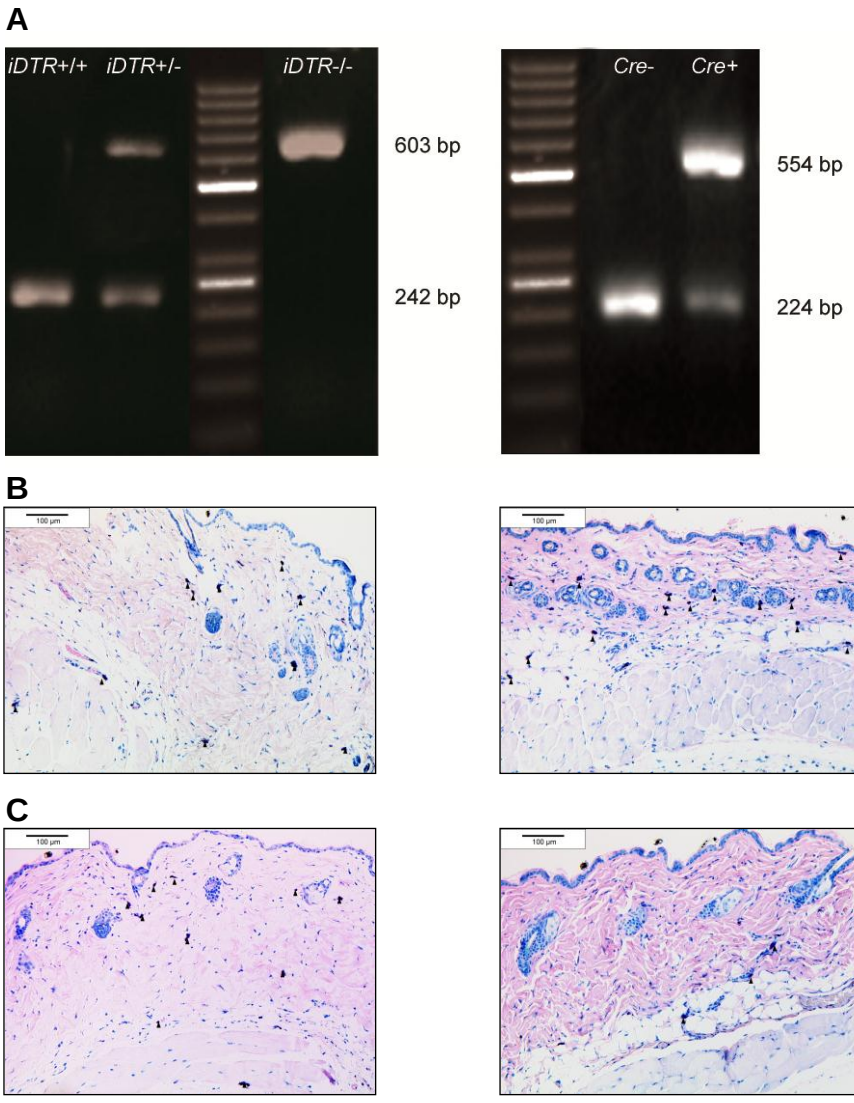

Figure 19. Mouse model of inducible mast cell deficiency. (A) Genotyping of *iDTR* (left) and *Mcpt5-Cre* (right) mice by PCR. The 242 bp fragment represents the *iDTR* gene, whereas the 603 bp fragment shows the wild type allele. For *Mcpt5-Cre*, the 554 bp fragment indicates the presence of the gene encoding the *Cre* recombinase (*Cre+*). The 224 bp fragment indicates the wild type (*Cre-*) allele. **(B)** *Mcpt5-Cre-/iDTR+* skin biopsy before (left) and after (right) i.p. DT injections, magnification 100x. **(C)** *Mcpt5-Cre+/iDTR+* skin biopsy before (left) and after (right) i.p. DT injections, magnification 100x. Giemsa staining, mast cells are marked by black arrows.

To exclude that multiple DT injections may influence tumor growth, we additionally used a mouse model of constitutive mast cell deficiency. Crossing *Mcpt5-Cre* animals to the *R-DTA* line[36] also showed, in double positive littermates (Figure 19A, right; Figure 20A), depletion of connective tissue mast cells (Figure 20B).

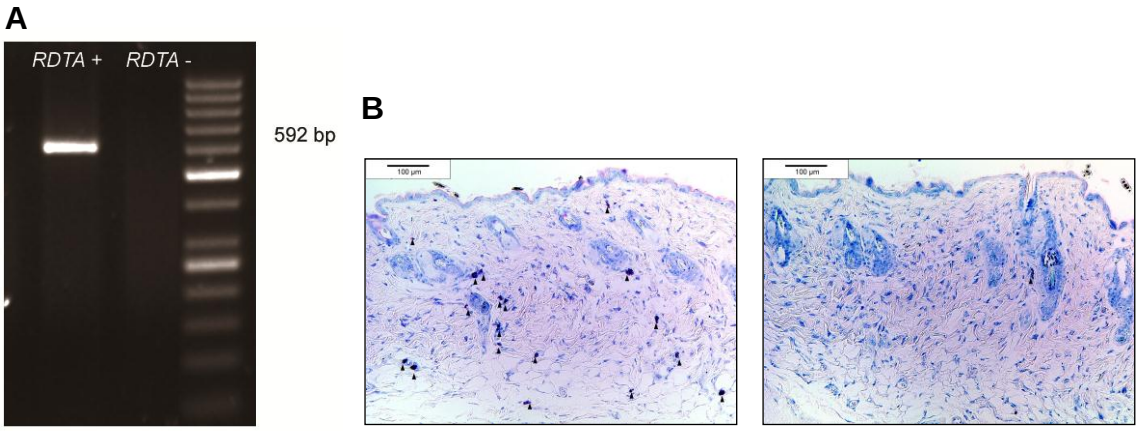

Figure 20. Mouse model of constitutive mast cell deficiency. (A) Genotyping of *R-DTA* mice by PCR. The 592 bp fragment represents the *R-DTA* gene. **(B)** *Mcpt5-Cre-/R-DTA+* (left) and *Mcpt5-Cre+/iDTR+* (right) skin biopsy, magnification 100x. Giemsa staining, mast cells are marked by black arrows.

Furthermore, to analyze the role of mast cells in tumor neoangiogenesis, we used *Mcpt5-Cre+/VEGF*$^{fl/fl}$ mice that lack mast cell-derived VEGF. For comparison, we also analyzed tumor growth in the traditionally used mast cell-deficient C57BL/6 *Kit*$^{W\text{-}sh/W\text{-}sh}$ line, which shows several other defects in addition to the deficiency of mast cells due to a genetic conversion in the *Kit* gene promoter[30,32], and in WT C57BL/6 controls.

4.2.3. Mast cell-deficient mice show decreased growth of subcutaneously injected tumors

In analogy to a recently published mouse model of CTCL[79], we injected the mouse T-cell lymphoma cell line EL4 subcutaneously in *Mcpt5-Cre+/iDTR+*, *Mcpt5-Cre+/R-DTA+*, *Mcpt5-Cre+/VEGF*$^{fl/fl}$, C57BL/6 *Kit*$^{W\text{-}sh/W\text{-}sh}$ and the appropriate control mice. Tumor volume (right) and area (left) were significantly decreased in the mast cell-deficient *Mcpt5-Cre+/iDTR+* and C57BL/6 *Kit*$^{W\text{-}sh/W\text{-}sh}$ mice compared to the *Mcpt5-Cre-/iDTR+* and WT C57BL/6 controls (Figure 21A, upper panels). Subcutaneous injection of two other tumor cell lines, the pancreatic cancer cell line Pan02 (Figure 21B) and the Lewis lung carcinoma cell line LLC (Figure 21C), showed similar results. Comparing *Mcpt5-Cre+/R-DTA+* and their controls, the difference was not as obvious, which may be due to possible additional effects of *R-DTA* (Figure 21A, lower panels). Depleting mast cell-derived VEGF slightly decreased tumor volume and tumor area (not significant), but not to the same level as in the mast cell-deficient animals. These data suggest that mast cell-derived VEGF may participate in tumor growth, but other mediators may play more significant roles. On the other hand, the lack of mast cell-derived VEGF may also be compensated for by other factors.

A

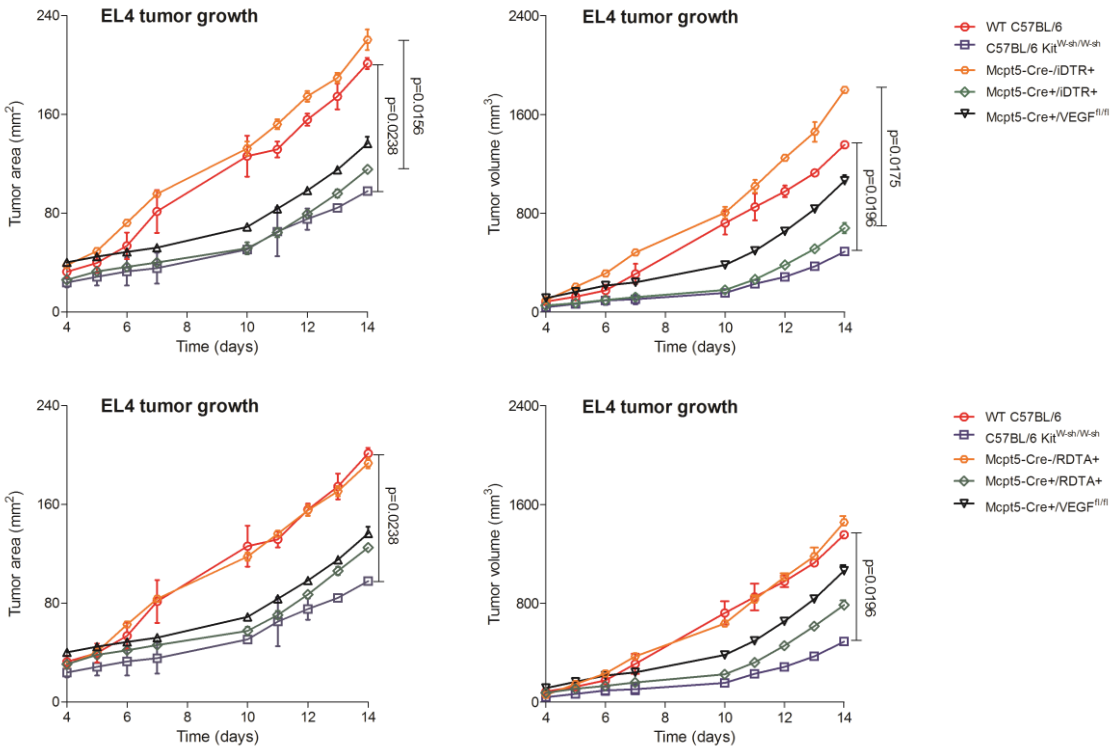

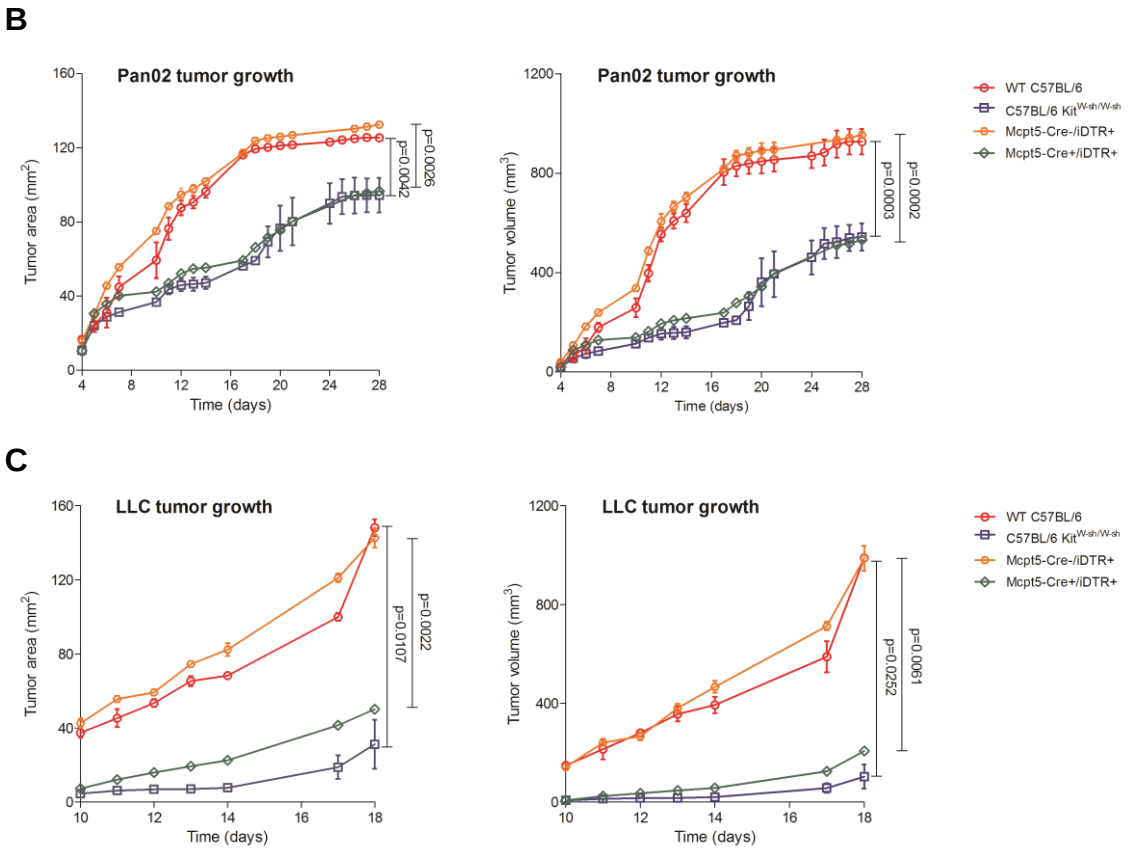

Figure 21. Mast cell-deficient mice show decreased growth of subcutaneously injected tumors. (A) 1x10^6 cells of the murine T-cell lymphoma cell line EL4 were injected s.c. into the flanks of mast cell-deficient *Mcpt5-Cre+/iDTR+* (upper panels) or *Mcpt5-Cre+/R-DTA+* (lower panels) and C57BL/6 *Kit*$^{W\text{-}sh/W\text{-}sh}$ mice and *Mcpt5-Cre-/iDTR+* (upper panels) or *Mcpt5-Cre-/R-DTA+* (lower panels) and WT C57BL/6 control mice as well as *Mcpt5-Cre+/VEGF*$^{fl/fl}$ mice and tumor area (left) and tumor volume (right) were assessed for 14 days using a Mitutoyo Quick Mini caliper. Data represent the mean ± SD of 4-6 tumors (n=4, C57BL/6 *Kit*$^{W\text{-}sh/W\text{-}sh}$ and WT C57BL/6 mice; n=6, *Mcpt5-Cre+/iDTR+*, *Mcpt5-Cre-/iDTR+*, *Mcpt5-Cre+/R-DTA+*, *Mcpt5-Cre-/R-DTA+* and *Mcpt5-Cre+/VEGF*$^{fl/fl}$). When error bars are not shown, they were too small to be diagrammed. Statistical significance was assessed by two-tailed Student´s *t*-test. **(B)** 1x10^6 cells of the murine cell line Pan02 were injected s.c. into the flanks of mast cell-deficient *Mcpt5-Cre+/iDTR+* and C57BL/6 *Kit*$^{W\text{-}sh/W\text{-}sh}$ mice as well as *Mcpt5-Cre-/iDTR+* and WT C57BL/6 control mice and (left) tumor area (left) and tumor volume (right) were assessed for 28 days using a Mitutoyo Quick Mini caliper. Data represent the mean ± SD of 4-6 tumors (n=4, C57BL/6 *Kit*$^{W\text{-}sh/W\text{-}sh}$ and WT C57BL/6 mice; n=6, *Mcpt5-Cre+/iDTR+* and *Mcpt5-Cre-/iDTR+*). When error bars are not shown, they were too small to be diagrammed. Statistical significance was assessed by two-tailed Student´s *t*-test. **(C)** 1x10^6 cells of the murine cell line LLC were injected s.c. into the flanks of mast cell-deficient *Mcpt5-Cre+/iDTR+* and C57BL/6 *Kit*$^{W\text{-}sh/W\text{-}sh}$ mice as well as *Mcpt5-Cre-/iDTR+* and WT C57BL/6 control mice and tumor area (left) and tumor volume (right) were assessed for 18 days using a Mitutoyo Quick Mini caliper. Data represent the mean ± SD of 4-6 tumors (n=4, C57BL/6 *Kit*$^{W\text{-}sh/W\text{-}sh}$ and WT C57BL/6 mice; n=6, *Mcpt5-Cre+/iDTR+* and *Mcpt5-Cre-/iDTR+*). When error bars are not shown, they were too small to be diagrammed. Statistical significance was assessed by two-tailed Student´s *t*-test.

Histologically, EL4 tumors in WT C57BL/6 (Figure 22A) and *Mcpt5-Cre-/iDTR+* (Figure 22B) controls were characterized by marked accumulation of mast cells along the tumor rim, similar to the mast cell infiltration in human CTCL (Figure 8B, C). In contrast, a smaller tumor infiltrate and only few mast cells were found in mast cell-deficient *Mcpt5-Cre+/iDTR+* mice (Figure 22C). To also analyze microvessel density in EL4 tumors in analogy to MF patients, we stained tumor tissue with anti-CD31 antibody and observed, as expected, a decreased microvessel density in *Mcpt5-Cre+/iDTR+* mice (Figure 22F) compared to WT C57BL/6 (Figure 22D) and *Mcpt5-Cre-/iDTR+* controls (Figure 22E).

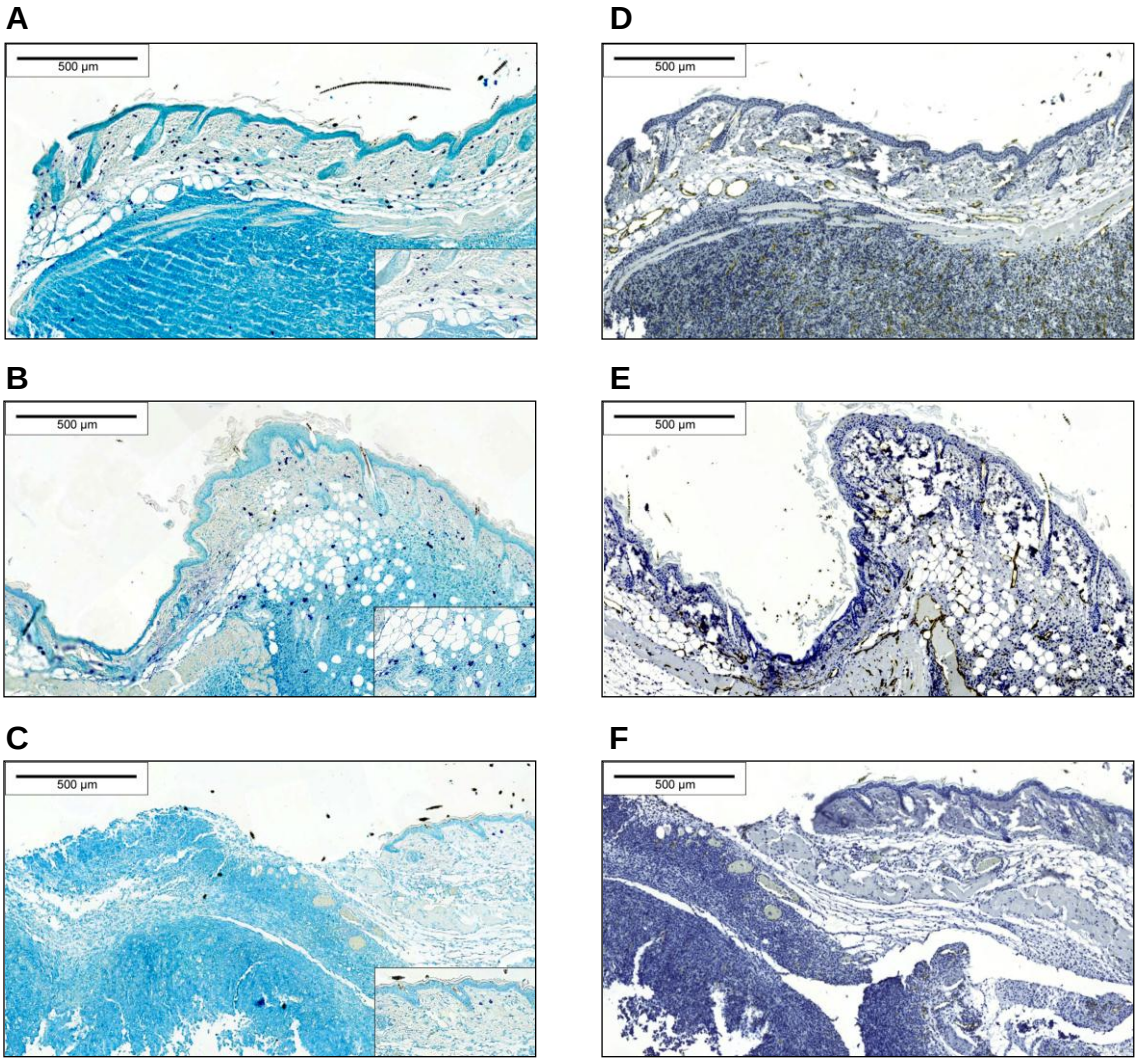

Figure 22. Mast cell-deficient mice show decreased growth of subcutaneously injected tumors and decreased microvessel density. (A) WT C57BL/6, skin biopsy of EL4 tumor at day 14, magnification 100x. **(B)** *Mcpt5-Cre-/iDTR+*, EL4 tumor, magnification 100x. **(C)** *Mcpt5-Cre+/iDTR+*, EL4 tumor, magnification 100x. Toluidine blue staining, mast cells (dark blue). Inserts show mast cells at 400x magnification. **(D)** WT C57BL/6 **(E)** *Mcpt5-Cre-/iDTR+* **(F)** *Mcpt5-Cre+/iDTR+*, skin biopsy of EL4 tumor at day 14, magnification 100x, CD31 staining.

4.2.4. Mast cell-deficient mice show decreased chemically induced carcinogenesis

Besides subcutaneous injection of tumor cell lines, we also performed the well-established two-step skin carcinogenesis model, where animals are treated with a single DMBA application followed by multiple TPA treatments. We observed decreased mast cell numbers and a reduced number of papillomas in mast cell-deficient *Mcpt5-Cre+/iDTR+* and C57BL/6 *Kit*$^{W\text{-}sh/W\text{-}sh}$ mice (Figure 23). In *Mcpt5-Cre+/iDTR+* animals, we were not able, after several weeks, to keep mast cells away from the developing papillomas by additional subcutaneous DT injections. The increase in papilloma number (Figure 23B) followed the increase in the number of mast cells (Figure 23A). Histologically, WT C57BL/6 (Figure 24A) and *Mcpt5-Cre-/iDTR+* (Figure 24C) controls showed accumulation of mast cells directly under the papilloma area (right panel), whereas in *Mcpt5-Cre+/iDTR+* (Figure 24D) and C57BL/6 *Kit*$^{W\text{-}sh/W\text{-}sh}$ (Figure 24B) mice, only few mast cells were detectable. All animals showed a thickened epidermis. Together, these results show that mast cells also promote chemically induced carcinogenesis.

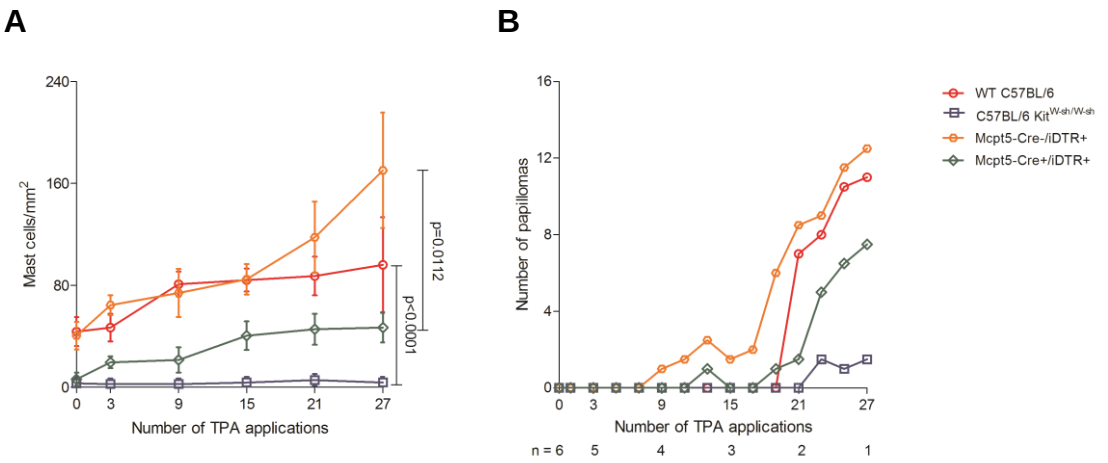

Figure 23. Mast cell-deficient mice show decreased chemically induced carcinogenesis. Mast cell-deficient *Mcpt5-Cre+/iDTR+* and C57BL/6 *Kit*$^{W\text{-}sh/W\text{-}sh}$ mice and *Mcpt5-Cre-/iDTR+* and WT C57BL/6 control mice were treated with DMBA/TPA. **(A)** Skin biopsies were stained at different time points by Giemsa staining and number of mast cells was analyzed by microscopic counting of 5 high power fields at 200x magnification and calculating the mean number of mast cells per mm^2. Data represent the mean ± SD. Statistical significance was assessed by two-tailed Student´s *t*-test. **(B)** Papillomas were counted macroscopically at different time points. Due to the low number of mice at later time points, statistical significance could not be assessed for this experiment.

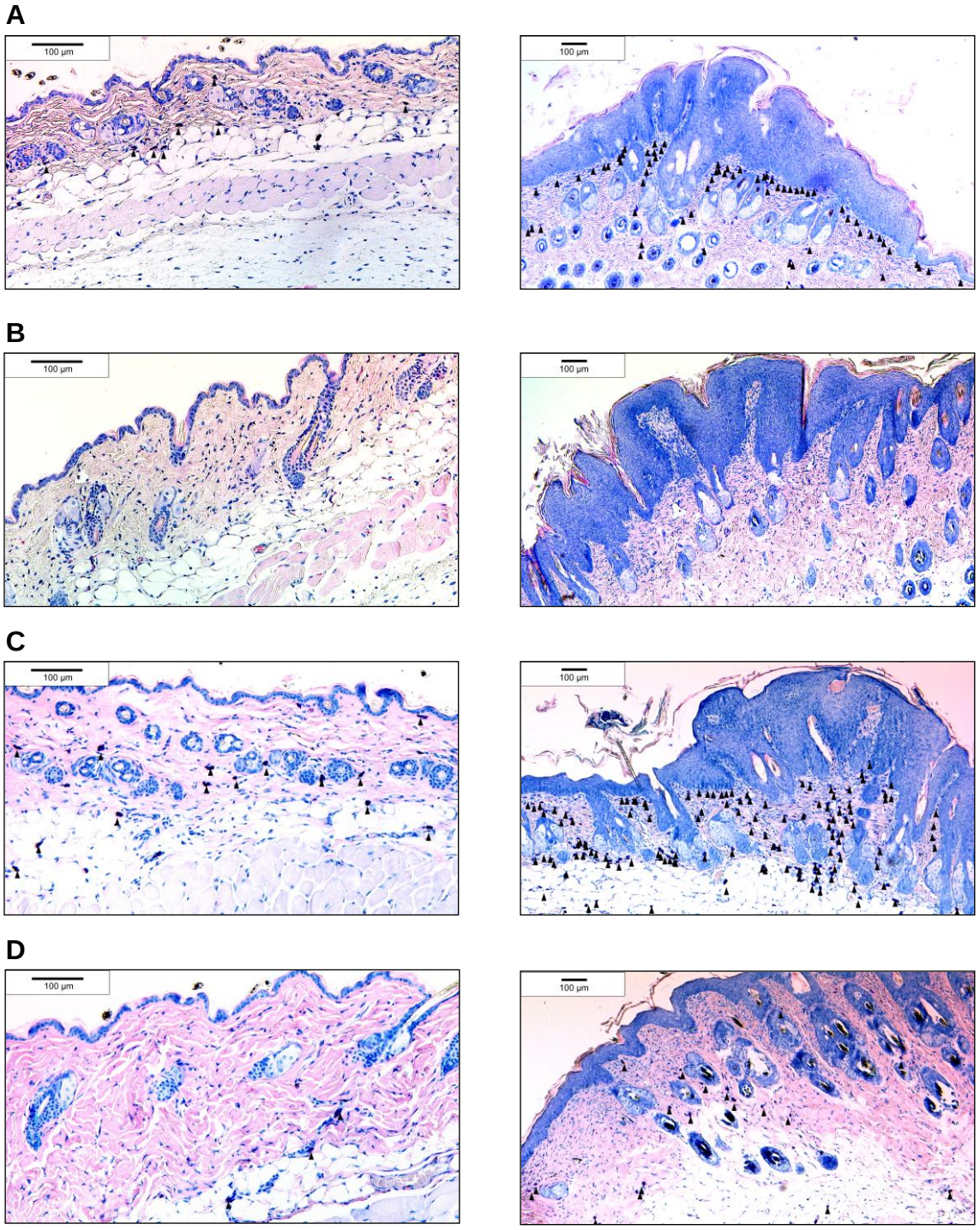

Figure 24. Histological analyses revealed that mast cell-deficient mice show decreased chemically induced carcinogenesis. (A) WT C57BL/6 skin biopsy, before (left, magnification 100x) and after (right, magnification 50x) DMBA/TPA treatment. **(B)** C57BL/6 *Kit*$^{W\text{-}sh/W\text{-}sh}$ skin biopsy, before (left, magnification 100x) and after (right, magnification 50x) DMBA/TPA treatment. **(C)** *Mcpt5-Cre-/iDTR+* skin biopsy, before (left, magnification 100x) and after (right, magnification 50x) DMBA/TPA treatment. **(D)** *Mcpt5-Cre+/iDTR+* skin biopsy, before (left, magnification 100x) and after (right, magnification 50x) DMBA/TPA treatment. Giemsa staining, mast cells are marked by black arrows.

5. Discussion

5.1. Increased mast cell number and microvessel density in primary cutaneous lymphoma

Mast cell numbers are increased in many cancers.[44-55] However, the functional role of mast cells in cancers is not well defined. Recent studies demonstrated that mast cells are probably not only innocent bystanders, but actively participate in modulating tumor growth.[41-43,59,60] They have been shown to exert relevant pro-[44-51] and antitumorigenic[52-54] effects. In the present study, we report for the first time on a protumorigenic role of mast cells in primary cutaneous lymphoma. The number of mast cells in skin sections of CTCL and CBCL patients is highly increased compared to normal skin and inflammatory cutaneous diseases. Mast cell infiltration is most prominent in the periphery of CTCL, especially at the rims of the infiltrate.

Our data on mast cell numbers in normal skin (Figure 7A) are in agreement with several recent studies, which also reported on an average of 40 mast cells/mm^2.[95-97] In these studies, no differences in skin mast cell numbers or distribution have been described when comparing skin obtained from male or female, and from young or old individuals.[95] However, mast cell numbers were found to vary to some degree between different sites of the body. The highest numbers of mast cells were observed in the most superficial skin layers and at peripheral skin sites, like chin and nose.[95] To exclude variability in mast cell numbers in our study, we analyzed skin biopsies from comparable sites and layers of the body. Furthermore, we included an appropriate number of control subjects reflecting similar sampling locations. There are also few reports on higher mast cell numbers in normal skin[98,99], which may correspond to different fixation, staining or counting methods.[96] In addition, there are several studies on the number and activation of mast cells in urticaria, psoriasis and atopic dermatitis.[100-118] Here, numbers of mast cells were increased to levels well comparable to the mast cell counts that we observed in inflammatory cutaneous diseases (Figure 7A). Thus, we believe our method of staining and counting mast cells results in reliable data. With this method, we observed for the first time highly increased numbers of mast cells in PCL, which even exceed the mast cell counts in inflammatory cutaneous diseases.

Our observation that mast cell numbers correlate with disease progression in CTCL (Figure 7C, Figure 9) is of potential significance for clinical management of patients with CTCL. Possibly, mast cell infiltration could serve as additional diagnostic criterion, as prognostic parameter or as follow-up marker. To definitively clarify whether mast cell counts are useful as diagnostic or prognostic marker in CTCL, however, further studies, especially prospective studies, with sufficient number of patients and statistical power are necessary.

Our data also support a rationale for therapeutic inhibition of mast cells, e.g. by antihistamines, cromolyn or, in the near future, by targeted drugs, which is predicted to decrease growth of PCLs or even lead to regression of the disease. The concept of inhibiting tumor progression by antihistamines has been studied, to some extent, in various cancer models.[119-122] For example, antihistamines have been found to inhibit growth of xenograft colon carcinomas and melanomas in mice and to delay proliferation of several human colon carcinoma cell lines.[119,120] In breast cancer, treatment with H_2-receptor antagonists resulted in complete remission of 70% of experimentally induced tumors.[121] However, in clinical trials, H_2-receptor antagonists showed only limited success in treatment of breast and colon cancer.[122] In murine xenograft models of prostate adenocarcinoma[44] and thyroid cancer[45], treatment with cromolyn, known to inhibit degranulation of mast cells and release of inflammatory cytokines, blocked growth of tumors, supporting our observation that mast cell supernatant of cromolyn-treated mast cells is not able to induce proliferation of tumor cells *in vitro* (Figure 17). Since patients with CTCL often suffer from pruritus, particularly those with MF and SS, antihistamines are already administered to many CTCL patients. However, no studies exist until now that compare the development of CTCL in the presence or absence of antihistamines.

In addition, an increasing number of studies in different types of tumors demonstrate that the tumor microenvironment interacts with tumor cells in a complex manner and crucially influences tumor growth.[37,61,123] For instance, in H&E-stained sections of our 43 patients with CTCL and CBCL, we also observed increased numbers of eosinophils associated with mast cell infiltration (Figure 11C). Similarly, in Hodgkin´s lymphoma, aggregation of eosinophils together with mast cells has been described.[62] Several studies have also

demonstrated that mast cell-derived mediators play important roles in eosinophil chemotaxis, activation and function.[124-127]

Besides the interaction with other cell types of the tumor microenvironment, mast cells can also influence structural components in the tumor surrounding. For example, in lung cancer[63] and squamous cell carcinomas of the esophagus[64] and cervix[65], mast cell infiltrates have been correlated with both microvessel density and tumor progression, comparable to our results (Figure 12). In agreement, Karpova et al[128] reported on increased blood vessel density and lymphangiogenesis in patients with Sézary syndrome. This observation was also confirmed by Mazur et al, who reported on significantly increased CD34-positive microvessels in MF compared to normal skin.[129] Similarly, an elevated number of CD31-positive vessels has been described in cutaneous B-cell lymphomas.[130]

5.2. Stimulation of tumor growth by mast cells *in vitro* and *in vivo*

We also report for the first time on a functional role of mast cells in cutaneous lymphoma performing *in vitro* and *in vivo* experiments. *In vitro*, mast cell supernatant is able to induce changes in cytokine production and proliferation of malignant cells (Figure 16 – Figure 18).

In addition, mast cell products can influence other immune cells. As mentioned above, studies from different laboratories demonstrated that mast cell-derived mediators are pivotal in eosinophil maturation and chemotaxis.[124-127] Among the mast cell products that affect eosinophils are cytokines, such as IL-1, IL-3, IL-4, IL-5, IL-13, TNF and GM-CSF, and chemokines, including CXCL8 (IL-8), CCL5 (RANTES) and CCL2 (MCP-1).[127] As shown in Figure 14, we were able to detect high levels of CCL2 and CXCL8 in supernatants of the human mast cell line HMC1. Comparably, in lesional biopsies of basal cell carcinoma, tryptase-positive mast cells have been shown to express CXCL8 (IL-8) and CCL5 (RANTES).[131] Furthermore, human lung mast cells activated with SCF and anti-IgE have been found to express CCL2 (MCP-1).[132] Whereas human mast cell lines activated by dengue virus secreted CCL5 (RANTES) and MIP-1, but not CXCL8 (IL-8)[133], similarly activated cord blood-derived mast cells expressed CCL5 (RANTES).[133]

5.2.1. Potential effects of mast cells on different hallmarks of cancer

Inflammation plays an important role in different stages of tumor development, including initiation, promotion, malignant conversion, invasion and metastasis.[134] Here, tumor-infiltrating immune cells are known to participate in an extensive and dynamic crosstalk with cancer cells.[134] Several basic concepts linking inflammation and cancer have now been developed, for example the concept that chronic inflammation as well as "undetectable" inflammation, e.g. obesity-induced inflammation, increase cancer risk.[134] Moreover, it is well known that different types of immune cells are usually present within tumors and affect cancer cells through the production of cytokines, chemokines, growth factors, prostaglandins, reactive oxygen and nitrogen species. In developing tumors, antitumorigenic and protumorigenic immune mechanism often coexist, however, if the tumor is not rejected, the protumorigenic effect increasingly dominates.[134] The immune cells that infiltrate the tumor microenvironment include innate immune cells, such as macrophages, neutrophils, mast cells, myeloid-derived suppressor cells, dendritic cells and natural killer cells, and adaptive immune cells, like T and B lymphocytes. Although investigations on the role of mast cells in tumors are still at the very beginning, mast cells have been demonstrated to actively participate in several hallmarks of cancer, described below.[37,123]

Recent studies demonstrated that mast cells can exert mitogenic, proangiogenic and proinvasive functions within the microenvironment of tumors. Moreover, they have been reported to recruit other tumor-infiltrating immune cells and to suppress the cytotoxic activity of the NK/T-cells. Figure 25 depicts the potential participation of mast cells in the scheme of Hanahan and Weinberg[37] illustrating the different hallmarks of cancer:

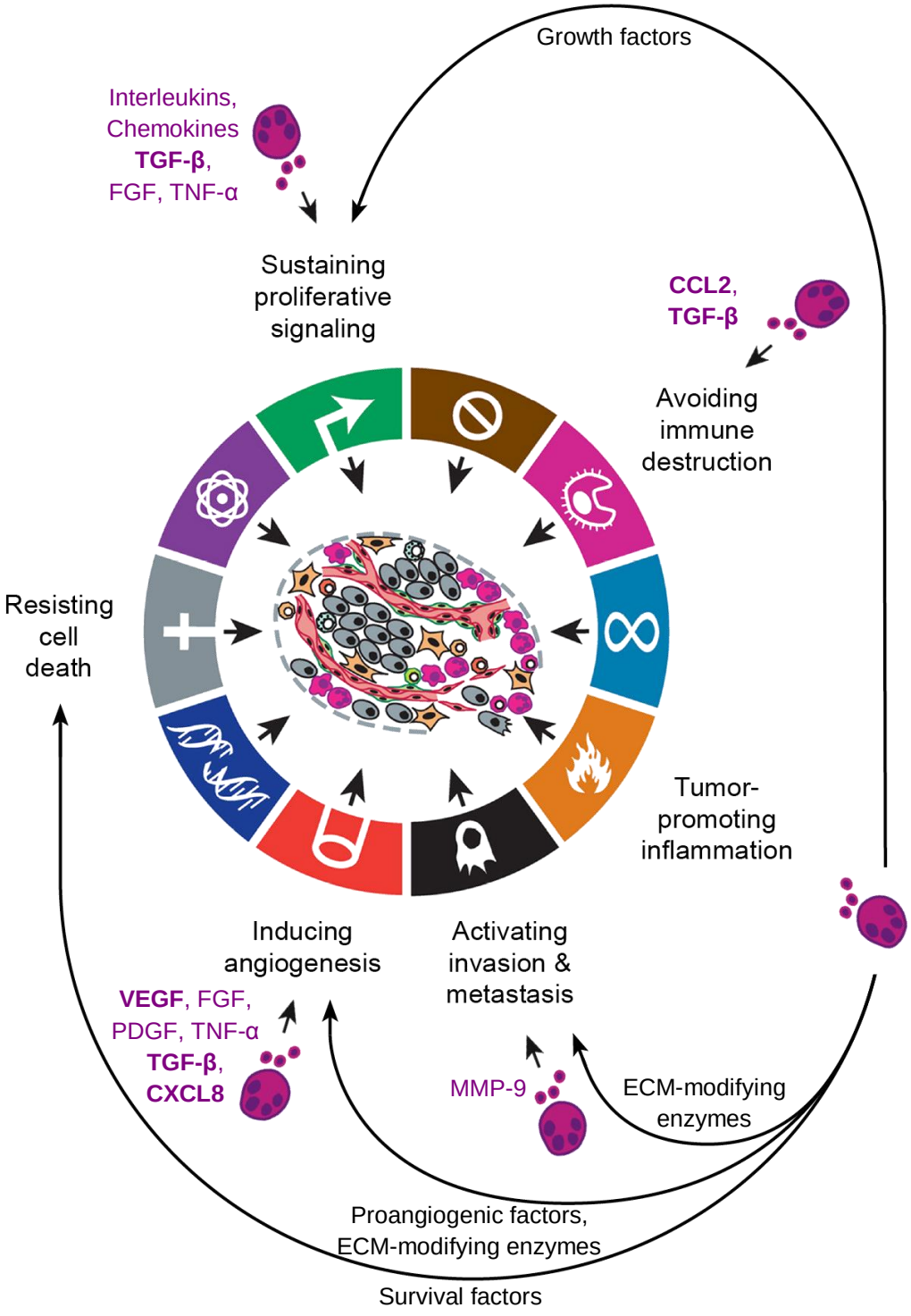

Figure 25. Potential participation of mast cells in different hallmarks of cancer. Adapted from Hanahan and Weinberg, 2011[37] and Hanahan and Coussens, 2012[123]. Mast cells are shown as violet cells. Mast cell mediators are shown in violet, bold violet mediators are the mediators that have been identified to participate in PCL in the present study.

5.2.1.1. Sustaining proliferative signaling

Proliferation of cancer cells can be mediated by autocrine production of growth factors[135] as well as by paracrine mechanisms, whereby surrounding cells produce mediators that induce proliferation of cancers.[135] Here, mast cells may contribute directly or indirectly by release of mediators such as TGF-β, TNF-α, FGF, various interleukins, chemokines and histamine.[123,136] In the present study, we observed that HMC1 cells produced especially high levels of TGF-β1 and CCL2 (MCP-1) (Figure 14).

CCL2 primarily recruits tumor-associated macrophages (TAMs).[136] TAMs accumulate in the microenvironment of tumors, especially in hypoxic areas[136-138], due to HIF-1-dependent upregulation of the chemokine receptor CXCR4[139], which is also present on mast cells. In response to for example TGF-β, TAMs acquire M2 properties, promoting tumor proliferation and progression.[136] Interestingly, a recent study using Hodgkin´s lymphoma cell lines demonstrated that mouse mast cells do not affect proliferation of all Hodgkin´s lymphoma cell lines, but subcutaneous injection of these cell lines together with mast cells gave rise to significantly larger tumors compared to injection of Hodgkin´s lymphoma cells alone.[140] Furthermore, Mizuno et al[140] showed that mast cells incubated with the proteasome inhibitor bortezomib released significantly less CCL2 than untreated mast cells.

5.2.1.2. Avoiding immune destruction

Although the immunosuppressive activity of mast cells is not well characterized, it is known that they can indirectly regulate immunosuppression by releasing cytokines that recruit MDSCs and T_{regs}.[43] Again, the cytokines CCL2 and TGF-β1 may play a major role in this process. CCL2 recruits monocytes, memory T cells, and dendritic cells to sites of tissue injury, infection and inflammation. TGF-β acts on surrounding stromal cells, immune cells, endothelial and smooth-muscle cells. Thereby, TGF-β promotes immunosuppression and angiogenesis, which in turn facilitate invasion of cancers.[141] In normal cells and early stages of tumorigenesis, TGF-β has been reported to block the cell cycle at the G1 stage, leading to inhibition of proliferation, enhanced differentiation or induction of apoptosis.[142] This might be a reason for the decreased TGF-β production in PCL cell lines upon incubation with HMC1 cell supernatant, in the present study

(Figure 16), because PCL cells were harvested at early phases of tumor cell expansion and mast cell supernatant stimulates them to overcome this early phase of minor proliferation. This hypothesis is also supported by the proliferation curves, shown in Figure 17, which show that PCL cells start their major growth phase after the second addition of mast cell supernatant. Later, in older tumor cells, parts of the TGF-β signaling pathway are mutated, and TGF-β no longer controls the tumor cells.[141] Moreover, the increased IL-6 production in PCL cells upon stimulation with HMC1 cell supernatant (Figure 16) promotes inflammation and serves as a detrimental signal for the tumor, by inducing apoptosis of tumor cells.[55]

5.2.1.3. Activating invasion and metastasis

In addition to unlimited proliferation of cancer cells, a large variety of coordinated cellular processes control invasion and metastasis.[143] For example, specific factors stimulate attachment of tumor cells to host extracellular matrix, tumor cell-mediated proteolysis of host barriers, migration of tumor cells and colony formation of tumor cells in the target organ for metastasis.[143]

Mast cells and macrophages are known to produce a series of proteases (MMPs) that promote tissue invasion by remodeling structural components of the extracellular matrix.[123] One of these proteases is MMP-9, which is primarily produced by mast cells and causes degradation of the extracellular matrix. Recently, mast cell-derived MMP-9 has been demonstrated to promote invasiveness of prostate cancer by Pittoni et al.[44] Analyzing the role of mast cells in transgenic mouse prostate tumors showed that mast cells are essential players in the initial stages of prostate tumor progression, by supplying MMP-9 to the tumor microenvironment.[44] MMP-9 is also involved in the mobilization of VEGF from the extracellular matrix[144], supporting the switch from vascular quiescence to neoangiogenesis.[44] Comparable to our first experiments investigating *Mcpt5-Cre*/*VEGF*$^{fl/fl}$ mice (Figure 21), one could imagine experiments with *Mcpt5-Cre*/*MMP-9*$^{fl/fl}$ mice[44] to clarify the specific contribution of mast cell-derived MMP-9 to tumor neo-angiogenesis and invasiveness.

5.2.1.4. Inducing angiogenesis

Most cancers are associated with the formation of new vessels from existing vasculature, which is called tumor-induced sprouting angiogenesis. Whereas normal angiogenesis ensures that developing or healing tissues receive an adequate supply of nutrients, the availability of nutrients is limited by competition among different proliferating cells in tumors. As a result, tumor cells induce sprouting of new vessels to secure their nutrient supply. The mechanisms by which cancer cells stimulate pathological neovascularization closely mimic those utilized by normal cells to foster physiological angiogenesis.[145]

In this process, the cytokine vascular endothelial growth factor (VEGF) plays a prominent role. VEGF is known to increase endothelial cell permeability, to stimulate endothelial cell proliferation, to inhibit endothelial cell apoptosis and to enhance endothelial cell migration.[145] In tumors, VEGF is released by tumor cells as well as by cells of the tumor microenvironment, then diffuses through the extracellular matrix and finally stimulates endothelial cells lining existing vessels in the proximity of the tumor to form new vessel sprouts. In addition to VEGF, several other cytokines have been shown to participate in angiogenesis. For example, FGF can also stimulate endothelial cell proliferation and enhance endothelial cell migration.[145] In contrast, TNF-α inhibits endothelial cell proliferation.[145] TGF-β increases the stability of vessel walls, supports anchorage-independent growth of fibroblasts, is chemotactic for monocytes and fibroblasts and stimulates angiogenesis in the presence of inflammatory responses *in vivo*.[145] PDGF has been shown to induce DNA synthesis in endothelial cells and to stimulate proliferation of smooth muscle cells and pericytes.[145] Furthermore, GM-CSF promotes endothelial cell proliferation and migration and Ang-1 induces endothelial cell sprout formation *in vitro* and increases girth and stability of the endothelium.[145]

Mediators produced by mast cells, namely VEGF, FGF, TNF-α, TGF-β, PDGF, GM-CSF, Ang-1, CXCL8 and prostaglandins, have been demonstrated to regulate vascular cell survival, proliferation and motility, along with tissue remodeling and new vessel formation.[41,146] In the present study, we also observed release of high levels of VEGF, TGF-β1 and CXCL8 from human mast cells (Figure 14). Further supporting our hypothesis that mast cells participate in

neovascularization of PCL, we observed an increased microvessel density correlating with mast cell counts (Figure 12). In addition, growth of EL4 tumors was delayed to some degree (not significant) in mast cell-specific VEGF knockout mice (Figure 21).

5.2.2. Decreased growth of subcutaneously injected tumors and decreased chemically induced carcinogenesis in mast cell-deficient mice

In the present study, we took advantage of a new transgenic mast cell-deficient mouse model, the *Mcpt5-Cre/iDTR* model, focusing for the first time on tumor research (Figure 21, Figure 23). To investigate growth of lymphomas *in vivo*, we chose to use subcutaneous injections of the mouse lymphoma cell line EL4, which we thought would best mimic cutaneous lymphoma in mice and which closely resembles the model of Wu et al (2011)[79]. Our results show significant differences in growth of subcutaneously injected tumors and chemically induced papillomas between mast cell-deficient *Mcpt5-Cre+/iDTR+* animals and *Mcpt5-Cre-/iDTR+* controls, while both groups received repeated diphtheria toxin injections before and during the experiments. These data demonstrate that mast cells are a crucial component within the tumor microenvironment able to control tumor progression.

In our experiments, we observed similarly delayed tumor growth in *Mcpt5-Cre+/iDTR+* animals like in C57BL/6 *Kit*$^{W\text{-}sh/W\text{-}sh}$ mice (Figure 21, Figure 23). This observation suggests that the previously reported reduced development of various tumors in mast cell-deficient WBBF1-*Kit*$^{W/Wv}$ [147] and C57BL/6 *Kit*$^{W\text{-}sh/W\text{-}sh}$ [148] mice is also based on the absence of mast cells and not on the other immunological alterations present in these models. In the past, these additional defects had led to misinterpretation of results and false attribution of certain tasks to mast cells, such as suppression of contact allergy.[34] Despite the similar response of *Mcpt5-Cre+/iDTR+* and C57BL/6 *Kit*$^{W\text{-}sh/W\text{-}sh}$ mice in our experiments, we can, however, not exclude that particular effects of mast cells on tumor development have to be newly defined in the context of the more specific *Mcpt5-Cre/iDTR* model.

Investigating the growth of subcutaneously injected tumor cell lines, we were only able to follow tumor growth for a limited period of time (Figure 21). After maximally 30 days, the tumors were too large and animals had to be sacrificed.

To exclude possible differences in tumor growth between mast cell-deficient mice and controls at later time points, we therefore also used a model of chemically induced carcinogenesis, which allowed us to follow papilloma growth for 20 weeks (Figure 23). These experiments, however, revealed that the *Mcpt5-Cre/iDTR* model is also associated with certain disadvantages. As Figure 23 shows, we were not able to sufficiently deplete mast cells for longer time periods, not even with additional injections of DT subcutaneously around the developing papillomas. After around 15 applications of TPA, at treatment week 7, mast cell numbers started to increase again and only 1 week later the number of papillomas also increased. On the other hand, besides the selective depletion of mast cells, an essential advantage of the *Mcpt5-Cre* model is the additional possibility of analyzing mast cell-specific products in tumor growth by cross breeding *Mcpt5-Cre* with different "floxed" lines.

Taken together, we could show that mast cell numbers are significantly increased in human primary cutaneous lymphoma. Patients with advanced stages of the disease showed higher mast cell counts than stable patients and mast cell numbers in different clinical stages correlated with disease progression. *In vitro*, we observed enhanced production of cytokines and increased proliferation of PCL cells in response to treatment with mast cell supernatant. *In vivo*, growth of subcutaneously injected tumors and chemically induced carcinogenesis was significantly decreased in mast cell-deficient transgenic mice.

To further define the role of mast cells in tumors, systematic analyses of different human tumor entities in different tumor stages are recommended. In addition, systematic investigations on growth of genetic tumor models in mast cell-deficient mice and on interactions of mast cells with tumor cells and other immune cells are suggested. Results of these studies may serve to better understand the pathogenesis of tumors and to develop more efficient treatments for cancer patients.

6. References

1. Ehrlich P. Beiträge zur Kenntnis der Anilinfärbungen und ihrer Verwendung in der mikroskopischen Technik. *Arch Mikro Anat*. 1877;13 (1):263-277.

2. Kitamura Y, Ito A. Mast cell-committed progenitors. *Proc Natl Acad Sci USA*. 2005;102(32):11129-11130.

3. Okayama Y, Kawakami T. Development, migration, and survival of mast cells. *Immunol Res*. 2006;34(2):97-115.

4. Galli SJ, Grimbaldeston M, Tsai M. Immunomodulatory mast cells: negative, as well as positive, regulators of immunity. *Nat Rev Immunol*. 2008;8(6):478-486.

5. Galli SJ, Nakae S. Mast cells to the defense. *Nat Immunol*. 2003;4(12):1160-1162.

6. Metcalfe DD, Baram D, Mekori YA. Mast cells. *Physiol Rev*. 1997;77(4):1033-1079.

7. Shelburne CP, Abraham SN. The Mast Cell in Innate and Adaptive Immunity. *Adv Exp Med Biol*. 2011;716:162-185.

8. Tsai M, Grimbaldeston M, Galli SJ. Mast Cells and Immunoregulation/Immunomodulation. *Adv Exp Med Biol*. 2011;716:186-211.

9. Gilfillan AM, Austin SJ, Metcalfe DD. Mast Cell Biology: Introduction and Overview. *Adv Exp Med Biol*. 2011;716:2-12.

10. Dawicki W, Marshall JS. New and emerging roles for mast cells in host defence. *Curr Opin Immunol*. 2007;19(1):31-38.

11. Echtenacher B, Mannel DN, Hultner L. Critical protective role of mast cells in a model of acute septic peritonitis. *Natur*e. 1996;381(6577):75-77.

12. Marshall JS. Mast-cell responses to pathogens. *Nat Rev Immunol*. 2004;4(10):787-799.

13. Marshall JS, Jawdat DM. Mast cells in innate immunity. *J Allergy Clin Immunol*. 2004;114(1):21-27.

14. Galli SJ, Kalesnikoff J, Grimbaldeston MA, Piliponsky AM, Williams CMM, Tsai M. Mast cells as “tunable” effector and immunoregulatory cells: Recent Advances. *Annu Rev Immunol*. 2005;23(1):749-786.

15. Mekori YA, Metcalfe DD. Mast cells in innate immunity. *Immunol Rev*. 2000;173(1):131-140.

16. Gilfillan AM, Tkaczyk C. Integrated signalling pathways for mast-cell activation. *Nat Rev Immunol*. 2006;6(3):218-230.

17. Grimbaldeston MA, Metz M, Yu M, Tsai M, Galli SJ. Effector and potential immunoregulatory roles of mast cells in IgE-associated acquired immune responses. *Curr Opin Immunol*. 2006;18(6):751-760.

18. Sayed BA, Christy A, Quirion MR, Brown MA. The Master Switch: The Role of Mast Cells in Autoimmunity and Tolerance. *Annu Rev Immunol*. 2008;26(1):705-739.

19. Lu L-F, Lind EF, Gondek DC, et al. Mast cells are essential intermediaries in regulatory T-cell tolerance. *Nature*. 2006;442(7106):997-1002.

20. Trautmann A, Toksoy A, Engelhardt E, Bröcker E-B, Gillitzer R. Mast cell involvement in normal human skin wound healing: expression of monocyte chemoattractant protein-1 is correlated with recruitment of mast cells which synthesize interleukin-4 in vivo. *J Pathol*. 2000;190(1):100-106.

21. Weller K, Foitzik K, Paus R, Syska W, Maurer M. Mast cells are required for normal healing of skin wounds in mice. *FASEB J*. 2006;20(13):E1628-E1635.

22. Liu J, Divoux A, Sun J, et al. Genetic deficiency and pharmacological stabilization of mast cells reduce diet-induced obesity and diabetes in mice. *Nat Med*. 2009;15(8):940-945.

23. Bachelet I, Levi-Schaffer F, Mekori YA. Mast Cells: Not Only in Allergy. *Immunol Allergy Clin North Am*. 2006;26(3):407-425.

24. Lee DM, Friend DS, Gurish MF, Benoist C, Mathis D, Brenner MB. Mast Cells: A Cellular Link Between Autoantibodies and Inflammatory Arthritis. *Science*. 2002;297(5587):1689-1692.

25. Secor VH, Secor WE, Gutekunst C-A, Brown MA. Mast Cells Are Essential for Early Onset and Severe Disease in a Murine Model of Multiple Sclerosis. *J Exp Med*. 2000;191(5):813-822.

26. Sun J, Sukhova GK, Wolters PJ, et al. Mast cells promote atherosclerosis by releasing proinflammatory cytokines. *Nat Med*. 2007;13(6):719-724.

27. Galli SJ, Nakae S, Tsai M. Mast cells in the development of adaptive immune responses. *Nat Immunol*. 2005;6(2):135-142.

28. Kitamura YY. Heterogeneity of mast cells and phenotypic change between subpopulations. *Annu Rev Immunol*. 1989;7:59-76.

29. Wilson BS, Oliver JM, Lidke DS. Spatio-Temporal Signaling in Mast Cells. *Adv Exp Med Biol*. 2011;716:91-106.

30. Grimbaldeston MA, Chen C-C, Piliponsky AM, Tsai M, Tam S-Y, Galli SJ. Mast Cell-Deficient W-sash c-kit Mutant KitW-sh/W-sh Mice as a Model for Investigating Mast Cell Biology in Vivo. *Am J Pathol*. 2005;167(3):835-848.

31. Zhou JS, Xing W, Friend DS, Austen KF, Katz HR. Mast cell deficiency in KitW-sh mice does not impair antibody-mediated arthritis. *J Exp Med*. 2007;204(12):2797-2802.

32. Nigrovic PA, Gray DHD, Jones T, et al. Genetic Inversion in Mast Cell-Deficient Wsh Mice Interrupts Corin and Manifests as Hematopoietic and Cardiac Aberrancy. *Am J Pathol*. 2008;173(6):1693-1701.

33. Scholten J, Hartmann K, Gerbaulet A, et al. Mast cell-specific Cre/loxP-mediated recombination in vivo. *Transgenic Res*. 2008;17(2):307-315.

34. Dudeck A, Dudeck J, Scholten J, et al. Mast Cells Are Key Promoters of Contact Allergy that Mediate the Adjuvant Effects of Haptens. *Immunity*. 2011;34(6):973-984.

35. Buch T, Heppner FL, Tertilt C, et al. A Cre-inducible diphtheria toxin receptor mediates cell lineage ablation after toxin administration. *Nat Methods*. 2005;2(6):419-426.

36. Voehringer D, Liang H-E, Locksley RM. Homeostasis and Effector Function of Lymphopenia-Induced “Memory-Like” T Cells in Constitutively T Cell-Depleted Mice. *J Immunol*. 2008;180(7):4742-4753.

37. Hanahan D, Weinberg RA. Hallmarks of Cancer: The Next Generation. *Cell*. 2011;144(5):646-674.

38. Nagy JA, Chang SH, Shih SC, Dvorak AM, Dvorak HF. Heterogeneity of the Tumor Vasculature. *Semin Thromb Hemost*. 2010;36(3):321-331.

39. Crivellato E, Beltrami CA, Mallardi F, Ribatti D. The mast cell: an active participant or an innocent bystander? *Histol Histopathol*. 2004;19(1):259-270.

40. Vasievich EA, Huang L. The Suppressive Tumor Microenvironment: A Challenge in Cancer Immunotherapy. *Mol Pharm*. 2011;8(3):635-641.

41. Maltby S, Khazaie K, McNagny KM. Mast cells in tumor growth: Angiogenesis, tissue remodelling and immune-modulation. *Biochim Biophys Acta*. 2009;1796(1):19-26.

42. Ribatti D, Crivellato E. Mast Cells, Angiogenesis and Cancer. *Adv Exp Med Biol*. 2011;716:270-288.

43. Wasiuk A, De Vries VC, Hartmann K, Roers A, Noelle RJ. Mast cells as regulators of adaptive immunity to tumours. *Clin Exp Immunol*. 2009;155(2):140-146.

44. Pittoni P, Tripodo C, Piconese S, et al. Mast Cell Targeting Hampers Prostate Adenocarcinoma Development but Promotes the Occurrence of Highly Malignant Neuroendocrine Cancers. *Cancer Res*. 2011;71(18):5987-5997.

45. Melillo RM, Guarino V, Avilla E, et al. Mast cells have a protumorigenic role in human thyroid cancer. *Oncogene*. 2010;29(47):6203-6215.

46. Ribatti D, Ennas MG, Vacca A, et al. Tumor vascularity and tryptase-positive mast cells correlate with a poor prognosis in melanoma. *Eur J Clin Invest*. 2003;33(5):420-425.

47. Molin D, Edström A, Glimelius I, et al. Mast cell infiltration correlates with poor prognosis in Hodgkin's lymphoma. *Br J Haematol*. 2002;119(1):122-124.

48. Zhu Y, Ghosh P, Charnay P, Burns DK, Parada LF. Neurofibromas in NF1: Schwann Cell Origin and Role of Tumor Environment. *Science*. 2002;296(5569):920-922.

49. Terada T, Matsunaga Y. Increased mast cells in hepatocellular carcinoma and intrahepatic cholangiocarcinoma. *J Hepatol*. 2000;33(6):961-966.

50. Ribatti D, Vacca A, Marzullo A, et al. Angiogenesis and mast cell density with tryptase activity increase simultaneously with pathological progression in B-cell non-Hodgkin's lymphomas. *Int J Cancer*. 2000;85(2):171-175.

51. Takanami I, Takeuchi K, Naruke M. Mast cell density is associated with angiogenesis and poor prognosis in pulmonary adenocarcinoma. *Cancer*. 2000;88(12):2686-2692.

52. Tan SY, Fan Y, Luo HS, Shen ZX, Guo Y, Zhao LJ. Prognostic significance of cell infiltrations of immunosurveillance in colorectal cancer. *World J Gastroenterol*. 2005;11(8):1210-1214.

53. Rajput A, Turbin D, Cheang M, et al. Stromal mast cells in invasive breast cancer are a marker of favourable prognosis: a study of 4,444 cases. *Breast Cancer Res Treat*. 2008;107(2):249-257.

54. Amini R-M, Aaltonen K, Nevanlinna H, et al. Mast cells and eosinophils in invasive breast carcinoma. *BMC Cancer*. 2007;7(1):165.

55. Theoharides TC, Conti P. Mast cells: the JEKYLL and HYDE of tumor growth. *Trends Immunol*. 2004;25(5):235-241.

56. Nico B, Mangieri D, Crivellato E, Vacca A, Ribatti D. Mast Cells Contribute to Vasculogenic Mimicry in Multiple Myeloma. *Stem Cells Dev*. 2008;17(1):19-22.

57. Strouch MJ, Cheon EC, Salabat MR, et al. Crosstalk between Mast Cells and Pancreatic Cancer Cells Contributes to Pancreatic Tumor Progression. *Clin Cancer Res*. 2010;16(8):2257-2265.

58. Toth-Jakatics R, Jimi S, Takebayashi S, Kawamoto N. Cutaneous malignant melanoma: Correlation between neovascularization and peritumor accumulation of mast cells overexpressing vascular endothelial growth factor. *Hum Pathol*. 2000;31(8):955-960.

59. Gounaris E, Erdman SE, Restaino C, et al. Mast cells are an essential hematopoietic component for polyp development. *Proc Natl Acad Sci USA*. 2007;104(50):19977-19982.

60. Soucek L, Lawlor ER, Soto D, Shchors K, Swigart LB, Evan GI. Mast cells are required for angiogenesis and macroscopic expansion of Myc-induced pancreatic islet tumors. *Nat Med*. 2007;13(10):1211-1218.

61. Liu J, Zhang Y, Zhao J, et al. Mast cell: insight into remodeling a tumor microenvironment. *Cancer Metastasis Rev*. 2011;30(2):177-184.

62. Enblad G, Sundstrom C, Glimelius B. Infiltration of eosinophils in Hodgkin's disease involved lymph nodes predicts prognosis. *Hematol Oncol*. 1993;11(4):187-193.

63. Tomita M, Matsuzaki Y, Onitsuka T. Effect of mast cells on tumor angiogenesis in lung cancer. *Ann Thorac Surg*. 2000;69(6):1686-1690.

64. Elpek GÖ, Gelen T, Aksoy NH, et al. The prognostic relevance of angiogenesis and mast cells in squamous cell carcinoma of the oesophagus. *J Clin Pathol*. 2001;54(12):940-944.

65. Benítez–Bribiesca L, Wong A, Utrera D, Castellanos E. The Role of Mast Cell Tryptase in Neoangiogenesis of Premalignant and Malignant Lesions of the Uterine Cervix. *J Histochem Cytochem*. 2001;49(8):1061-1062.

66. Willemze R, Dreyling M, On behalf of the EGWG. Primary cutaneous lymphoma: ESMO Clinical Recommendations for diagnosis, treatment and follow-up. *Ann Oncol*. 2009;20(suppl 4):iv115-iv118.

67. Stadler R, Assaf C, Klemke C-D, et al. Short German guidelines: Cutaneous lymphomas. *J Dtsch Dermatol Ges*. 2008;6:S25-S31.

68. Willemze R, Jaffe ES, Burg G, et al. WHO-EORTC classification for cutaneous lymphomas. *Blood*. 2005;105(10):3768-3785.

69. Dummer R, Stadler R, Sterry W. Cutaneous lymphomas. *J Dtsch Dermatol Ges*. 2007;5(7):605-617.

70. Arulogun SO, Prince HM, Ng J, et al. Long-term outcomes of patients with advanced-stage cutaneous T-cell lymphoma and large cell transformation. *Blood*. 2008;112(8):3082-3087.

71. Olsen EA, Whittaker S, Kim YH, et al. Clinical End Points and Response Criteria in Mycosis Fungoides and Sézary Syndrome: A Consensus Statement of the International Society for Cutaneous Lymphomas, the United States Cutaneous Lymphoma Consortium, and the Cutaneous Lymphoma Task Force of the European Organisation for Research and Treatment of Cancer. *J Clin Oncol*. 2011;29(18):2598-2607.

72. Golling P, Cozzio A, Dummer R, French L, Kempf W. Primary cutaneous B-cell lymphomas - clinicopathological, prognostic and therapeutic characterisation of 54 cases according to the WHO-EORTC classification and the ISCL/EORTC TNM classification system for primary cutaneous lymphomas other than mycosis fungoides and Sezary syndrome. *Leuk Lymphoma*. 2008;49(6):1094-1103.

73. Cirée A, Michel L, Camilleri-Bröet S, et al. Expression and activity of IL-17 in cutaneous T-cell lymphomas (mycosis fungoides and sezary syndrome). *Int J Cancer*. 2004;112(1):113-120.

74. Krejsgaard T, Ralfkiaer U, Clasen-Linde E, et al. Malignant Cutaneous T-Cell Lymphoma Cells Express IL-17 Utilizing the Jak3/Stat3 Signaling Pathway. *J Invest Dermatol*. 2011;131(6):1331-1338.

75. Döbbeling U, Dummer R, Laine E, Potoczna N, Qin J-Z, Burg G. Interleukin-15 Is an Autocrine/Paracrine Viability Factor for Cutaneous T-Cell Lymphoma Cells. *Blood*. 1998;92(1):252-258.

76. Krejsgaard T, Vetter-Kauczok CS, Woetmann A, et al. Jak3- and JNK-dependent vascular endothelial growth factor expression in cutaneous T-cell lymphoma. *Leukemia*. 2006;20(10):1759-1766.

77. Vacca A, Moretti S, Ribatti D, et al. Progression of mycosis fungoides is associated with changes in angiogenesis and expression of the matrix metalloproteinases 2 and 9. *Eur J Cancer*. 1997;33(10):1685-1692.

78. Kopp KLM, Kauczok CS, Lauenborg B, et al. COX-2-dependent PGE2 acts as a growth factor in mycosis fungoides (MF). *Leukemia*. 2010;24(6):1179-1185.

79. Wu X, Sells RE, Hwang ST. Upregulation of Inflammatory Cytokines and Oncogenic Signal Pathways Preceding Tumor Formation in a Murine Model of T-Cell Lymphoma in Skin. *J Invest Dermatol*. 2011;131(8):1727-1734.

80. Rashid G, Bernheim J, Green J, Benchetrit S. Parathyroid hormone stimulates endothelial expression of atherosclerotic parameters through protein kinase pathways. *Am J Physiol Renal Physiol*. 2007;292(4):F1215-F1218.

81. Nagineni CN, Cherukuri KS, Kutty V, Detrick B, Hooks JJ. Interferon-γ differentially regulates TGF-β1 and TGF-β2 expression in human retinal pigment epithelial cells through JAK-STAT pathway. *J Cell Physiol*. 2007;210(1):192-200.

82. Saavedra E, Herrera M, Gao W, Uemura H, Pereira MA. The Trypanosoma cruzi trans-Sialidase, through Its Cooh-Terminal Tandem Repeat, Upregulates Interleukin 6 Secretion in Normal Human Intestinal Microvascular Endothelial Cells and Peripheral Blood Mononuclear Cells. *J Exp Med*. 1999;190(12):1825-1836.

83. Olsen E, Vonderheid E, Pimpinelli N, et al. Revisions to the staging and classification of mycosis fungoides and Sézary syndrome: a proposal of the International Society for Cutaneous Lymphomas (ISCL) and the cutaneous lymphoma task force of the European Organization of Research and Treatment of Cancer (EORTC). *Blood*. 2007;110(6):1713-1722.

84. Kadin ME, Cavaille-Coll MW, Gertz R, Massagué J, Cheifetz S, George D. Loss of receptors for transforming growth factor beta in human T-cell malignancies. *Proc Natl Acad Sci USA*. 1994;91(13):6002-6006.

85. Kaltoft K, Bisballe S, Dyrberg T, Boel E, Rasmussen PB, Thestrup-Pedersen K. Establishment of two continuous T-cell strains from a single plaque of a patient with mycosis fungoides. *In Vitro Cell Dev Biol*. 1992;28A(3 Pt 1):161-167.

86. Kaltoft K, Bisballe S, Rasmussen HF, Thestrup-Pedersen K, Thomsen K, Sterry W. A continuous T-cell line from a patient with Sézary syndrome. *Arch Dermatol Res*. 1987;279(5):293-298.

87. Klein G, Lindahl T, Jondal M, et al. Continuous lymphoid cell lines with characteristics of B cells (bone-marrow-derived), lacking the Epstein-Barr virus genome and derived from three human lymphomas. *Proc Natl Acad Sci USA*. 1974;71(8):3283-3286.

88. Schneider U, Schwenk HU, Bornkamm G. Characterization of EBV-genome negative "null" and "T" cell lines derived from children with acute lymphoblastic leukemia and leukemic transformed non-Hodgkin lymphoma. *Int J Cancer*. 1977;19(5):621-626.

89. McKenzie RCT, Jones CL, Tosi I, Caesar JA, Whittaker SJ, Mitchell TJ. Constitutive activation of STAT3 in Sezary syndrome is independent of SHP-1. *Leukemia*. 2012;26(2):323-331.

90. Drube S, Heink S, Walter S, et al. The receptor tyrosine kinase c-Kit controls IL-33 receptor signaling in mast cells. *Blood*. 2010;115(19):3899-3906.

91. Corbett TH, Roberts BJ, Leopold WR, et al. Induction and Chemotherapeutic Response of Two Transplantable Ductal Adenocarcinomas of the Pancreas in C57BL/6 Mice. *Cancer Res*. 1984;44(2):717-726.

92. Pfaffl M. A new mathematical model for relative quantification in real-time RT-PCR. *Nucleic Acids Res*. 2001;29(9):e45.

93. Gerber HP, Hillan KJ, Ryan AM, et al. VEGF is required for growth and survival in neonatal mice. *Development*. 1999;126(6):1149-1159.

94. Rabenhorst A, Schlaak M, Heukamp LC, et al. Mast cells play a protumorigenic role in primary cutaneous lymphoma. *Blood*. 2012;120(10):2042-2054.

95. Weber A, Knop J, Maurer M. Pattern analysis of human cutaneous mast cell populations by total body surface mapping. *Br J Dermatol*. 2003;148(2):224-228.

96. Damsgaard TE, Olesen AB, Sorensen FB, Thestrup-Pedersen K, Schiotz PO. Mast cells and atopic dermatitis. Stereological quantification of mast cells in atopic dermatitis and normal human skin. *Arch Dermatol Res*. 1997;289(5):256-260.

97. Weber A, Maurer M. Skin site mast cell numbers correlate with rates of nodular growth, but not incidence, of basal cell carcinoma. *Dermatology*. 2005;211(3):298-299.

98. Mikhail GR, Miller-Milinska A. Mast cell population in human skin. *J Invest Dermatol*. 1964;43:249-254.

99. Janssens AS, Heide R, den Hollander JC, Mulder PGM, Tank B, Oranje AP. Mast cell distribution in normal adult skin. *J Clin Pathol*. 2005;58(3):285-289.

100. Jiang WY, Chattedee AD, Raychaudhuri SP, Raychaudhuri SK, Farber EM. Mast cell density and IL-8 expression in nonlesional and lesional psoriatic skin. *Int J Dermatol*. 2001;40(11):699-703.

101. Lin AM, Rubin CJ, Khandpur R, et al. Mast Cells and Neutrophils Release IL-17 through Extracellular Trap Formation in Psoriasis. *J Immunol*. 2011;187(1):490-500.

102. Kneilling M, Röcken M. Mast cells: novel clinical perspectives from recent insights. *Exp Dermatol*. 2009;18(5):488-496.

103. Kawakami T, Ando T, Kimura M, Wilson BS, Kawakami Y. Mast cells in atopic dermatitis. *Curr Opin Immunol*. 2009;21(6):666-678.

104. Ackermann L, Harvima IT. Mast cells of psoriatic and atopic dermatitis skin are positive for TNF-α and their degranulation is associated with expression of ICAM-1 in the epidermis. *Arch Dermatol Res*. 1998;290(7):353-359.

105. Ackermann, Harvima, Pelkonen, Ritamäki S, Naukkarinen, Horsmanheimo. Mast cells in psoriatic skin are strongly positive for interferon-gamma. *Br J Dermatol*. 1999;140(4):624-633.

106. Naukkarinen A, Järvikallio A, Lakkakorpi J, Harvima IT, Harvima RJ, Horsmanheimo M. Quantitative histochemical analysis of mast cells and sensory nerves in psoriatic skin. *J Pathol*. 1996;180(2):200-205.

107. Harvima IT, Naukkarinen A, Paukkonen K, et al. Mast cell tryptase and chymase in developing and mature psoriatic lesions. *Arch Dermatol Res*. 1993;285(4):184-192.

108. Harvima IT, Naukkarinen A, Harvima RJ, Horsmanheimo M. Enzyme- and immunohistochemical localization of mast cell tryptase in psoriatic skin. *Arch Dermatol Res*. 1989;281(6):387-391.

109. Harvima IT, Naukkarinen A, Harvima RJ, Aalto ML, NeittaanmÄki H, Horsmanheimo M. Quantitative enzyme-histochemical analysis of tryptase- and chymase-containing mast cells in psoriatic skin. *Arch Dermatol Res*. 1990;282(7):428-433.

110. Goodfield M, Macdonald Hull S, Holland D, et al. Investigations of the 'active' edge of plaque psoriasis: vascular proliferation precedes changes in epidermal keratin. *Br J Dermatol*. 1994;131(6):808-813.

111. van de Kerkhof PCM, Goos M, Christophers E, Baudin M, Dupuy P. Inhibitor of the Release of Mast Cell Mediators Does Not Improve the Psoriatic Plaque. *Skin Pharmacol*. 1995;8(1-2):25-29.

112. Petersen LJ, Hansen U, Kristensen JK, Nielsen H, Skov PS, Nielsen HJ. Studies on mast cells and histamine release in psoriasis: the effect of ranitidine. *Acta Derm Venereol*. 1998;78(3):190-193.

113. Kreuter R, Steigleder GK, Pullmann H. Mast cell numbers in initial psoriasis vulgaris. *Z Hautkr*. 1978;53(21):756-758.

114. Töyry S, Fräki J, Tammi R. Mast cell density in psoriatic skin. The effect of PUVA and corticosteroid therapy. *Arch Dermatol Res*. 1988;280(5):282-285.

115. Toruniowa B, Jablońska S. Mast cells in the initial stages of psoriasis. *Arch Dermatol Res*. 1988;280(4):189-193.

116. Eriksson, Hagforsen, Lundin, Micha Ëlsson. Palmoplantar pustulosis: a clinical and immunohistological study. *Br J Dermatol*. 1998;138(3):390-398.

117. Stewart G. Histopathology of chronic urticaria. *Clin Rev Allergy Immunol*. 2002;23(2):195-200.

118. Haas N, Hermes B, Henz BM. Adhesion molecules and cellular infiltrate: histology of urticaria. *J Investig Dermatol Symp Proc*. 2001;6(2):137-138.

119. Medina VA, Rivera ES. Histamine receptors and cancer pharmacology. *Br J Pharmacol*. 2010;161(4):755-767.

120. Ruffell B, Coussens LM. Histamine restricts cancer: nothing to sneeze at. *Nat Med*. 2011;17(1):43-44.

121. Rivera ES, Cricco GP, Engel NI, Fitzsimons CP, Martín GA, Bergoc RM. Histamine as an autocrine growth factor: an unusual role for a widespread mediator. *Semin Cancer Biol*. 2000;10(1):15-23.

122. Bolton E, King J, Morris DL. H2-antagonists in the treatment of colon and breast cancer. *Semin Cancer Biol*. 2000;10(1):3-10.

123. Hanahan D, Coussens Lisa M. Accessories to the Crime: Functions of Cells Recruited to the Tumor Microenvironment. *Cancer Cell*. 2012;21(3):309-322.

124. Rothenberg ME. Eosinophilia. *N Engl J Med*. 1998;338(22):1592-1600.

125. Lampinen, Rak, Venge. The role of interleukin-5, interleukin-8 and RANTES in the chemotactic attraction of eosinophils to the allergic lung. *Clin Exp Allergy*. 1999;29(3):314-322.

126. Oliveira SH, Faccioli LH, Ferreira SH, FQ. C. Participation of interleukin-5, interleukin-8 and leukotriene B4 in eosinophil accumulation in two different experimental model. *Mem Inst Oswaldo Cruz*. 1997;92(Suppl 2):205-2010.

127. Shakoory B, Fitzgerald SM, Lee SA, Chi DS, Krishnaswamy G. The role of human mast cell-derived cytokines in eosinophil biology. *J Interferon Cytokine Res*. 2004;24(5):271-281.

128. Karpova MB, Fujii K, Jenni D, Dummer R, Urosevic-Maiwald M. Evaluation of lymphangiogenic markers in Sézary syndrome. *Leuk Lymphoma*. 2011;52(3):491-501.

129. Mazur G, Woźniak Z, Wróbel T, Maj J, Kuliczkowski K. Increased angiogenesis in cutaneous T-cell lymphomas. *Pathol Oncol Res*. 2004;10(1):34-36.

130. Schaerer L, Schmid MH, Mueller B, Dummer RG, Burg G, Kempf W. Angiogenesis in cutaneous lymphoproliferative disorders: microvessel density discriminates between cutaneous B-cell lymphomas and B-cell pseudolymphomas. *Am J Dermatopathol*. 2000;22(2):140-143.

131. Aoki M, Pawankar R, Niimi Y, Kawana S. Mast Cells in Basal Cell Carcinoma Express VEGF, IL-8 and RANTES. *Int Arch Allergy Immunol*. 2003;130(3):216-223.

132. Baghestanian M, Hofbauer R, Kiener HP, et al. The c-kit Ligand Stem Cell Factor and Anti-IgE Promote Expression of Monocyte Chemoattractant Protein-1 in Human Lung Mast Cells. *Blood*. 1997;90(11):4438-4449.

133. King CA, Anderson R, Marshall JS. Dengue Virus Selectively Induces Human Mast Cell Chemokine Production. *J Virol*. 2002;76(16):8408-8419.

134. Grivennikov SI, Greten FR, Karin M. Immunity, Inflammation, and Cancer. *Cell*. 2010;140(6):883-899.

135. Rambaldi A, Torcia M, Bettoni S, et al. Modulation of cell proliferation and cytokine production in acute myeloblastic leukemia by interleukin-1 receptor antagonist and lack of its expression by leukemic cells. *Blood*. 1991;78(12):3248-3253.

136. Balkwill F, Charles KA, Mantovani A. Smoldering and polarized inflammation in the initiation and promotion of malignant disease. *Cancer Cell*. 2005;7(3):211-217.

137. Bingle L, Brown NJ, Lewis CE. The role of tumour-associated macrophages in tumour progression: implications for new anticancer therapies. *J Pathol*. 2002;196(3):254-265.

138. Pollard JW. Tumour-educated macrophages promote tumour progression and metastasis. *Nat Rev Cancer*. 2004;4(1):71-78.

139. Schioppa T, Uranchimeg B, Saccani A, et al. Regulation of the Chemokine Receptor CXCR4 by Hypoxia. *J Exp Med*. 2003;198(9):1391-1402.

140. Mizuno H, Nakayama T, Miyata Y, et al. Mast cells promote the growth of Hodgkin's lymphoma cell tumor by modifying the tumor microenvironment that can be perturbed by bortezomib. *Leukemia*. 2012. Epub ahead of print

141. Blobe GC, Schiemann WP, Lodish HF. Role of Transforming Growth Factor β in Human Disease. *N Engl J Med*. 2000;342(18):1350-1358.

142. Hill J, Tremblay T-L, Cantin C, O'Connor-McCourt M, Kelly J, Lenferink A. Glycoproteomic analysis of two mouse mammary cell lines during transforming growth factor (TGF)-beta induced epithelial to mesenchymal transition. *Proteome Sci*. 2009;7(1):2.

143. Liotta LA, Stetler-Stevenson WG. Tumor Invasion and Metastasis: An Imbalance of Positive and Negative Regulation. *Cancer Res*. 1991;51(18 Supplement):5054s-5059s.

144. Melani C, Sangaletti S, Barazzetta FM, Werb Z, Colombo MP. Amino-Biphosphonate–Mediated MMP-9 Inhibition Breaks the Tumor-Bone Marrow Axis Responsible for Myeloid-Derived Suppressor Cell Expansion and Macrophage Infiltration in Tumor Stroma. *Cancer Res*. 2007;67(23):11438-11446.

145. Papetti M, Herman IM. Mechanisms of normal and tumor-derived angiogenesis. *Am J Physiol Cell Physiol*. 2002;282(5):C947-C970.

146. Coussens LM, Raymond WW, Bergers G, et al. Inflammatory mast cells up-regulate angiogenesis during squamous epithelial carcinogenesis. *Genes Dev*. 1999;13(11):1382-1397.

147. Starkey JR, Crowle PK, Taubenberger S. Mast-cell-deficient W/Wv mice exhibit a decreased rate of tumor angiogenesis. *Int J Cancer*. 1988;42(1):48-52.

148. Oldford SA, Haidl ID, Howatt MA, Leiva CA, Johnston B, Marshall JS. A Critical Role for Mast Cells and Mast Cell-Derived IL-6 in TLR2-Mediated Inhibition of Tumor Growth. *J Immunol*. 2010;185(11):7067-7076.

Figure Index

Figure 1. Mast cell development 7
Figure 2. *Mcpt5-Cre/iDTR* – A mouse model of inducible mast cell deficiency 10
Figure 3. *Mcpt5-Cre/R-DTA* – A mouse model of constitutive mast cell deficiency 10
Figure 4. Hallmarks of cancer 11
Figure 5. Treatment regimen for C57BL/6 $Kit^{W\text{-}sh/W\text{-}sh}$ and WT C57BL/6 animals 37
Figure 6. Treatment regimen for *Mcpt5-Cre+/iDTR+* and *Mcpt5-Cre-/iDTR+* animals 37
Figure 7. Mast cell numbers are increased in PCL 43
Figure 8. Histological analyses showed that mast cell numbers are increased in PCL 44
Figure 9. Mast cell numbers correlate with progression of PCL 46
Figure 10. Mast cell degranulation stages 47
Figure 11. Mast cell degranulation is increased in PCL 48
Figure 12. Microvessel density is increased in MF 50
Figure 13. Histological analyses showed that microvessel density is increased in MF 51
Figure 14. Mast cells release mediators that promote tumor growth 52
Figure 15. Unstimulated PCL cells produce proinflammatory cytokines 54
Figure 16. Mast cell supernatant induces changes in cytokine production of PCL cells 55
Figure 17. Mast cell supernatant induces proliferation of PCL cells 57
Figure 18. Murine mast cell supernatant induces cytokine release and proliferation of mouse T-cell lymphoma cell line EL4 59
Figure 19. Mouse model of inducible mast cell deficiency 60
Figure 20. Mouse model of constitutive mast cell deficiency 61
Figure 21. Mast cell-deficient mice show decreased growth of subcutaneously injected tumors 63

Figure 22. Mast cell-deficient mice show decreased growth of subcutaneously injected tumors and decreased microvessel density 64
Figure 23. Mast cell-deficient mice show decreased chemically induced carcinogenesis 65
Figure 24. Histological analyses revealed that mast cell-deficient mice show decreased chemically induced carcinogenesis 66
Figure 25. Potential participation of mast cells in different hallmarks of cancer 71

Table Index

Table 1. Mediators produced by mast cells exerting beneficial effects on tumor growth 16
Table 2. Mediators produced by mast cells exerting detrimental effects on tumor growth 16
Table 3. Frequently used chemicals and solutions 23
Table 4. Chemical composition of frequently used buffers 23
Table 5. Primer used for animal genotyping 24
Table 6. Primer used for quantitative real-time PCR 24
Table 7. Frequently used laboratory equipment 25
Table 8. Software used for data collection and analysis 25
Table 9. Summary of PCR cycling profiles for genotyping 35
Table 10. Clinical characteristics of PCL patients participating in the study 41

Acknowledgments

I would like to thank especially Karin Hartmann for the opportunity to work with her at this very interesting topic, for her support, helpful advices and constructive discussions.

I also want to thank the present lab members Anja Förster and Silke Leja, as well as the former members of the lab Stefan Grotha and Carmen Berns for discussion, instructions and continuous help.

Furthermore, I would like to thank Dr. Max Schlaak, PD Dr. Peter Kurschat and Prof. Dr. Dr. Cornelia Mauch from the Department of Dermatology, Dr. Lukas Heukamp and Prof. Dr. Reinhard Büttner from the Institute of Pathology, as well as Dr. Sebastian Theurich and PD Dr. Dr. Michael von Bergwelt-Baildon from the Department I of Internal Medicine for contributing patient samples and data.

I would also like to thank Alexandra Florin from the Institute of Pathology for excellent technical assistance and Prof. Dr. Christine Neumann for helpful discussions.

I also wish to thank my parents, grandparents and brother for their great support and for making all this possible.

Many sincere thanks to Bastian for always being at my side and for distracting me whenever I needed it.

Erklärung

Ich versichere, dass ich die von mir vorgelegte Dissertation selbständig angefertigt, die benutzten Quellen und Hilfsmittel vollständig angegeben und die Stellen der Arbeit – einschließlich Tabellen, Karten, und Abbildungen –, die anderen Werken im Wortlaut oder dem Sinn nach entnommen sind, in jedem Einzelfall als Entlehnung kenntlich gemacht habe; dass diese Dissertation noch keiner anderen Fakultät oder Universität zur Prüfung vorgelegen hat; dass sie – abgesehen von unten angegebenen Teilpublikationen – noch nicht veröffentlicht worden ist sowie, dass ich eine solche Veröffentlichung vor Abschluss des Promotionsverfahrens nicht vornehmen werde. Die Bestimmungen der Promotionsordnung sind mir bekannt. Die von mir vorgelegte Dissertation ist von PD Dr. Karin Hartmann betreut worden.

Teilpublikationen:

Anja Rabenhorst, Max Schlaak, Lukas C. Heukamp, Anja Förster, Reinhard Büttner, Sebastian Theurich, Michael von Bergwelt-Baildon, Peter Kurschat, Cornelia Mauch, Axel Roers, Karin Hartmann: Mast cells play a protumorigenic role in primary cutaneous lymphoma. *Blood*, 2012, 120(10):2042-2054

Katrin Peschke, Anne Dudeck, **Anja Rabenhorst**, Karin Hartmann, Axel Roers: Investigation of mast cell *in vivo* function using novel mouse models of mast cell deficiency and mast cell-specific gene inactivation. *Methods Mol Biol*, 2012, *in press*

Teile dieser Arbeit wurden auf folgenden Kongressen vorgestellt:

Oral presentations:

Mast cells in cutaneous T- and B-cell lymphomas. 5th International Symposium on the Biology and Immunology of Cutaneous Lymphoma, 2011, Berlin, Germany

Mast cells play a protumorigenic role in primary cutaneous lymphoma. International Mast Cell and Basophil Meeting, 2011, Southampton, United Kingdom

Mast cells play a protumorigenic role in primary cutaneous lymphoma. 15th Meeting of the AGMZB-Mast cell and Basophil Section of the ADF, 2011, Mainz, Germany

Poster presentations:

Anja Rabenhorst*, Max Schlaak* (*first authors), Lukas Heukamp, Reinhard Büttner, Peter Kurschat, Cornelia Mauch, Karin Hartmann: Mast cells in cutaneous T-and B-cell lymphomas. International Mast Cell and Basophil Meeting, 2010, Berlin, Germany

Max Schlaak*, **Anja Rabenhorst*** (*first authors), Lukas Heukamp, Reinhard Büttner, Peter Kurschat, Cornelia Mauch, Karin Hartmann: Increased number and degranulation of mast cells in cutaneous lymphomas. 38. Jahrestagung der ADF (Arbeitsgemeinschaft Dermatologische Forschung), 2011, Tübingen, Germany

Anja Rabenhorst, Max Schlaak, Lukas C. Heukamp, Anja Förster, Sebastian Theurich, Michael v. Bergwelt, Reinhard Büttner, Peter Kurschat, Cornelia Mauch, Axel Roers, Karin Hartmann: Mast cells play a protumorigenic role in primary cutaneous lymphoma. 39. Jahrestagung der ADF (Arbeitsgemeinschaft Dermatologische Forschung), 2012, Marburg, Germany

Karin Hartmann, **Anja Rabenhorst**: Modulation of tumor microenvironment and anti-tumor immunity by mast cells. SFB832-International Symposium, 2012, Bad Neuenahr, Germany

Anja Rabenhorst, Max Schlaak, Lukas C. Heukamp, Anja Förster, Sebastian Theurich, Michael v. Bergwelt, Reinhard Büttner, Peter Kurschat, Cornelia Mauch, Axel Roers, Karin Hartmann: Mast cells play a protumorigenic role in primary cutaneous lymphoma. Keystone Symposia-The Role of Inflammation during Carcinogenesis, 2012, Dublin, Ireland

Ich versichere, dass ich alle Angaben wahrheitsgemäß nach bestem Wissen und Gewissen gemacht habe und verpflichte mich, jedmögliche, die obigen Angaben betreffenden Veränderungen, dem Promotionsausschuss unverzüglich mitzuteilen.

Köln, den ……..

_____

Anja Rabenhorst

Curriculum vitae

Name	Anja Rabenhorst
Date of birth	06. December 1981
Place of birth	Wismar, Germany
Nationality	German

Education

August 2010 – present	University of Cologne, Department of Dermatology PhD student in Biological Sciences PhD thesis: "The role of mast cells in the microenvironment of tumors" PhD student membership in "Graduate School for Biological Sciences", associated in the (IPMM) "Interdisciplinary Program in Molecular Medicine"
2007 – 2010	University of Mainz, Institute for Molecular Biophysics PhD student funded by scholarship of "Graduate School of Immunotherapy"
2003 – 2007	University of Mainz Studies in Biology Diploma thesis at the Institute for Molecular Biophysics: "Zur Kristallisation von multimeren Arthropoden-Hämocyaninen" (grade: 1.0) Diploma examination in Botany (grade: 2.0), Zoology (grade: 1.0), Molecular Biophysics (grade: 1.3)
2000 – 2003	University of Heidelberg Studies in Medicine
June 2000	Gerhart-Hauptmann-Gymnasium, Wismar Abitur (grade: 1.0)

Workshops and Trainings

BioScript Workshop	Advanced Scientific Writing
BioScript Workshop	Designing and Presenting a Poster
BioScript Workshop	Getting Funded
Technical Training	In vivo imaging of Luciferase expression by BLI
Training	Grundlagen der medizinischen Statistik

Awards

Poster Award 39. Jahrestagung der ADF (AG Dermatologische Forschung), 2012, Marburg, Germany

Publications

Christian Meesters, Bruno Pairet, **Anja Rabenhorst**, Heinz Decker, Elmar Jaenicke: Monte Carlo-based rigid body modelling of large protein complexes against small angle scattering data. *Comput Biol Chem*, 2010, 34(3):158-64

Anja Rabenhorst, Max Schlaak, Lukas C. Heukamp, Anja Förster, Reinhard Büttner, Sebastian Theurich, Michael von Bergwelt-Baildon, Peter Kurschat, Cornelia Mauch, Axel Roers, Karin Hartmann: Mast cells play a protumorigenic role in primary cutaneous lymphoma. *Blood*, 2012, 120(10):2042-2054

Anja Förster, Franco H. Falcone, Bernhard F. Gibbs, Liane M. Preussner, Britta S. Fiebig, Hülya Altunok, Jens M. Seeger, Sabine Cerny-Reiterer, **Anja Rabenhorst**, Kerstin Papenfuss, Peter Valent, Hamid Kashkar, Karin Hartmann: Anti-Fas/CD95 and tumor necrosis factor-related apoptosis-inducing ligand (TRAIL) differentially regulate apoptosis in normal and neoplastic human basophils. *Leuk Lymphoma,* 2012, [Epub ahead of print]

Katrin Peschke, Anne Dudeck, **Anja Rabenhorst**, Karin Hartmann, Axel Roers: Investigation of mast cell *in vivo* function using novel mouse models of mast cell deficiency and mast cell-specific gene inactivation. *Methods Mol Biol*, 2012, *in press*

Karin Hartmann*, Nicola Wagner*, **Anja Rabenhorst*** (*first authors), Liselotte Pflanz, Silke Leja, Anja Förster, Manuela Gehring, Alexander Kapp, Ulrike Raap: Serum levels of IL-31 are increased in a subset of patients with mastocytosis and correlate with disease severity in adult patients. *J Allergy Clin Immunol*, 2012, [Epub ahead of print]

Oral Presentations

Mast cells in cutaneous T- and B-cell lymphomas. 5th International Symposium on the Biology and Immunology of Cutaneous Lymphoma, 2011, Berlin, Germany

Mast cells play a protumorigenic role in primary cutaneous lymphoma. International Mast Cell and Basophil Meeting, 2011, Southampton, United Kingdom

Mast cells play a protumorigenic role in primary cutaneous lymphoma. 15th Meeting of the AGMZB-Mast cell and Basophil Section of the ADF, 2011, Mainz, Germany

Poster Presentations

Anja Rabenhorst*, Max Schlaak* (*first authors), Lukas Heukamp, Reinhard Büttner, Peter Kurschat, Cornelia Mauch, Karin Hartmann: Mast cells in cutaneous T-and B-cell lymphomas. International Mast Cell and Basophil Meeting, 2010, Berlin, Germany

Max Schlaak*, **Anja Rabenhorst*** (*first authors), Lukas Heukamp, Reinhard Büttner, Peter Kurschat, Cornelia Mauch, Karin Hartmann: Increased number and degranulation of mast cells in cutaneous lymphomas. 38. Jahrestagung der ADF (Arbeitsgemeinschaft Dermatologische Forschung), 2011, Tübingen, Germany

Anja Rabenhorst, Max Schlaak, Lukas C. Heukamp, Anja Förster, Sebastian Theurich, Michael v. Bergwelt, Reinhard Büttner, Peter Kurschat, Cornelia Mauch, Axel Roers, Karin Hartmann: Mast cells play a protumorigenic role in primary cutaneous lymphoma. 39. Jahrestagung der ADF (Arbeitsgemeinschaft Dermatologische Forschung), 2012, Marburg, Germany

Anja Förster, Stefan Grotha, **Anja Rabenhorst**, Henning Walczak, Hamid Kashkar, Axel Roers, Karin Hartmann: Effect of TNF-related apoptosis-inducing ligand receptor (TRAILR) on homeostasis of murine mast cells. 39. Jahrestagung der ADF (Arbeitsgemeinschaft Dermatologische Forschung), 2012, Marburg, Germany

Karin Hartmann, **Anja Rabenhorst**: Modulation of tumor microenvironment and anti-tumor immunity by mast cells. SFB832-International Symposium, 2012, Bad Neuenahr, Germany

Anja Rabenhorst, Max Schlaak, Lukas C. Heukamp, Anja Förster, Sebastian Theurich, Michael v. Bergwelt, Reinhard Büttner, Peter Kurschat, Cornelia Mauch, Axel Roers, Karin Hartmann: Mast cells play a protumorigenic role in primary cutaneous lymphoma. Keystone Symposia-The Role of Inflammation during Carcinogenesis, 2012, Dublin, Ireland